Available online at www.sciencedirect.com
SCIENCE DIRECT®
Prog. Polym. Sci. 29 (2004) 1079–1141
PROGRESS IN POLYMER SCIENCE
www.elsevier.com/locate/ppolysci

Polymers containing fullerene or carbon nanotube structures

Changchun Wang[a,*], Zhi-Xin Guo[b], Shoukuan Fu[a], Wei Wu[b], Daoben Zhu[b]

[a]*Department of Macromolecular Science, The Key Laboratory of Polymer Molecular Engineering of Ministry of Education, Fudan University, Shanghai 200433, China*
[b]*Institute of Chemistry, Chinese Academy of Sciences, Beijing 100080, China*

Received 23 May 2003; revised 26 July 2004; accepted 2 August 2004
Available online 5 October 2004

Abstract

This review deals with recent progress in studies of polymeric covalent and noncovalent modifications of fullerenes (mainly C_{60}) and carbon nanotubes (CNTs), and their applications. By using functional polymers to react with fullerenes, or synthesizing polymers in the presence of fullerenes, various kinds of polymeric fullerenes can be prepared: side-chain polymers, main-chain polymers, dendritic fullerenes, star-shaped polymers, fullerene end-capped polymers, etc. Furthermore, by controlling the functional groups in polymer chains and reaction conditions, many well-defined fullerene polymers have been prepared. 'Living' polymerization methods have also been introduced for preparation of fullerene polymers, e.g. anionic polymerization, iniferter technique, stable free radical polymerization, and atom-transfer free-radical polymerisation. With these living methods, both the architecture of the fullerene polymers and the grafted polymer chains can be well-controlled. All of these methods establish a good platform for developing applications of fullerene polymers. The synthesis of polymeric CNTs is only in its infancy. However, present results show promise that the combination of the unique properties of CNTs with functional polymers will lead to novel materials with unusual mechanical, electrical, magnetic, and optical properties. Doping of polymeric systems with fullerenes in is also a very important research area, especially for preparation of electronic and optical materials. Both conducting and conventional polymers can be used as matrices in the preparation of functional composites. The structures and properties of these composites are strongly dependent on the properties and concentrations of the active components. CNT-doped polymers have also been prepared and show interesting properties. The combination of the unique properties of fullerenes and CNTs with polymers makes these materials potential candidates for many applications, such as data storage media, photovoltaic cells and photodiodes, optical limiting devices, photosensitive drums for printers, and so on. The applications of polymeric fullerenes and CNTs are also reviewed in this article.

Keywords: Fullerene (C_{60}); Carbon nanotubes (CNTs); Polymer fullerenes; Covalent modifications; Doping; Photoconductivity; Photorefractivity; Photovoltaic cells; Photodiodes; Optical limiting

* Corresponding author. Tel.: +86 21 6564 2385; fax: +86 21 6564 0293.
E-mail address: ccwang@fudan.edu.cn (C. Wang).

0079-6700/$ - see front matter © 2004 Elsevier Ltd. All rights reserved.
doi:10.1016/j.progpolymsci.2004.08.001

Contents

1. Introduction

1.1. A brief history of fullerene and carbon nanotubes

In 1985, Kroto et al. [1] first reported the existence of buckminsterfullerene C_{60} (Scheme 1a), theoretical speculation about carbon clusters [2] over 36 years was finally verified. Since then, this beautiful molecule has attracted ever more attention of theoretical and experimental scientists. Some chemists began to focus their research on the chemistry of this molecule, but real fullerene chemistry began only after 1990 when Krätschmer et al. described a method for preparing macroscopic quantities of C_{60} [3]. Then many of polymer scientists shifted their attention to this field. They tried to use this molecule as a building

Nomenclature

AIBN 2,2′-azobisisobutyronitrile
ATRP atom transfer radical polymerization
BAF benzylaminofullerene
BCBO benzocyclobutenone
BPO benzyl peroxide
BSA bovine serum albumin
C_{60}(St-PCHD-PS)$_6$ 6-*star*-fullerene[styrene-*block*-poly(1,3-cyclohexadiene)-*block*-polystyrene]
C_{60}(St-PPP-PS)$_6$ 6-*star*-fullerene[styrene-*block*-poly(1,4-phenylene)-*block*-polystyrene]
CNT carbon nanotube
CV cyclic voltammogram
DBU 1,8-diazabicyclo[5,4,0]undec-7-ene
DCV dicyanovinyl aniline
DLS dynamic light scattering
DMF dimethyl formamide
DSC differential scanning calorimetry
EPDM ethylene–propylene ethylidene norbornene terpolymer
GPC gel permeation chromatography
HOMO highest occupied molecular orbital
HPLC high performance liquid chromatography
IPCE incident photon-current efficiency for monochromatic light
ITO indium tin oxide
Jsc short circuit current
LC liquid crystal
LDPE low-density polyethylene
LED light-emitting diode
LESR light-induced electron-spin resonance
LUMO lowest unoccupied molecular orbital
MBP methyl 2-bromopropionate
MDDA didecylamine modified MWNTs
MEH-PPV poly[2-methoxy, 5-(ethyl-hexyloxy)-*p*-phenylene vinylene]
MWNT multiwalled carbon nanotube
NHS *N*-hydroxysuccinimide
NLO nonlinear optical
NMP *N*-methyl-2-pyrrolidone
OO-PPV poly(2,5-dioctyloxy-*p*-phenylene vinylene
OPV oligophenylenevinylene
P3OT poly(3-octylthiophene)
PANI polyaniline
PAT poly(3-alkylthiophene)
PBMA poly(*n*-butyl methacrylate)
PC polycarbonate
PDI polydispersity index
PE polyethylene
PEO poly(ethylene oxide)
PHDK poly[1,6-heptadiene]
PHEMA poly(hydroxyethyl methacrylate)
PIA photoinduced absorption
PL photoluminescence
PMMA poly(methyl methacrylate)
PMPS phenylmethyl polysilane
PmPV poly(*m*-phenylenevinylene-*co*-2,5-dioctoxy-*p*-phenylene vinylene)
PPA poly(phenylacetylene)
PPB poly(1-phenyl-1-butyne)
PPO poly(propylene oxide)
PPP poly(1-phenyl-1-propyne)
PPV poly(*p*-phenylene vinylene)
PPyPV PR poly{(2,6-pyridinylene-vinylene)-*co*-[(2,5-dioctyloxy-*p*-phenylene)vinylene]}photorefractive
PS polystyrene
PSS polystyrene sulfonate
PVDF polyvinylidene fluoride
PVK poly(*N*-vinylcarbazole)
PVP polyvinyl pyrrolidone
RSA reverse saturable absorption
sec-BuLi *sec*-butyllithium
SMCC succinimidyl 4-(*N*-maleimidomethyl) cyclohexane-1-carboxylate
STM scanning tunneling microscopy
SWNT single-walled carbon nanotube
$t_{1/2}$ decay half-time
TEM transmission electron microscopy
TEMPO 2,2,6,6-tetramethylpiperidinyl-1-oxy
T_g glass transition temperature
THF tetrahydrofuran
TMEDA *N*,*N*,*N*′,*N*′-tetramethylethylenediamine
TMEDA tetramethyl-ethylenediamine
TOF-MS time of flight-mass spectrum
TPA triphenylamine
UV/Vis ultraviolet visible
Voc open circuit voltage

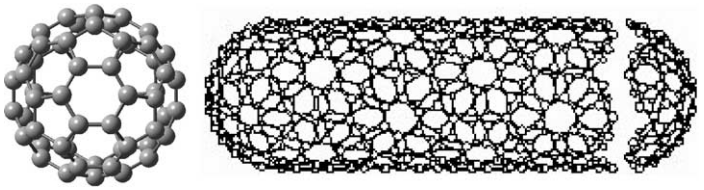

Scheme 1. Ideal structure of (a) C_{60} and (b) a single-walled carbon nanotube.

block to construct novel materials with unusual properties. With the sharp decrease of price and availability of large amounts of C_{60}, the first mass application appeared in 2003 in a very unexpected form: bowling balls with fullerene coatings [4]. Now, tons of C_{60} are produced by a Japanese venture company by burning toluene to produce fullerenes [5], and they have built a plant capable of producing 40 t/yr and plan production of 1500 t/yr in 2007 [6].

Carbon nanotubes (CNTs) (Scheme 1b), the macromolecular analog of fullerenes, were found by Iijima [7] in 1991. These are arrangements of carbon hexagons formed into tiny tubes. They may have diameters ranging from a few angstroms to tens of nanometers and can have lengths of up to several centimeters. CNTs can be viewed as hollow coaxial cylinders formed of graphite layers with both ends of the cylinder normally capped by fullerene-like structures. There are two kinds of CNTs, single-walled carbon nanotubes (SWNTs) formed by a single graphene sheet, and multiwalled nanotubes (MWNTs) formed with additional graphene sheets wrapped around the SWNT core. The development of CNT research began soon after the macroscopic production of C_{60} and the identification of CNTs in soot deposits formed during plasma arc experiments. CNTs possess unique mechanical and electronic properties depending on their geometry and dimensions. CNTs have very high moduli [8,9], and are believed to be the lightest and strongest materials so far discovered. Recently, uniformly conductive CNTs/Nylon 6 composites have been supplied by RTP company [10].

1.2. The scope of this review

This review of polymers containing fullerene or CNT structures will deal with two kinds of materials: polymer composites doped with fullerene or CNT and fullerene or CNTs covalently bonded to polymer chains.

Preparation of fullerene- or CNT-containing polymeric materials is noteworthy for several reasons. For instance, when a small amount of C_{60} or CNTs is introduced into a polymer system, many properties of the polymer are enhanced, such as photoconductivity [11], mechanical properties [12], optical limiting properties [13], etc. Another goal is to overcome the drawbacks of C_{60} or CNTs for large-scale applications, due to their insolubility, or near insolubility, in most solvents, and their tendency to aggregate [14]. These problems can be overcome by polymer modification of the fullerenes or CNTs [15–19], thus opening routes to tailor-made polymeric materials with interesting electronic, magnetic, mechanical, catalytic, and optical properties.

1.3. Classification of fullerene polymers

In the course of the rapid development of the fullerene chemistry, many types of polymeric derivatives have been prepared. A structural classification of polymeric fullerene derivatives is presented in Scheme 2.

Many chapters and reviews have been published on fullerenes [4,20–25]: some focus on their physical properties [20–22]; others focus on their synthesis [4, 23–35]. Our aim here to give a detailed account of progress, especially recent progress, on the several categories of fullerene-containing polymeric materials. CNT-containing polymers are also reviewed. Finally, we mention some interesting applications of these materials.

2. Polymeric derivatives of fullerenes

2.1. General aspects

As we know, when C_{60} is attached to a polymer chain, properties of the polymer will be changed and

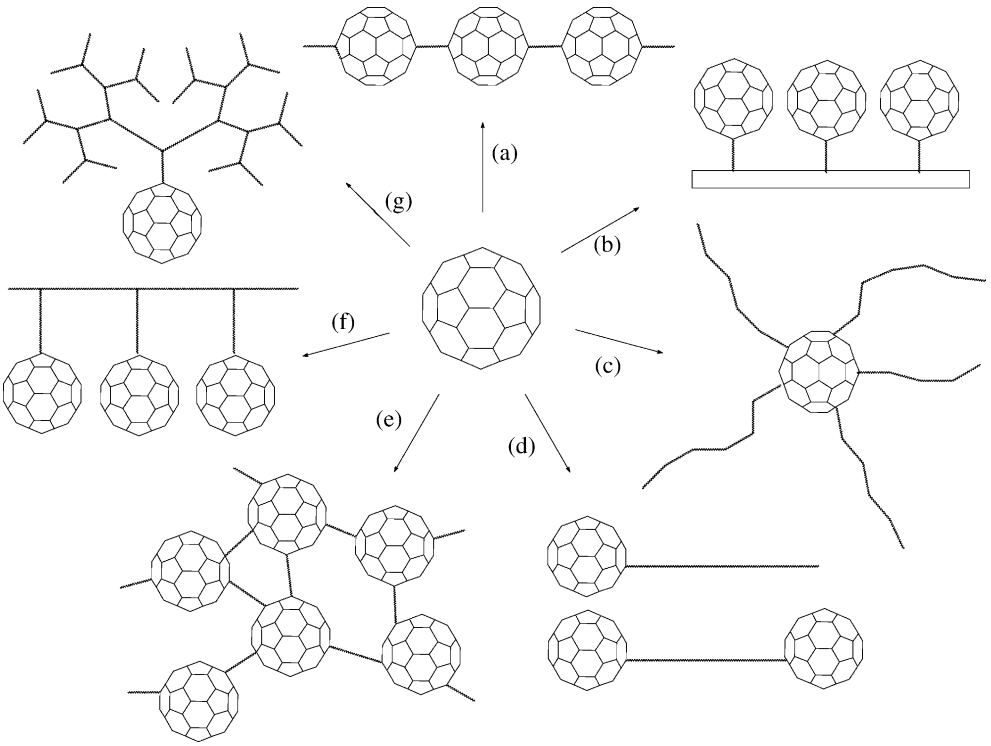

Scheme 2. Different types of polymeric C_{60} derivatives: (a) main-chain fullerene polymer; (b) immobilization of fullerenes on solid surface; (c) star-shaped fullerene polymers; (d) fullerene-end-capped polymers; (e) crosslinked polymeric fullerene derivatives; (f) side-chain fullerene polymers; (g) fullerodendrimer.

some new properties will appear. At the same time, the fullerene polymer may be soluble in common solvents. Through controlled modification of C_{60}, fullerene polymers with different structures can be obtained, such as side-chain polymers, main-chain polymers, star-shaped polymers, etc. In this section, the synthesis of fullerene-containing polymers is summarized systematically, with emphasis on recent progress.

2.2. *Side-chain fullerene polymers*

Research on polymeric fullerene derivatives has benefited from the rapid development of fullerene chemistry. The first attempt to produce side-chain fullerene polymers was by Wudl et al. [26]. They first prepared a low molecular weight bihydroxy-functional fullerene derivative and then obtained a C_{60}-containing polyester or polyurethane by polycondensation (Scheme 3). Because of the large steric hindrance of the C_{60} moiety, the degree of polymerization was very low.

Using different strategies, Geckeler and Hirsch prepared the first true side-chain fullerene polymers [27]. In order to overcome the influence of steric hinderance of the C_{60} moiety on the polymer molecular weight, they prepared the amino-polymer first, and then reacted this polymer with fullerene to obtain the side-chain fullerene polymer (Scheme 4). A similar method was used to synthesize fullerene-based polymers by covalently attaching fullerenes to amine-containing hydrocarbon polymers [28]. Some of these polymers are readily soluble in hexane or tetrahydrofuran (THF), although fullerene itself is essentially insoluble. Water-soluble fullerene polymer can also be prepared by this method [29]. In the reaction of an amine group with fullerene, control of reaction conditions is essential to avoid the formation of insoluble polymer, because C_{60} easily forms multi-addition products. Using different synthesis strategies, Hawker prepared a linear polymer with pendent C_{60} moieties by nitrogen bridging [30] (Scheme 5). In this kind of polymer, the content of C_{60} could be

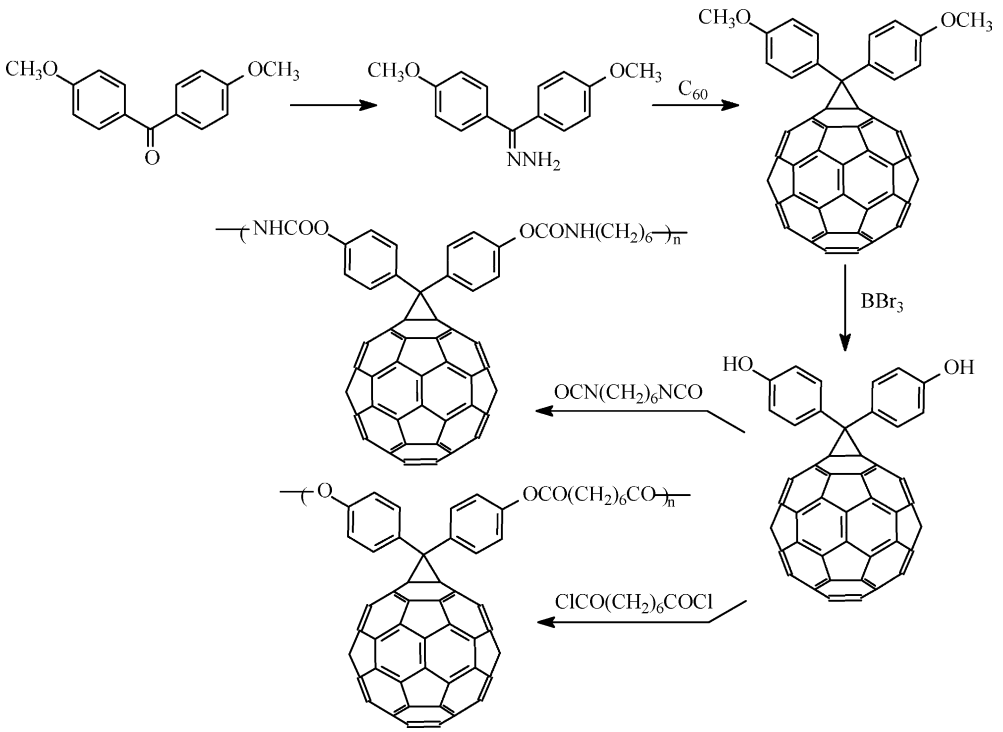

Scheme 3. Polyester and polyurethane derivatives of C_{60} [26].

controlled by using the azidomethyl units in preformed polymer. Because the azide group is easily introduced in the polymer chain and its reaction with C_{60} can be well controlled, this method has been widely used [31–35]. For example, using group-transfer polymerization, allyl methacrylate and methyl methacrylate (or *n*-butyl methacrylate) copolymer were synthesized [32]; then the pendant allyl

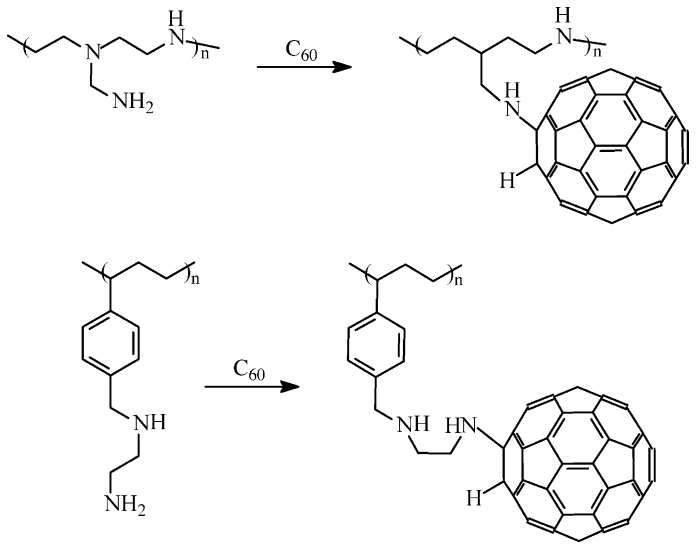

Scheme 4. Soluble macromolecular fullerenes obtained by covalent binding of C_{60} to amino polymers [27].

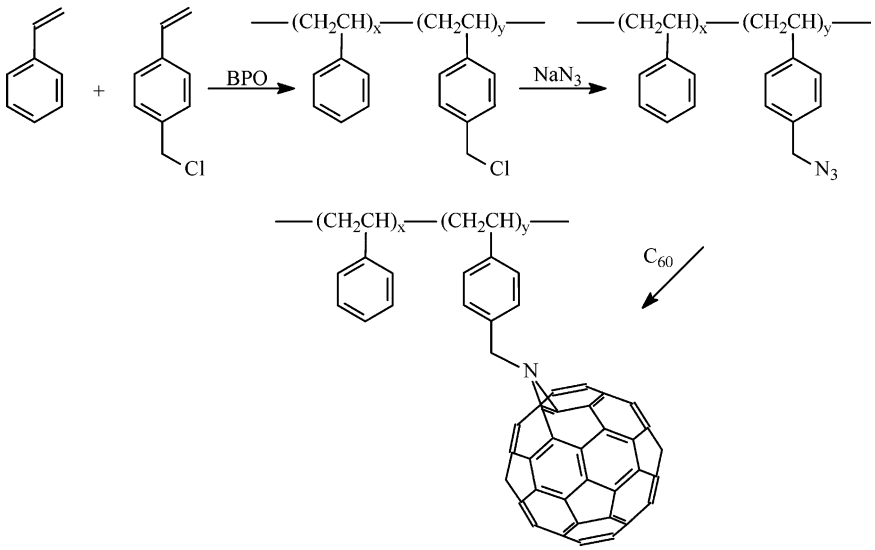

Scheme 5. Reaction of C_{60} with azido-functional polymer [30].

groups in the copolymers were hydrobrominated, followed by reaction with sodium azide; and finally fullerene was incorporated via an addition reaction (Scheme 6). The resulting fullerene-containing poly (alkyl methacrylate)s have fairly narrow polydispersities. Another interesting side-chain fullerene polymer (C_{60}-PHEMA) was synthesized by Goh et al. [33] by Hawker's method [30] (Scheme 7). These polymers had varying C_{60} content. Goh et al. found that C_{60} content greatly influences solubility of the final product. When C_{60} content is higher than 3.2 wt%, the solubility of the polymer in most organic solvents is limited.

Using the reaction of the azide group with fullerene, fullerene-containing monomers can also be prepared. Sato et al. [21] prepared methacrylate monomers (Scheme 8) containing fullerene. These monomers were copolymerized with *t*-butyl

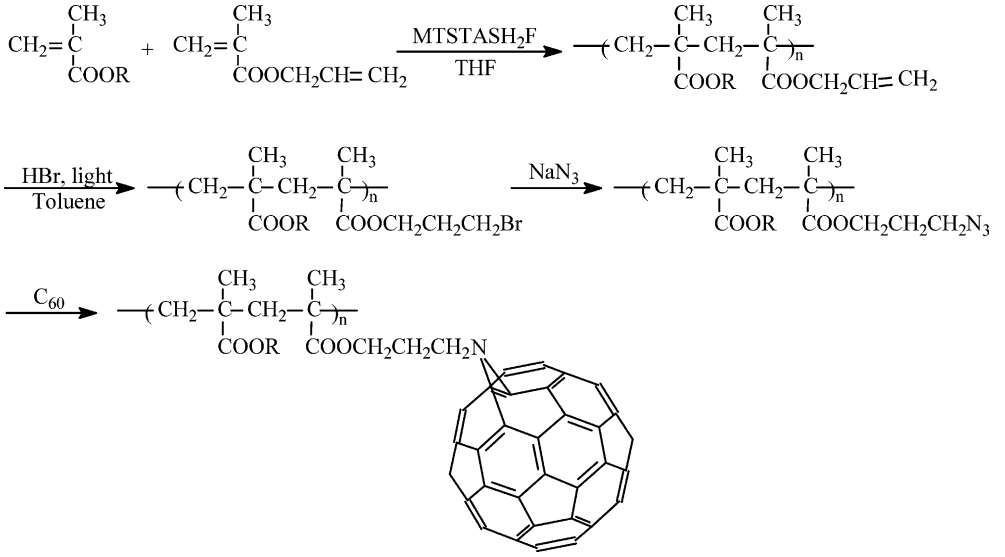

Scheme 6. Synthesis of C_{60}-containing poly(alkyl methacrylate) [32].

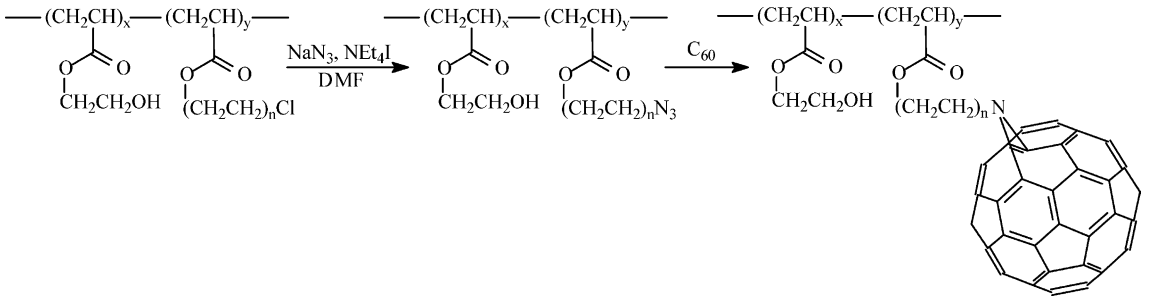

Scheme 7. Synthesis of C_{60}-containing polymethyacrylate [33].

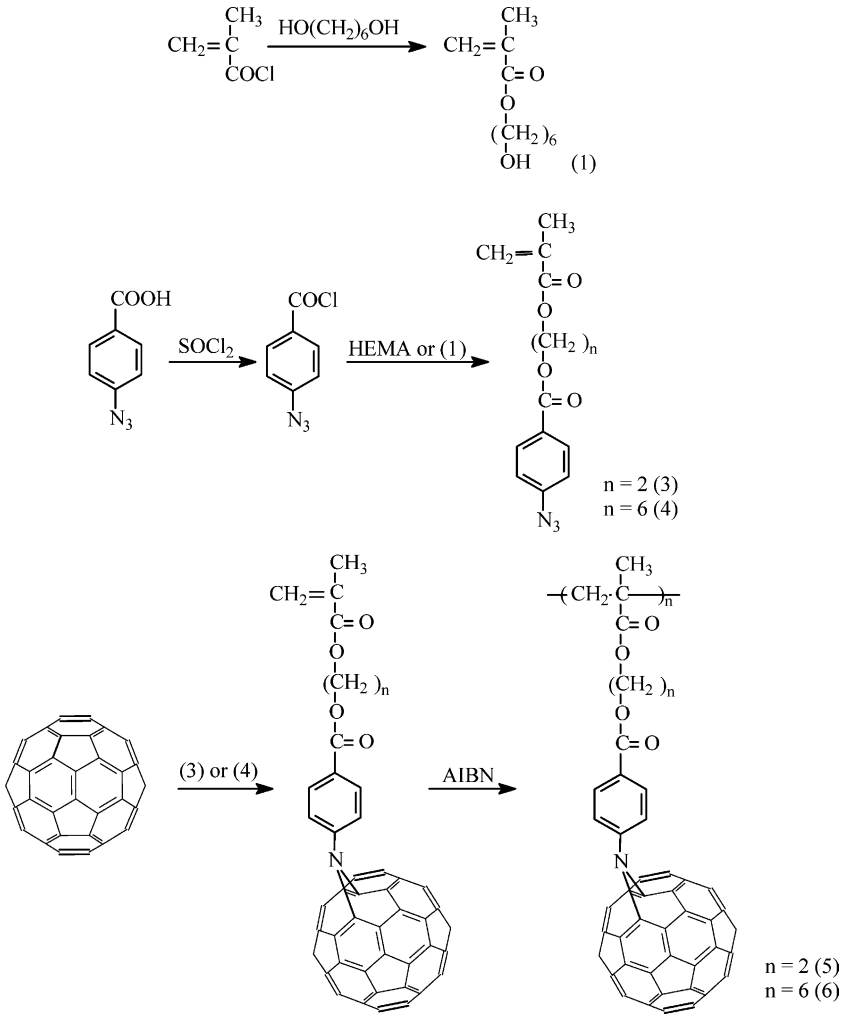

Scheme 8. Synthesis of C_{60}-containing polymer from azido-C_{60} monomer [34].

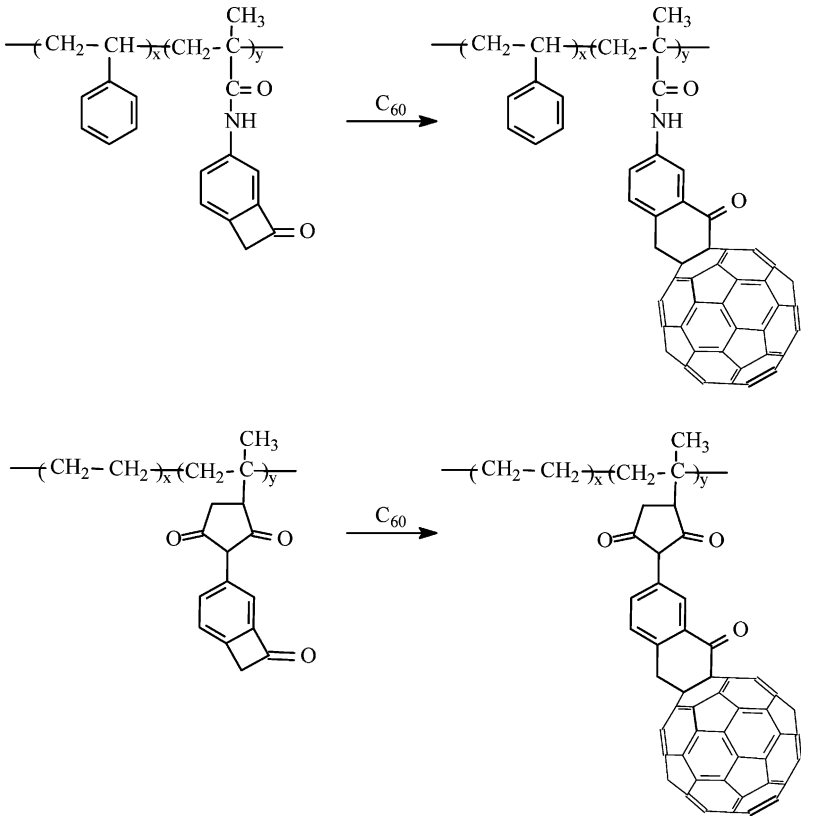

Scheme 9. Synthesis of C_{60}-containing polymer from BCBO monomer [36].

methacrylate by radical polymerization giving a copolymer with the fullerene moieties in the side chains. Because fullerene can terminate the free radical of the initiator, the structure with fullerene moieties in the side chains shown in Scheme 8 will not be completely realized.

The cycloaddition reaction is another important method for preparing side-chain fullerene polymers. The C_{60}-containing polymers are readily obtained from the reaction of benzocyclobutenone (BCBO)-PSt and C_{60} in refluxing 1,2-dichlorobenzene (Scheme 9) [36]. Experimental results show that incorporation of C_{60} into vinyl polymers based on the unique cycloaddition reaction of BCBO with C_{60} is nearly quantitative, and the copolymerizability of BCBO monomer with a wide range of vinyl monomers allows for the preparation of a variety of BCBO-containing polymers and, further, for C_{60}-containing polymers. The amount of C_{60} present in a polymer is dictated by its BCBO content, which can be easily controlled through copolymerization or grafting. Using the same reaction, fullerene can also be introduced into the side chain of poly(dimethylsiloxane) [37] to give polymers with excellent film-forming properties.

Fullerenated polycarbonates ($TCNEOC_{60}$-PCs) can be prepared by direct reaction of TCNEO-C_{60} with PC using $AlCl_3$ as a catalyst (Scheme 10) [38,39]. The studies cited showed that the electron-accepting ability of $TCNEOC_{60}$ is stronger than that of C_{60}, and $TCNEOC_{60}$-PCs limit 532 nm optical pulses more effectively than C_{60}-PCs. This suggests that increasing the electron-accepting ability of fullerene will generally be effective in improving the optical limiting properties of fullerene polymers. The fullerenated PCs had good thermal stability, and the glass transition temperatures (T_g) of the $TCNEOC_{60}$-PCs were about 20–30 °C lower than that of the starting PCs (148.5 °C). Interestingly, a linear relationship between the feed ratio and the

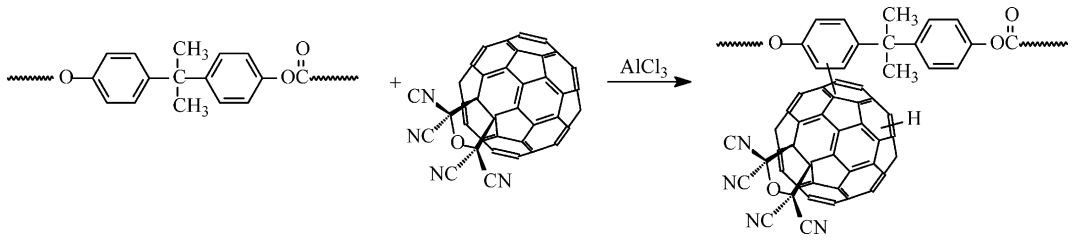

Scheme 10. Synthesis of polycarbonate containing a C_{60} derivative [38].

fullerene content was found for the fullerenation of polycarbonate. Similarly, C_{60} can be incorporated directly into uncrosslinked polystyrene by $AlCl_3$ catalysis, as reported by Liu et al. [40], who prepared C_{60}–PS polymers by Friedel–Crafts reactions.

Conjugated polymer-fullerene composites show very good photoconductivity [11]. The attachment of a fullerene moiety to the conducting polymer backbone is a very important result, since it can be expected to lead to new photoconductive materials with more intimate association of donor/acceptor sites. The attachment of fullerenes onto polythiophene derivatives was explored by Ferraris et al. [35] and Zhang [41] (Scheme 11). In these studies, soluble conjugated copolymers were reported, where a polythiophene main chain is substituted with solubilizing side chains and fullerene side groups. The covalent attachment of fullerene derivatives in substituted polythiophenes leads to good processing properties for polymer photodiodes. The inclusion of

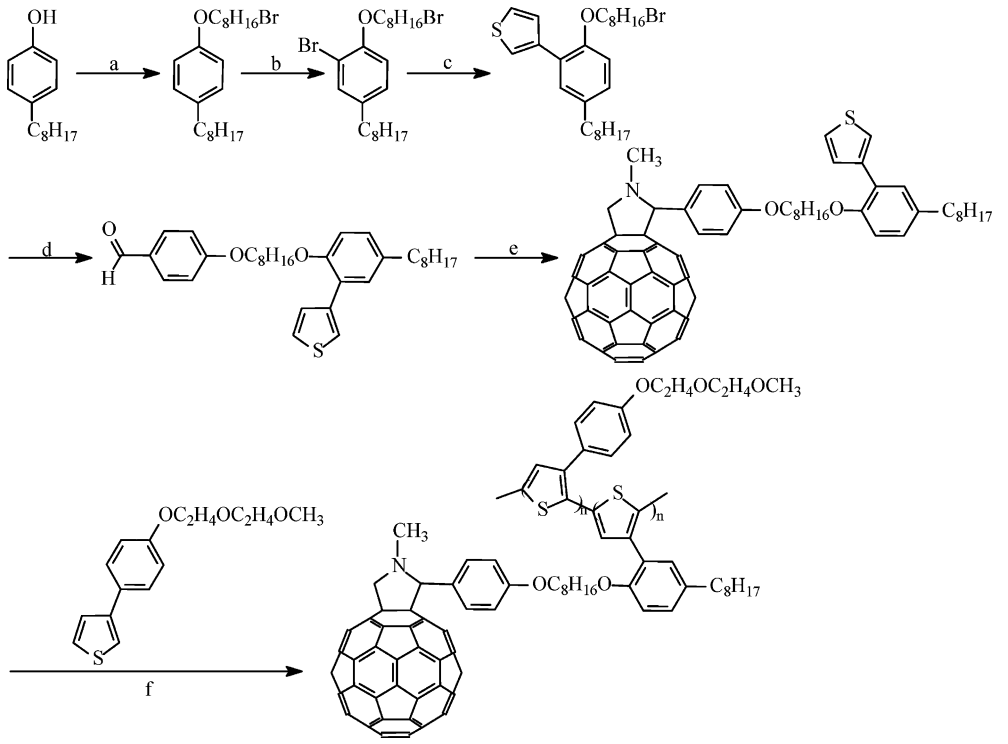

Scheme 11. Synthesis of C_{60} modified polythiophene copolymers. Reagents, reaction conditions and percent yield: (a) 1,8-dibromooctane, K_2CO_3, 2-butanol, reflux, 24 h, 66%; (b) *N*-bromosuccinimide (NBS), dimethylformamide (DMF), 20 h, RT, 94%; (c) 3-thiophene boronic acid, tetrakis(triphenylphosphine) palladium(0), $NaHCO_3$ (1 M), DMF, reflux, 10 h, 40%; (d) 4-hydroxybenzaldehyde, K_2CO_3, acetone, reflux, 36 h, 80%; (e) *N*-methylglycine, C_{60}, chlorobenzene, reflux, 5 h, 52%; (f) $FeCl_3$ (1:6) (0.05 M), chloroform, 5 h [41].

side-chain bonded fullerenes does not prevent the ordering of the polythiophene main chain at low concentrations. The organization of the polymer is not seriously disturbed even at 14 mol% fullerene in side chains, and the polymer chains are sufficiently mobile to accommodate geometric relaxation upon treatment with chloroform vapor. Rectifying junctions are found in thin film photodiodes, but only after illumination does the photovoltage increase to appreciable values. External quantum efficiencies are moderate, but the spectral coverage can extend to 700 nm in the ordered state of the copolymer. Using different main chains, Ramos et al. [42] prepared a processable π-conjugated polymer with covalently linked methano-fullerenes (Scheme 12). This polymer has very good solubility, and it can be applied via spin coating to form a photoconductive layer. This polymer, led to the first polymer solar cell based on a covalently linked donor–acceptor bulk-heterojunction. Ramos et al. found that photoexcitation of this polymer resulted in an electron-transfer reaction from the conjugated backbone to the pendant C_{60} moiety. These results indicate that a bicontinuous network of donor and acceptors, confined to a molecular scale, is an attractive approach to new materials for photovoltaic applications PPV-based C_{60}-containing, conjugated polymers, partly soluble in common organic solvents, have also been prepared in our laboratory [43–45]. A typical synthesis method is shown in Scheme 13 [44]. The polymers contained various percentages of C_{60}. CV analysis showed that the electronic characteristics were retained despite covalent attachment of C_{60} to the polymer by the cycloaddition reaction. Excited-state properties of PPV-AFCAR were investigated by steady-state spectroscopy and lifetime measurements [45]. After photoexcitation, photoinduced energy transfer from the oligomer chain to the pendant moiety occurred to a large extent, but a charge-separation process did not occur.

Another route to soluble fullerenated polymers by reacting carbanions on polymer chains with fullerenes was suggested by Chen et al. [46–48]. This method of adding C_{60} to a carbanion-containing polymer chain, such as polystyrene, poly(bromostyrene) and poly (vinylbenzylchloride), begins with an organometalic reaction (Scheme 14). Both the stereo electronic effect and the steric hindrance of C_{60} have been reported to have significant influences on the structure and physical properties of these polymers. Using carbanions on a polymer chain, Dai et al. [49,50] successfully attached C_{60} to 1,4-polydiene chains with fullerene buckyballs as the pendant groups

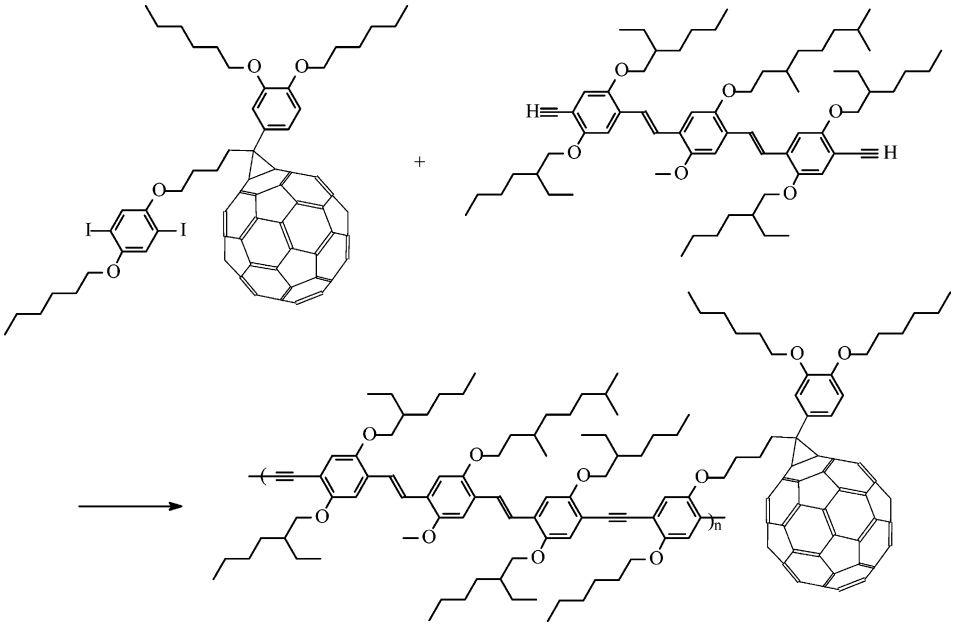

Scheme 12. Synthesis of conjugated polymer with pendent C_{60} [42].

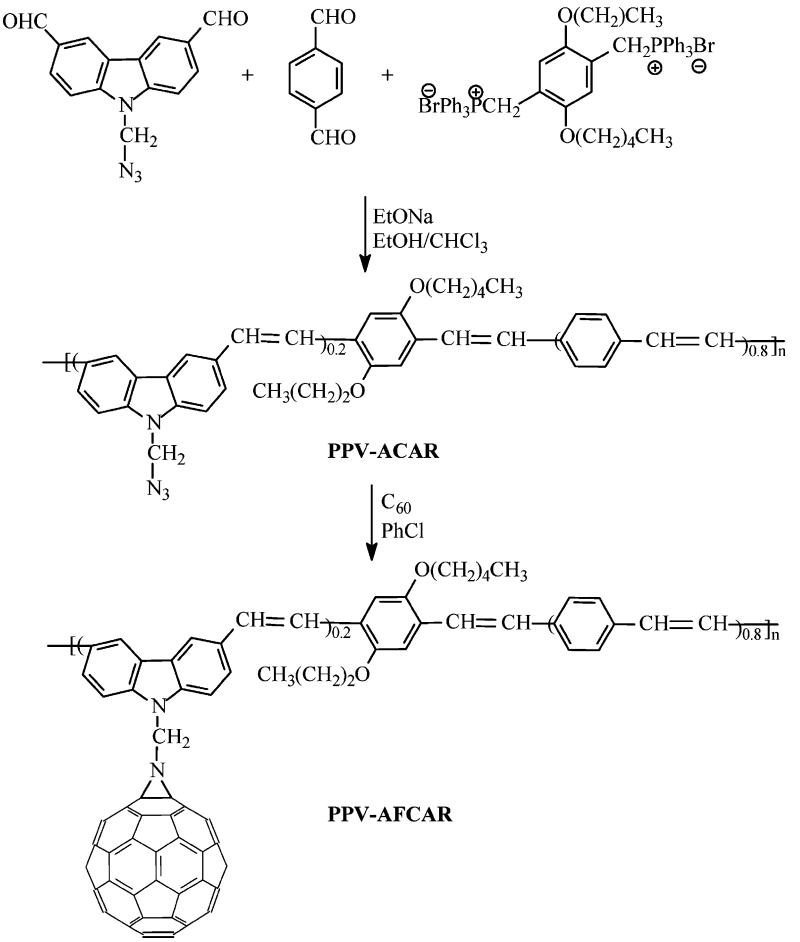

Scheme 13. Synthesis of C_{60}-containing conjugated PPV copolymer [44].

(Scheme 15). As shown in Scheme 15, the grafting reaction involves lithiation of polydiene chains with *sec*-BuLi in the presence of tetramethyl-ethylenediamine (TMEDA), followed by addition of C_{60} onto the lithiated living polydiene chains. The solubility of the resultant C_{60}-functionalized polydiene chains can be varied by changing the molar ratio [*sec*-BuLi]/[C_{60}]. For instance, the C_{60}-grafted polydiene materials with [*sec*-BuLi]/[C_{60}] < 1 are highly soluble in most common organic solvents owing largely to the

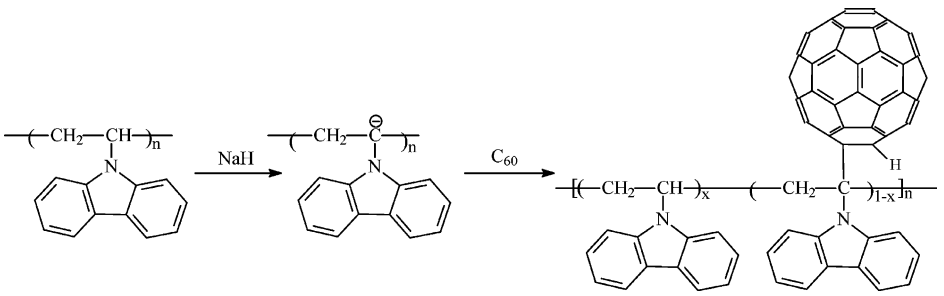

Scheme 14. Reaction of C_{60} with poly(*N*-vinylcarbazole) (PVK) [47].

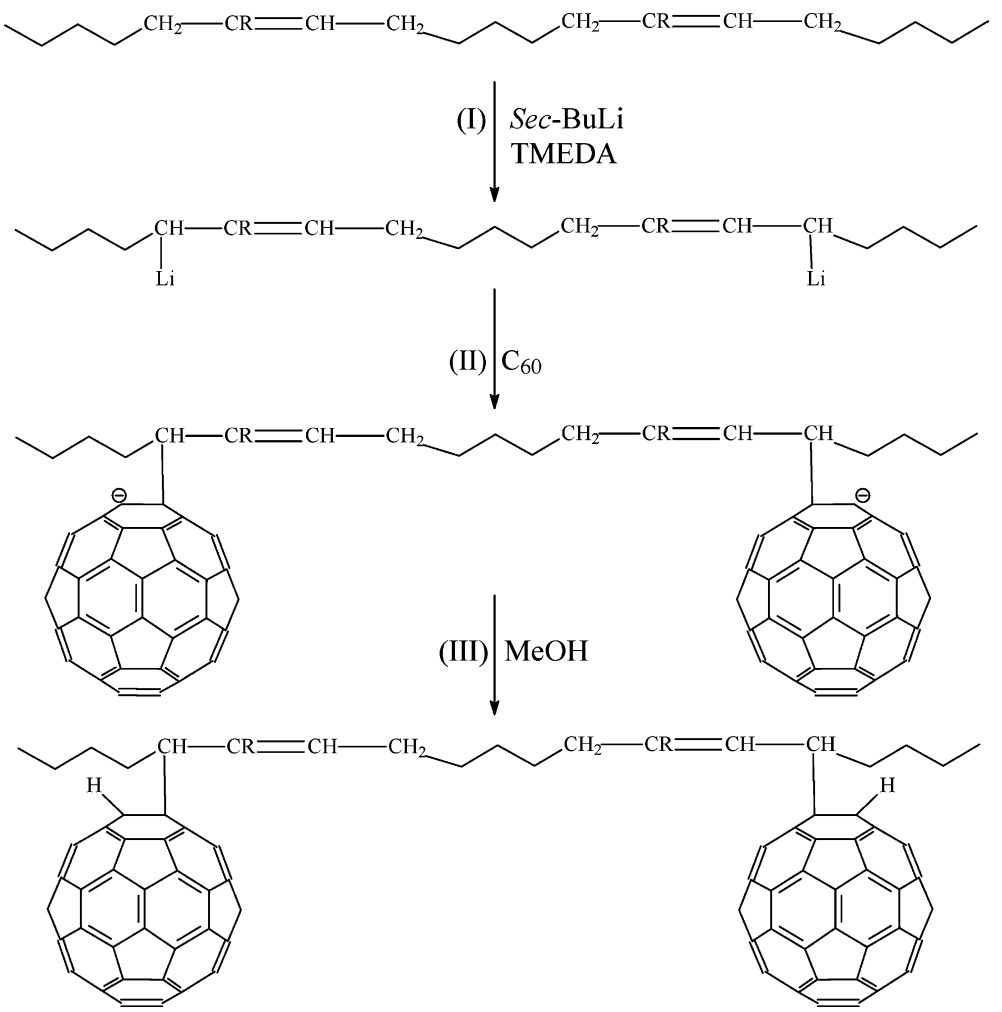

Scheme 15. Covalent grafting of C_{60} onto polydiene chains [49].

monoaddition of C_{60}, whereas fullerene crosslinked polymer gels are observed at high molar ratio of *sec*-BuLi to C_{60} (i.e. [*sec*-BuLi]/[C_{60}] > 1) [46]. Differential scanning calorimetric (DSC) analyses on the soluble material indicate that the chain rigidity of the polydienes increases slightly upon grafting with C_{60}, but the final product remains thermally processable. The unconjugated polydiene segments between two adjacent C_{60} pendant groups in the C_{60}-grafted polydiene chains could be converted into a conjugated structure by an I_2-induced conjugation reaction [51–53].

The first hydrogen-bonded fullerene supramolecular structure from a side-chain fullerene derivative was prepared by Sanchez et al. (Scheme 16) [54]. Interestingly, the chemical integrity of the monomeric moiety, its redox and UV/Vis behavior, is fully preserved in the highly dynamic polymeric state.

2.3. Main-chain fullerene polymers

The first main-chain fullerene polymer was prepared by Benincori et al. [55] via electrochemical polymerization. Subsequently, many papers have been published on such polymers [56–60]. A well-defined main-chain fullerene polymer was prepared by Okamura et al. [57]. Using the reaction of C_{60} with the polystyryl radical, they obtained a well-defined

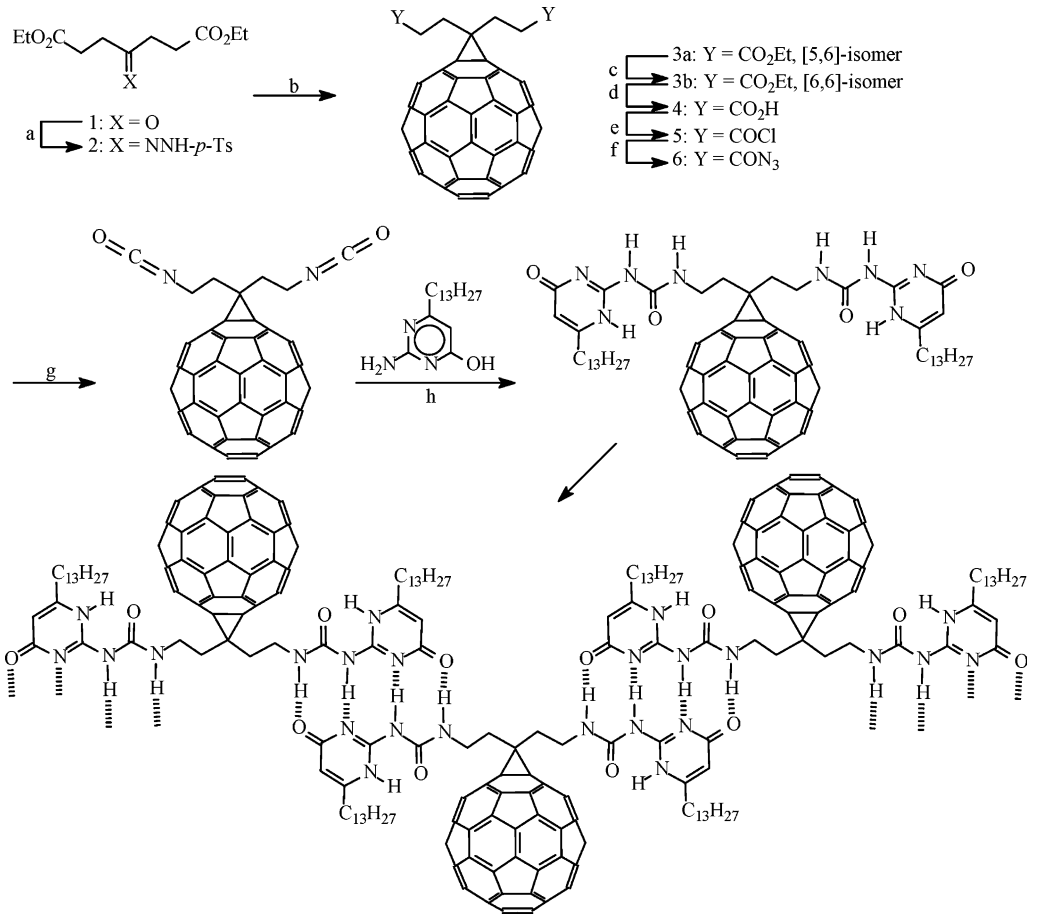

Scheme 16. Synthesis of hydrogen-bonded fullerene supramolecular polymer. Reagents, reaction condition and percent yield: (a) *p*-$TsNHNH_2$, EtOH, overnight, △, 85%; (b) NaOMe, py, 30 min, RT; then C_{60} in ODCB, 80 °C, 16 h; (c) ODCB, 500 W flood lamp, RT, overnight, 49% (b + c); (d) ODCB, AcOH, HCl, H_2O, △, overnight, 83%; (e) $SOCl_2$, 1 h; (f + g) NaN_3, ODCB,Me2NCOMe, 75 °C, 30 min; (h) 2-amino-4-hydroxy-6-tridecylpyrimidine, py, 100 °C, overnight, 43% (e–h); Ts: tosyl, py: pyridene, Ac: acetyl [54].

polymer derivatives of C_{60} from a narrow-polydispersity polystyryl adduct terminated with TEMPO (PS-TEMPO) (Scheme 17), where TEMPO is 2,2,6,6-tetramethylpiperidinyl-1-oxy. They heated PS-TEMPO, which was prepared by nitroxyl-mediated 'living' radical polymerization, with C_{60} in *o*-dichlorobenzene at 145 °C. The C_{60} derivatives thus obtained in 60–80% yield were found to be predominantly 1,4-dipolystyryldihydrofullerenes. The selective production of the bis-adducts in these systems was suggested to be due to a fourfold excess of C_{60} relative to PS-TEMPO in the feed and/or the potential barrier of the PS moieties of the bis-adducts that restricts further addition of PS radicals to the C_{60} moiety. Instability of the C_{60}-TEMPO and C_{60} dimers at high temperature might be another reason for the bis-adduct selectivity. The bisubstituted derivatives retained the redox properties of original C_{60}. C_{60} reacted with bis-anthracene by Diels–Alder cycloaddition to give a fullerene based copolymer [58]. The addition is fully reversible upon heating to 75 °C, providing a fully thermoreversible polymer. This example shows that this type of fullerene polymer could be used in applications requiring a recyclable and thermally processable.

The first true main-chain fullerene polymer was synthesized by Taki et al. [59]. C_{60} bisphenol was allowed to react with an equimolar amount of dibasic

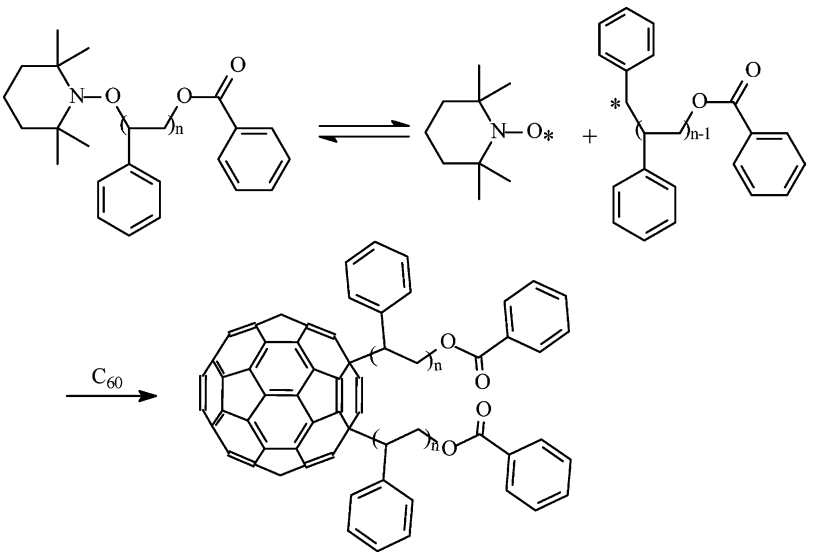

Scheme 17. Synthesis procedure of dipolystyryldihydrofullerenes [57].

acid dichloride at room temperature to afford linear polyesters containing the fullerene moiety in the main chain. Similarly, C_{60} pearl-necklace polymer, poly(4,49-carbonylbisphenylene-*trans*-2-fullerenobisacetamide), was synthesized by a direct polycondensation of *trans*-2-fullerenobisacetic acid with 4,49-diaminobenzophenone in the presence of large excess of triphenyl phosphite and pyridine (Scheme 18) [60]. In these polymers, fullerene 'pearls' and diamine linkers were attached to each other by methanocarbonyl connectors. The molecular weight M_w of the polymer was about 4.5×10^4 on the basis of TOF-MS. Another reactive fullerene polymer allowed the incorporation of fullerene units into the polymer backbone of polysiloxanes (Scheme 19) [37]. These polymers show excellent solubility in common solvents and high thermal stability up to about 435 °C. Moreover, the polymers possess good film-forming properties on nonpolar surfaces, which is an important property for many applications. For example, doping of conjugated polymers in photovoltaic cells with fullerenes or fullerene adducts results in dramatically increased quantum yields [61–63].

2.4. Fullerodendrimers

Owing to the capability of dendritic architectures to generate specific properties, dendrimers are attracting increased attention. Fullerenes possess electronic and photophysical properties which make them natural candidates for the preparation of functional

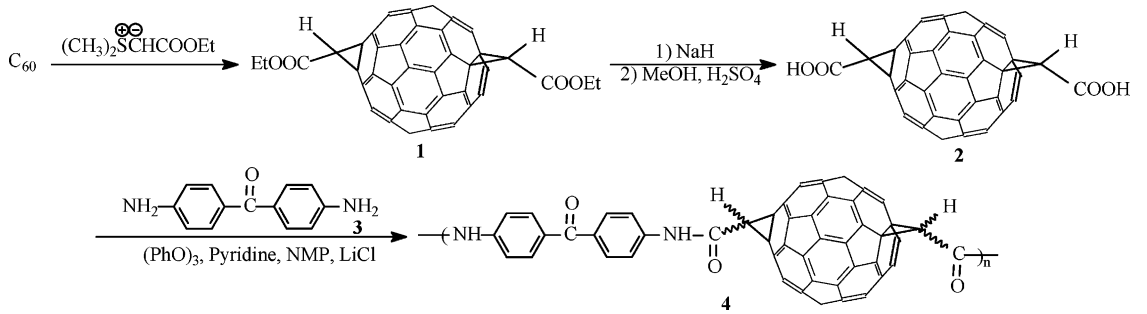

Scheme 18. Preparation of C_{60} pearl-necklace polymer [60].

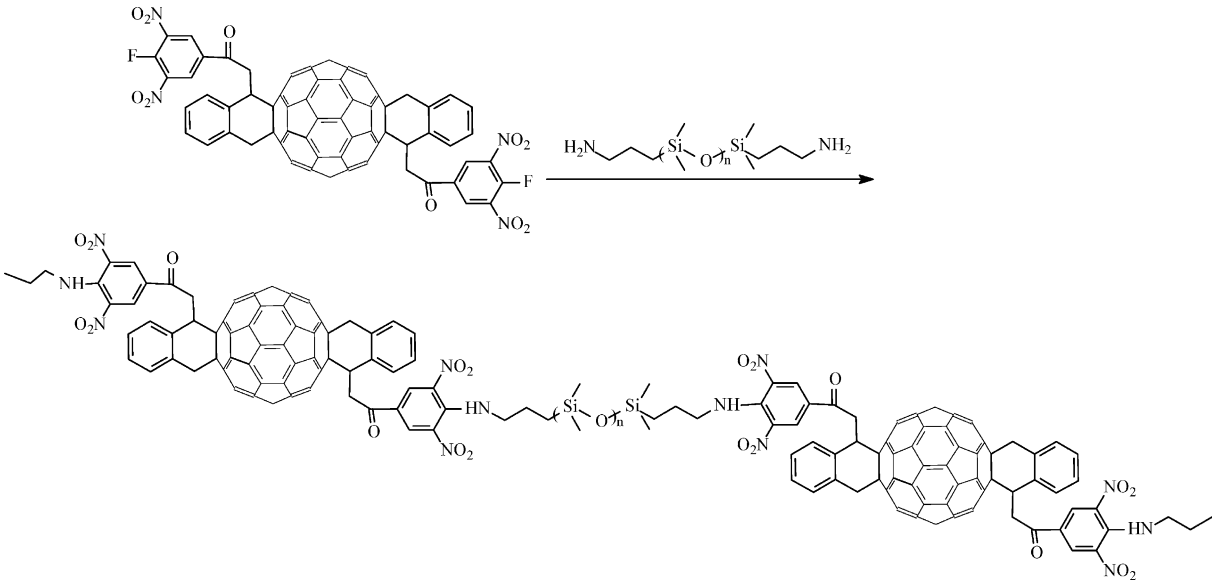

Scheme 19. Synthesis of C_{60}-containing polysilicone [37].

dendrimers. For example, a dendritic framework can surround active core molecules. Thus a dendritic shell can encapsulate a functional core moiety and to create a specific site-isolated microenvironment capable of affecting molecular properties [64]. A variety of experimental techniques have been employed to appraise the effect of shielding the core moiety by the dendritic shell [64,65]. Dendrimers with a fullerene core appear to be appealing candidates to evidence such effects. Effectively, the lifetime of the first triplet excited state of fullerene derivatives is sensitive to the solvent [66]. Therefore, lifetime measurements in different solvents can be used to evaluate the degree of isolation of the central C_{60} moiety from external contacts. A steady increase of lifetimes is found by increasing the dendrimer size in all solvents, suggesting that the dendritic wedges are able to shield, at least partially, the fullerene core from external contacts with the solvent and from quenchers such as molecular oxygen [67]. Furthermore, dendrimers can be used as traps for small molecules or ions with the aim of releasing them where needed (e.g. in biological tissues) [68].

Wooley et al. [69] prepared dendritic fullerene by attachment of poly(aryl ether)-based dendrimer to phenol-functionalized fullerenes (Scheme 20). The benzylic bromide moiety of the fourth-generation dendrimer reacts with the phenolic groups attached to fullerene, and thus two dendrimer building blocks couple with one fullerene to give the fullerene-based dendrimer. Using the cycloaddition reaction of azides with fullerenes, Wooley et al. prepared a new type of fullerodendrimer based on the benzylic bromide moiety of the fourth-generation dendrimer, as above [70]. The final products contained mono- and bi-addition products, but no higher addition products. The failure to obtain tri- or multisubstitution may be due to steric hindrance around the C_{60} nucleus and/or unfavorable electronic conditions after the bi-addition. Rio et al. [71] used a poly(aryl ether) dendrimer to obtain a series of fullerodendrimers (Scheme 21). Systematic changes in the photophysical properties in the series suggest increasing interaction between the poly(aryl ether) dendritic wedges and the fullerene core, which brings about increasing isolation of the central chromophore from the exterior. Rio et al. also incorporated these fullerodendrimers (1–4) into mesoporous silica glasses, and showed that these materials possess efficient optical limiting properties. Recently, Murata et al. [72] synthesized a series of poly(aryl ether) fullerodendrimers, $GnC_{60}H$ ($n \sim 1$–4). All the dendrimers were very soluble in common organic solvents. Electrochemical studies indicated that GnC_{60}^{-} ($n = 1$–4) anions can be electrochemically

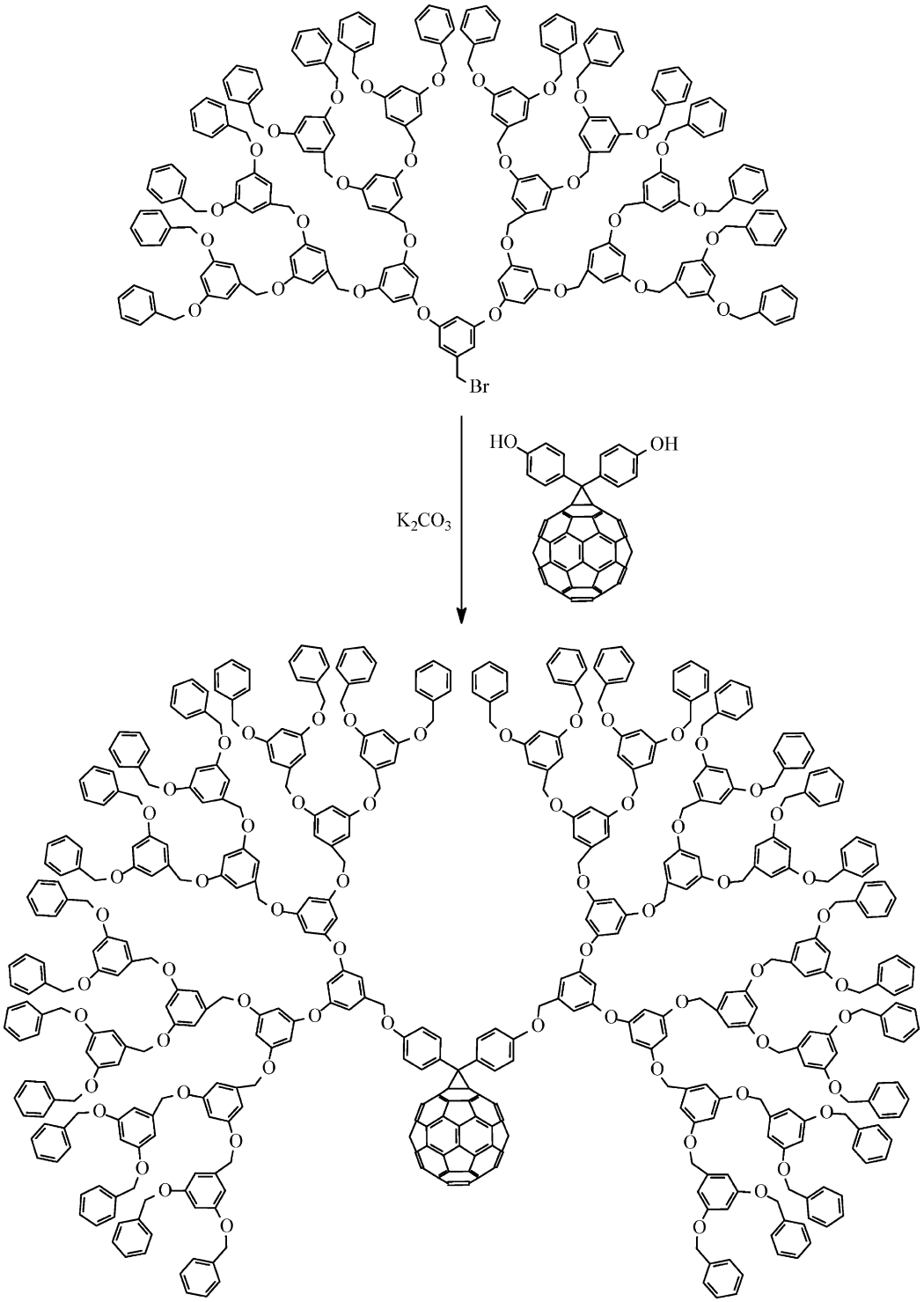

Scheme 20. Synthesis of fullerodendrimer with aromatic polyether dendritic branches [69].

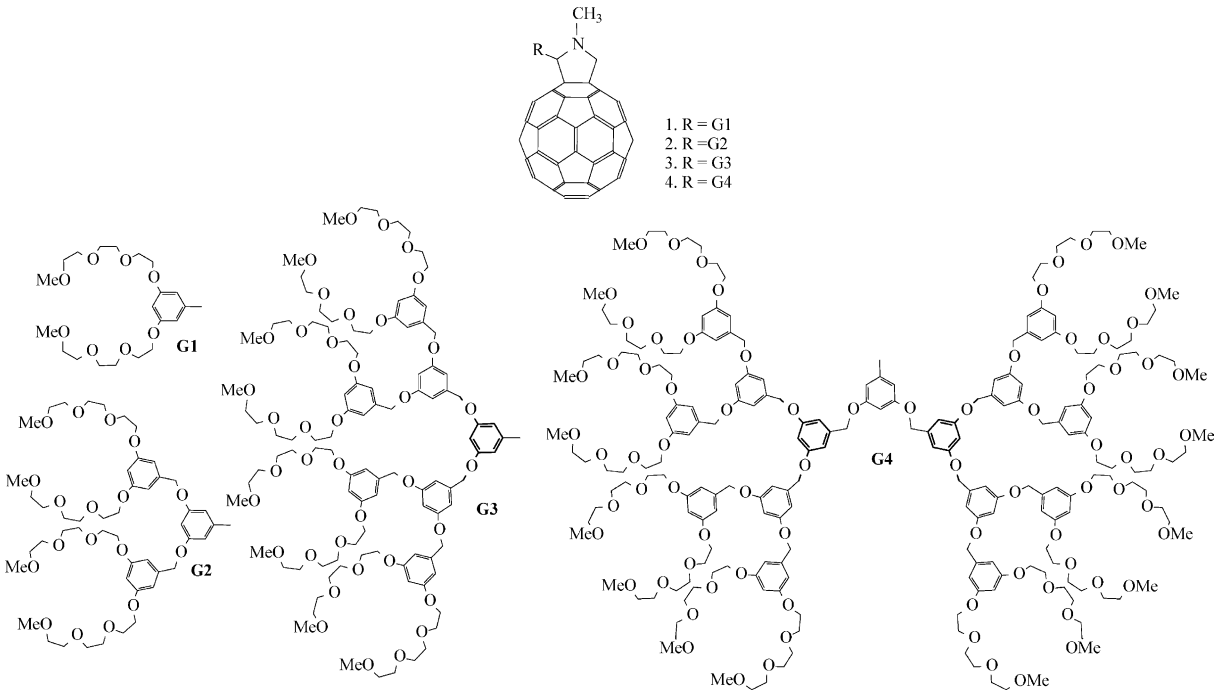

Scheme 21. Fullerodendrimer with poly(aryl ether) dendritic branches [71].

generated and are further reduced to the trianion stage. Anions GnC_{60}^{-} ($n=1$–4) subjected to chemical one-electron oxidation with iodine gave new fullerene dimers carrying a dendrimer unit on each fullerene cage.

A highly water-soluble fullerodendrimer was prepared by Brettreich and Hirsch [73] (Scheme 22). Using electronic absorption spectroscopy, and steady-state and time-resolved fluorescence [74], they studied singlet state fluorescence quenching and found that it originated from the external heavy-atom effect. They prepared another water-soluble fullerodendrimer by a Diels–Alder reaction of C_{60} with an anthryl dendron under extremely mild conditions following the synthesis route in Scheme 23. The results show the anthryl dendron affords a facile, efficient route to the fullerodendrimer. So far most syntheses of fullerodendrimers have been accomplished by means of a Hirsch–Bingel reaction, which requires CBr_4 and DBU as mediator. On the contrary, this approach, which is highly convergent without any reagent, highlights a useful preparation of water-soluble fullerodendrimer under convenient reaction conditions.

A fullerene-containing liquid-crystalline dendrimer was prepared by Dardel et al. (Scheme 24) [75]. This dendrimer showed good solubility in common organic solvents and good thermal stability. It formed an enantiotropic smectic A phase, which was identified by polarized optical microscopy from the observation of typical focal-conic and homeotropic textures. Dardel et al. [76] synthesized another series of liquid-crystalline fillerodendrimers by the addition reaction of mesomorphic malonate-based dendrimers (up to the fourth generation) with C_{60} (Scheme 25) [76]. The cyanobiphenyl unit was used as a liquid-crystalline promoter. The malonates presented nematic and/or smectic A phases. The fullerenes showed only smectic A phases, with the exception of the second generation dendrimer for which smectic A and nematic phases were observed. The supramolecular organization of the fullerene-based molecular units within the smectic A layers was investigated by X-ray diffraction. Two structural regimes were determined. For the low-generation dendrimers, the supramolecular organization is determined by steric factors. For the high-generation dendrimers, the mesogenic groups impose a microphase organization:

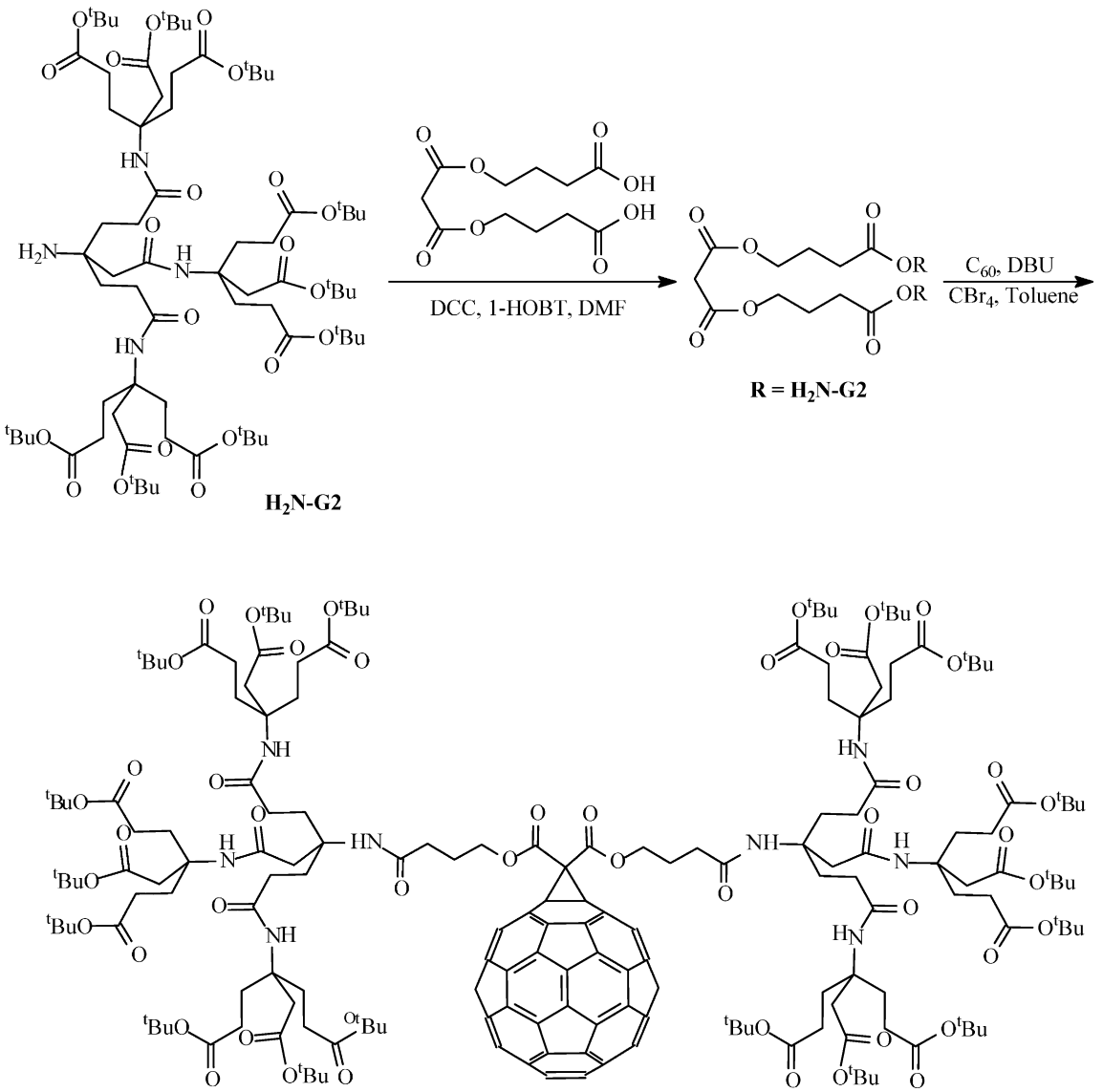

Scheme 22. Synthesis of water-soluble dendrofullerene [73].

owing to lateral extension of the branching part of the molecule, the cyanobiphenyl groups are arranged in parallel fashion as in classical smectic A phases, the rest of the macromolecule being located between the mesogenic sublayers.

2.5. Star-shaped fullerene polymers

Many papers have been published on radical polymerization in the presence of C_{60} [77–80]. A detailed description was given by Chen and Lin [79]. They conducted the radical polymerizations of styrene in the presence of C_{60} at 90 °C in benzene using benzoyl peroxide (BPO) as the initiator. The polymerization process was followed by monitoring BPO concentration, C_{60} content, and polymerization time. It was found that C_{60} acts like a radical absorber which multiply absorbs primary radicals of BPO and the propagating polymer radicals. Therefore, the yield of the polymerization and the molecular weight of

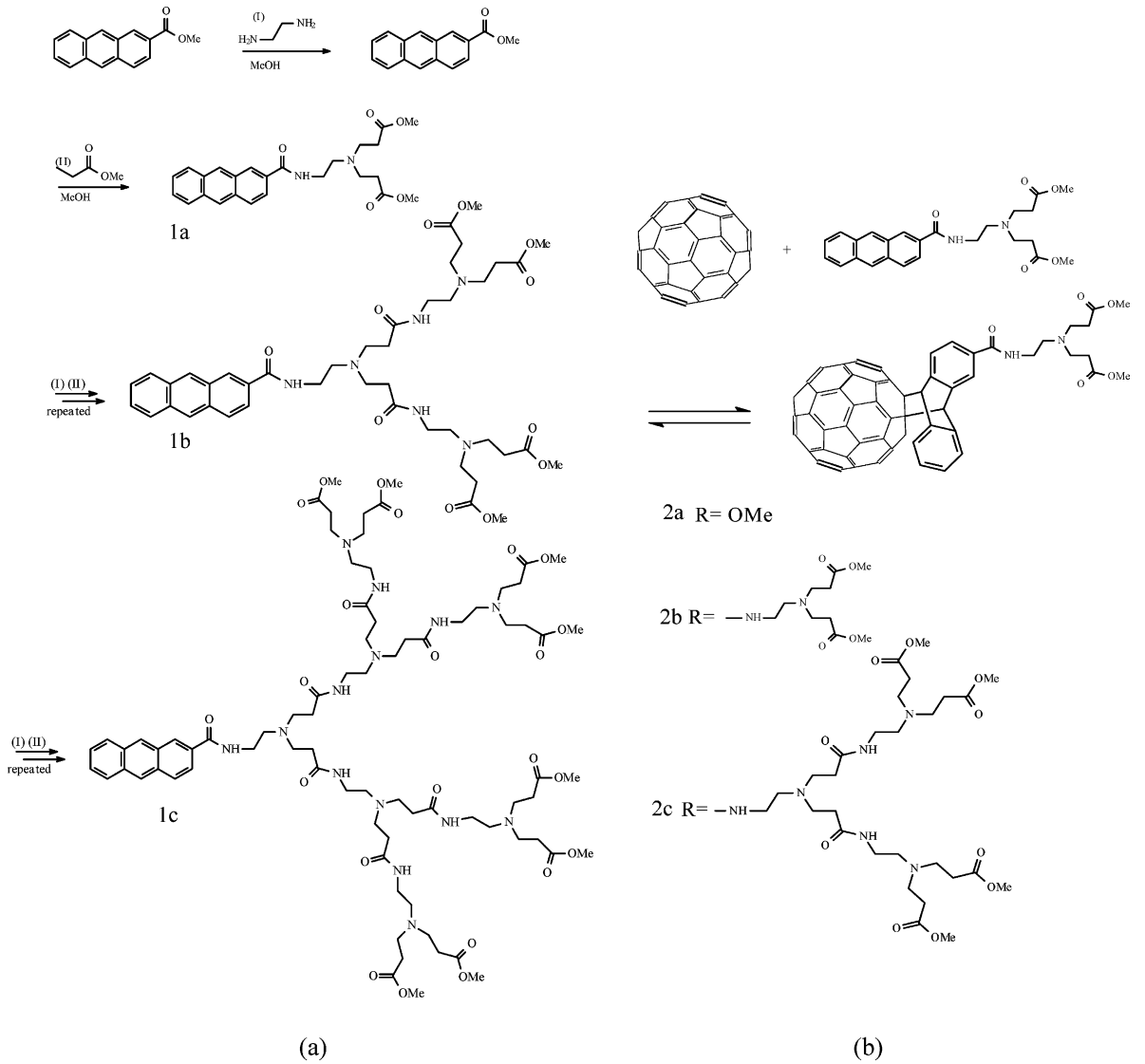

Scheme 23. (1) Synthesis of antryl dendrons (**1a**–**c**); (2) preparation of fulleodendrimer (**2a**–**c**) [74].

the polymer decrease significantly in the presence of C_{60}. However, the molecular weight distribution is narrowed by the coupling characteristics of the reaction. At the beginning of the reaction, chain-propagation is restricted by the radical-absorbing effect of C_{60}. However, the number of polystyrene chains added to C_{60} increases with polymerization time. Direct dilatometric experiments prove that C_{60} acts mainly as an inhibitor for radical polymerization of styrene initiated by BPO. Besides, the glass transition temperature T_g of the copolymers increases with increasing content of C_{60}. The final polymer is usually star-shaped (Scheme 26). Direct fullerenation of polycarbonate (PC), a commercially important optical polymer, can also yield star-shaped fullerene polymers. By simply irradiating a solution of PC and C_{60} at room temperature using a conventional UV lamp, or by warming a C_{60}/PC solution to 60 °C in the presence of AIBN, Tang et al. obtained a series of star-shaped fullerene PC [39] polymers. The extent of

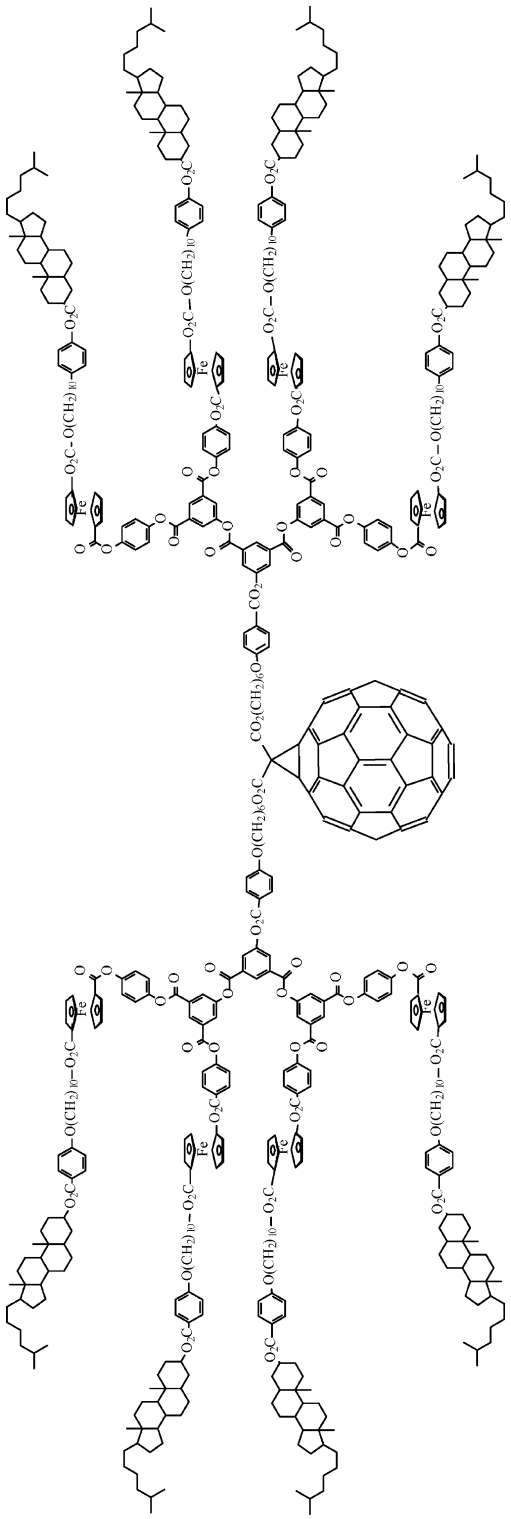

Scheme 24. C_{60}-ferrocene liquid-crystalline dendrimer [75].

fullerenation is controllable by varying the C_{60} feed ratio, and fullerenated PC with C_{60} content as high as 6.3 wt% (more than two C_{60} molecules per PC chain) is readily prepared in almost quantitative yield (99.7%). The molecular weight of the fullerenated PC is higher than that of the parent polymer, suggesting that the fullerenation proceeds by multiple additions to C_{60}, leading to a star-shaped molecule. The fullerenation involves a radical mechanism, and its general applicability to other polymer systems is demonstrated by the attachment of C_{60} to poly(vinyl chloride).

Fullerenols containing multiple hydroxy groups can be used to synthesize urethane-connected polyether star-shaped polymers [81]. Chiang et al. [81] first treated fullerenol with a diisocyanato-urethane polyether, following this by a termination reaction with urethane-connected polyether (Scheme 27). To completely eliminate the crosslinking reaction, they used an excess of the bifunctional isocyanate prepolymer (10 NCO group per each OH group of fullerenol). At the end of the reaction period, the intermediate mixtures were allowed to react further with dodecane-1-ol or 2,2′-dichloroethanol. Comparing the average molecular masses of arm chains (M_n 2600 and M_w 5450, polydispersity 2.11) and of the star-shaped polymer (M_n 18,000 and M_w 26,100, polydispersity 1.45), they found that one fullerenol-based star-shaped polymer contained six linear urethane-connected polymer arms on average. Wang et al. also prepared star-shaped polymers by reacting polyurethane with fullerenol [82]. The polymers exhibited enhanced thermal stability in comparison with the corresponding linear polyurethane and analogous elastomers crosslinked with 1,1,1-tris(hydroxymethyl)ethane.

Addition of living anionic polymers to C_{60} may offer unique opportunities to control the number of grafted chains on the fullerene, such as the molecular mass, and the polydispersity. Ederle and Mathis [83] showed that, when conducted under high-purity conditions, the addition of living anionic polymers can be controlled and used to prepare adducts with well-defined structures. In toluene, star-shaped polymers with up to six branches, from low to high mass, can be produced by using reactive carbanions such as styryl or isoprenyl. The number of additions to C_{60} (three to six) was controlled by stoichiometry. They

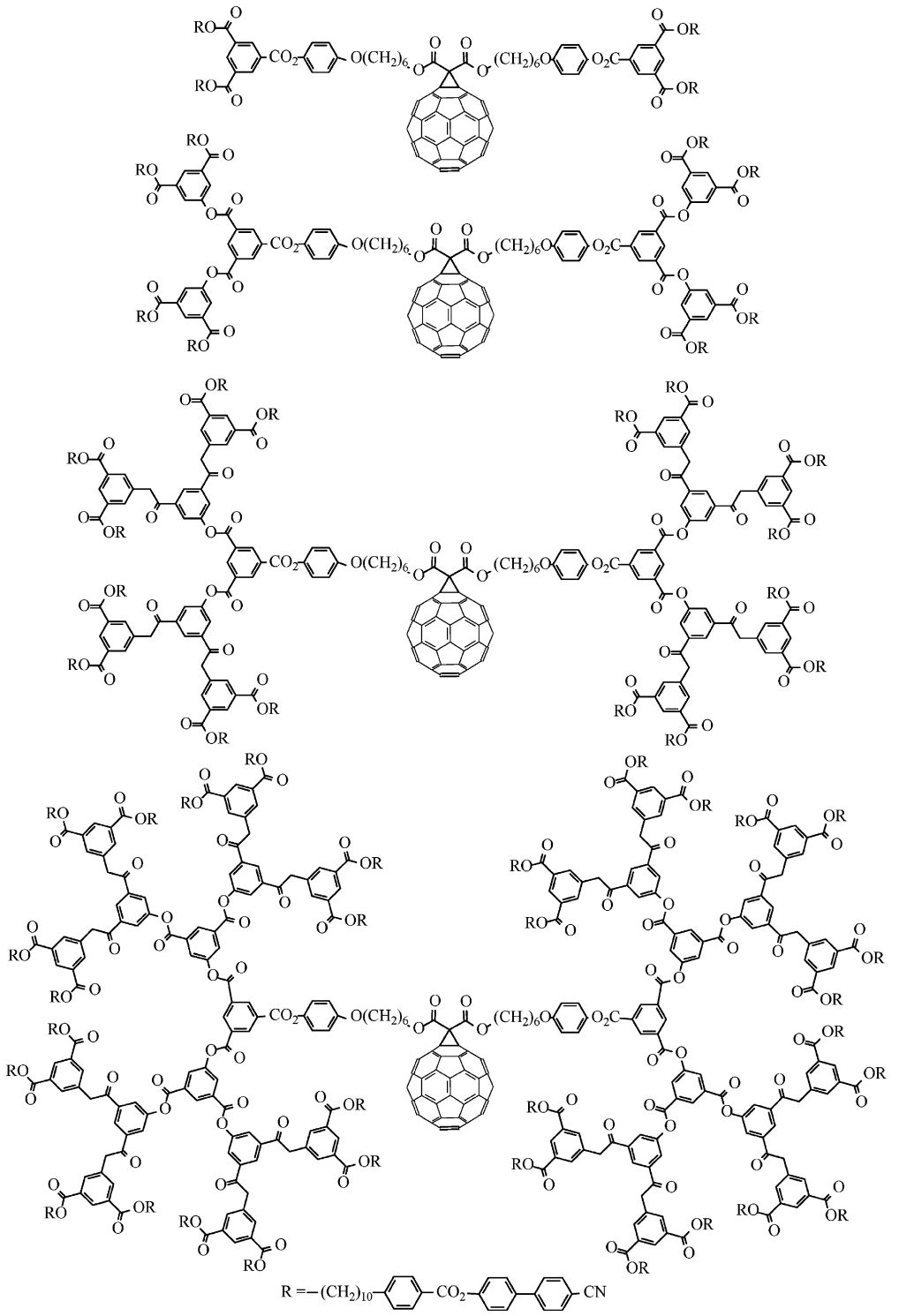

Scheme 25. C_{60}-containing dendrimers [76].

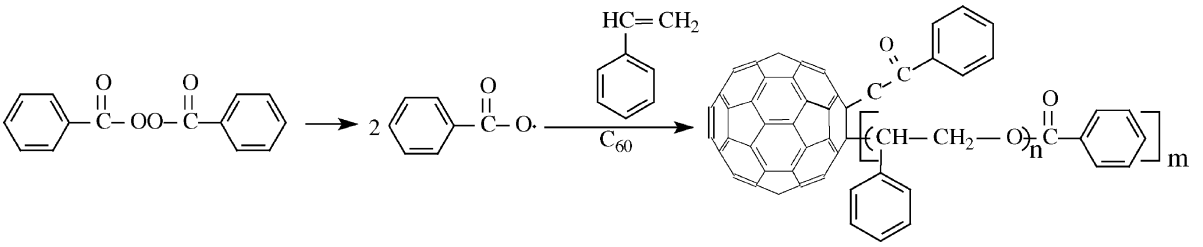

Scheme 26. Polymerization of styrene in the presence of C_{60}.

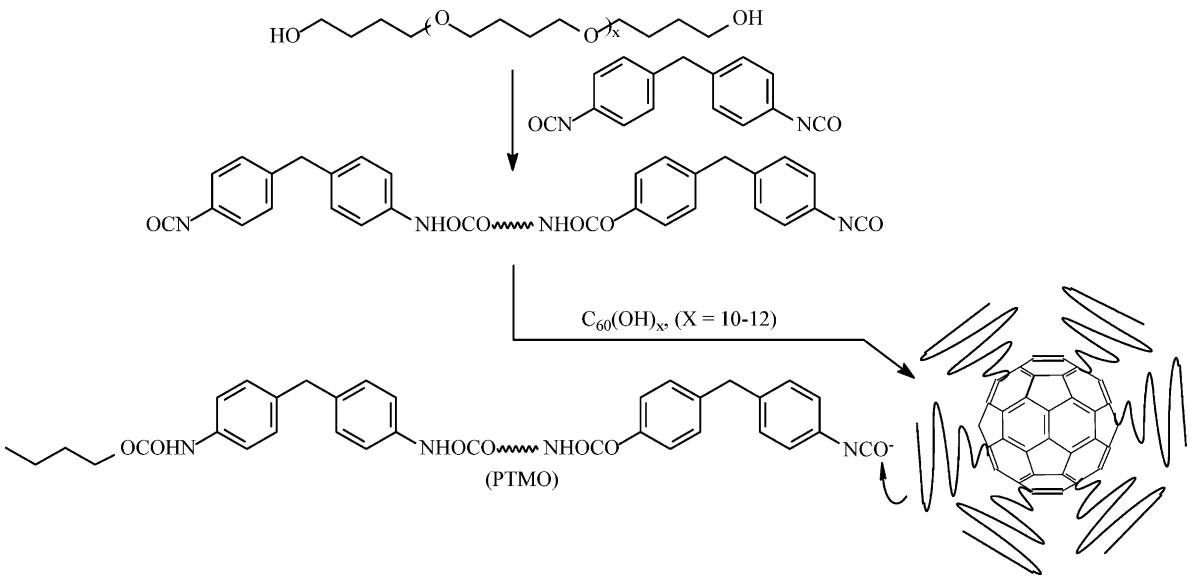

Scheme 27. Fullerenol-derived, urethane connected polyether [65].

also studied the influence of C_{60} anions to initiate living polymerization of PS or PMMA. They found that $C_{60}^{3-}(K^+)_3$ did not initiate polymerization of St or MMA [84] and that C_{60}^{6-} did not initiate polymerization of PS, but did initiate polymerization of MMA. Making the reaction ratio [PSLi]:[C_{60} = 6:1, Mathis and co-workers [85,86] obtained fairly pure star-shaped polymers with six branches and six carbanions located on the fullerene core. Of these six carbanions, only one is able to initiate anionic polymerization of styrene or isoprene to produce well-defined palm-tree-like architectures (Scheme 28a). At the final stage of the reaction, the out-growing chain end bears a carbanion that can be reacted with a coupling agent (dibromo-*p*-xylene or dibromohexane) to produce dumbbell-like structures (Scheme 28b). If C_{60} itself is allowed to react with the living palm tree, a third fullerene molecule is introduced at the center of the macromolecule. Mathis et al. [87] further studied the thermal stability of the bond between the fullerene and a grafted chain. At temperatures around 100 °C, the hexa-adduct is slowly converted into lower-arm adducts; i.e. the experimental results are coherent with a step-by-step mechanism where the six-arm stars are converted to five-arm stars, then to four-arm stars and so on, the kinetic constant decreasing as the functionality of the stars decreases. They also found that the thermal stability of the polymer decreases as the length of the grafts increases. Using the anionic polymerization and appropriate post-linking polymerization, a graft block copolymer chain can be obtained, such as the poly(styrene-*g*-isoprene) chain [88]. Using the same strategy, Mignard et al. [89] prepared two types of hexa-arm star copolymers with

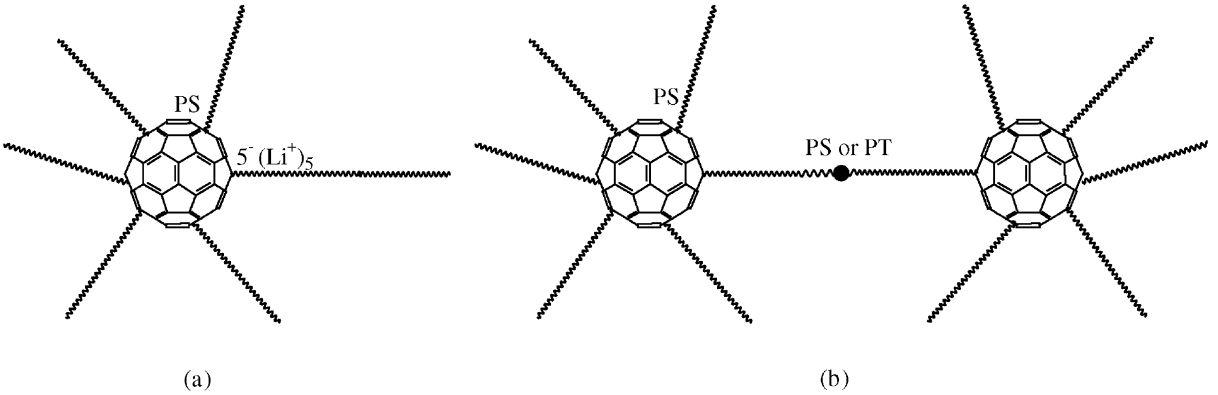

Scheme 28. 'Palm tree' (a) and 'dumbbell' (b) polymers based on C_{60} [85,86].

the aim of obtaining materials with different macroscopic properties. Scheme 29 shows the overall synthetic routes to C_{60}(St-PCHD-PS)$_6$ and C_{60}(St-PPP-PS)$_6$ (six-arm star-shaped polymers). In this reaction, the authors found some benefits from the star-shaped structures: (1) C_{60} was observed to control the limiting number of grafted polymers up to six. (2) The use of a PS 'shell' around the highly conjugated PPP segments enables the polymers to dissolve easily in common organic solvents. The good photoconductivity of these systems may provide a starting point for the design of photovoltaic devices. Anantharaj et al. (Scheme 30) [90] prepared another six-arm star-shaped fullerene polymer from hexanitrofullerene as a precursor. With chemically attached multiple oligoanilines on the C_{60} molecular core, the resulting starburst poly(oligoanilinated) fullerenes exhibit efficient three-dimensional intermolecular electron transport or hopping behavior among doped oligoanilino arms.

Using the living free radical technique (iniferter), He et al. (Scheme 31) [91] synthesized starlike C_{60}-bonding polymers. They used C_{60} with pendent *N*,*N*-diethyldithiocarbamate groups (C_{60}-SR) as a polyfunctional photoiniferter. The photopolymerization proceeded by a living-radical mechanism and gave soluble polyfunctional polymers (photoiniferters). These star-shaped fullerene polymers could be used

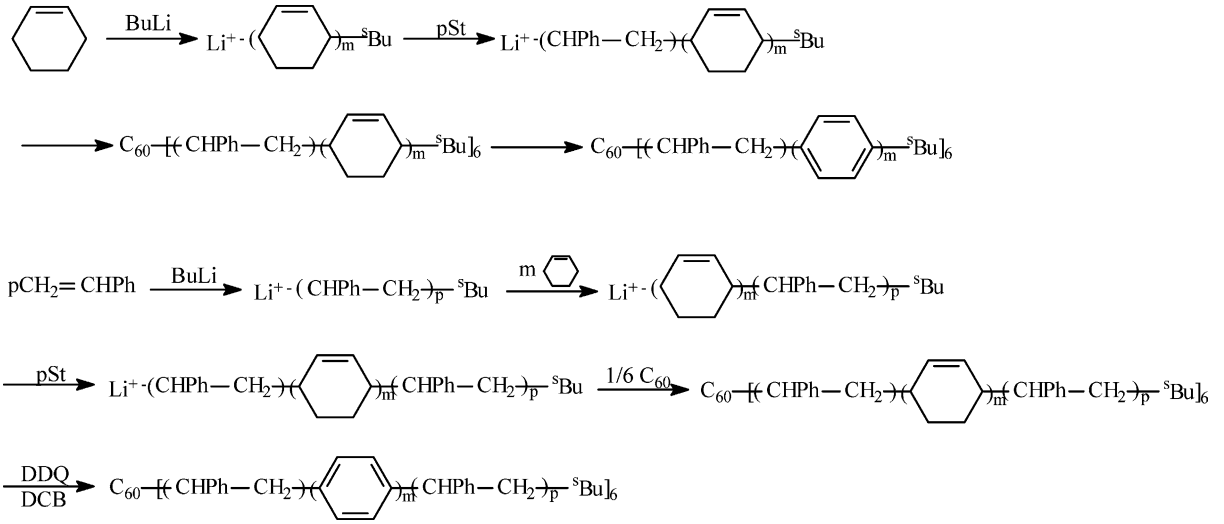

Scheme 29. Overall synthetic routes to 6-*star*-fullerene[styrene-*block*-poly(1,3-cyclohexadiene)-*block*-polystyrene], C_{60}(St-PCHD-PS)$_6$, and 6-*star*-fullerene[styrene-*block*-poly(1,4-phenylene)-*block*-polystyrene] C_{60}(St-PPP-PS)$_6$ [89].

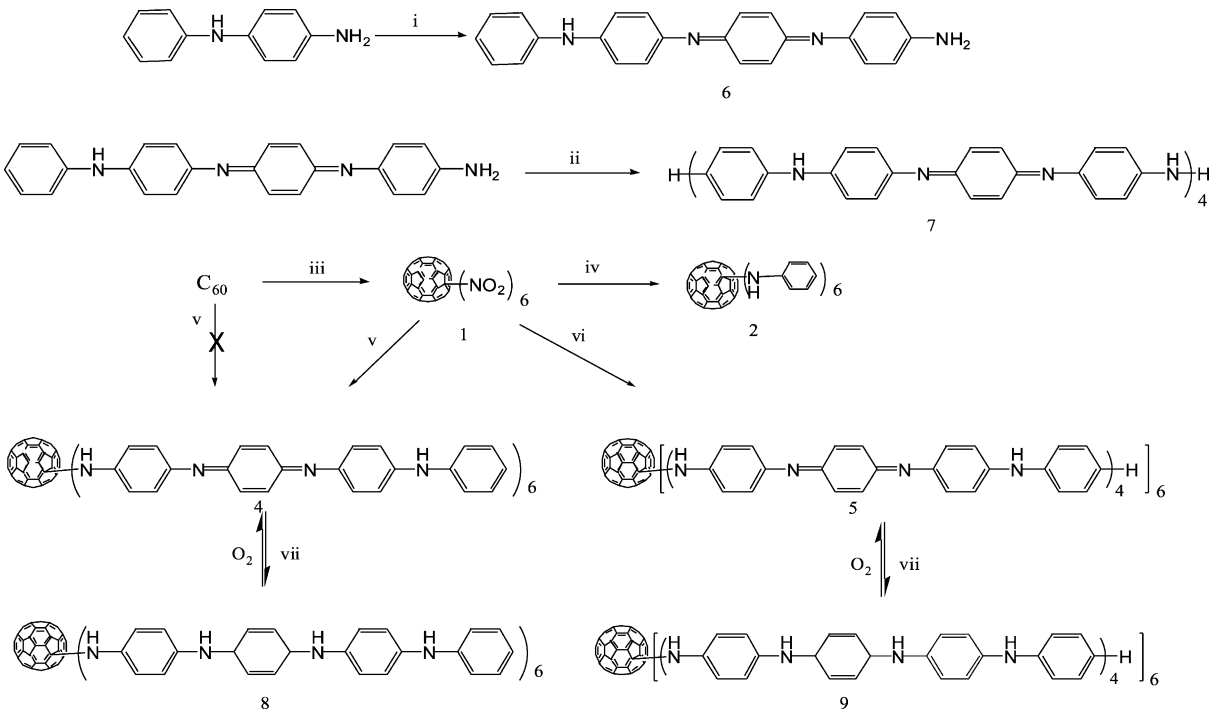

Scheme 30. Synthesis of hexa(oligoanilinated) C_{60} [90].

as excellent crosslinking agents. Similarly, Tang et al. [92] prepared star-shaped fullerene polymers by the addition C_{60} to WCl_6–Ph_4Sn, to convert the WCl_6–Ph_4Sn from a poor to an effective initiator for phenylalkyne polymerization. While polymerization of 1-phenyl-1-butyne (PB) initiated by WCl_6–Ph_4Sn at room temperature yields only small amounts of polymer (0.05–5.3%) with low molecular weight (M_n 8000–15,000) and narrow polydispersity index (PDI up to 1.09), addition of C_{60} to the initiator mixture

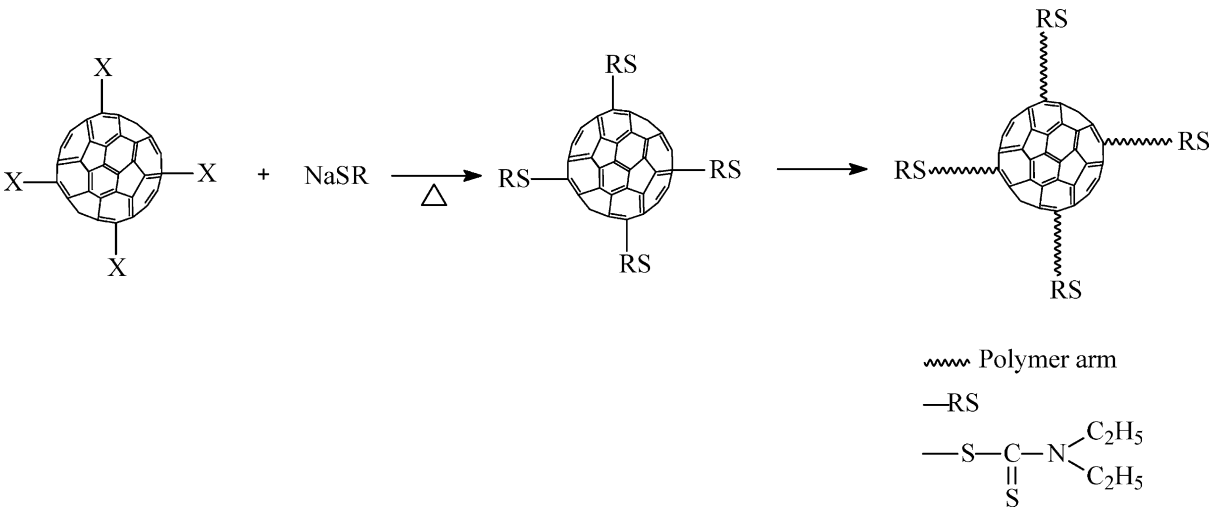

Scheme 31. Synthesis of starlike C_{60}-binding polymers [91].

dramatically boosts initiation activity, producing polymer with high M_n (up to 171,000) and broad PDI (larger than 2.2) in high yield (up to 99.5%). The resulting polymers consist of polyacetylene chains and covalently bound C_{60} cages (up to 9.1 wt%). The molecular weights of C_{60}-PPBs are much higher than that of the pure poly(1-phenyl-1-butyne) (PPB), suggesting multiple additions of PPB chains to one C_{60} cage. Upon photoexcitation the star-shaped C_{60}-PPBs emit strong blue light, which can effectively attenuate the power of a pulsed laser beam. Their saturation fluence is much lower than that of C_{60} at similar linear transmittance.

2.6. Fullerene end-capped polymers

The first mono-C_{60}-end-capped polystyrenes were prepared by reaction of amino-terminated polystyrene with C_{60} (Scheme 32) [93]. These polymers could easily be processed to homogeneous, transparent films containing up to 27 wt% C_{60}, and no microphase or nanophase separation was observed. Tang et al. [92] prepared mono-C_{60}-end-capped PPB by polymerization of 1-phenyl-1-propyne (PP) initiated by WCl_6–Ph_4Sn with C_{60} in the initiator mixture. Compared with the parent C_{60}, these polymers show better optical limiting performance. Using the reaction of TEMPOL (4-hydroxyl-2,2,6,6-tetramethyl-piperdinyloxyl)-terminated polystyrene with C_{60}, we prepared narrow-polydispersity mono-C_{60}-end-capped polystyrene in our laboratory [94]; we also found these polymeric derivatives to exhibit very good photoconductivity. Zhou et al. [95,96] prepared mono-C_{60}-end-capped PSt (PSt-C_{60}-Br) and PMMA (PMMA-C_{60}-Br) under atom transfer radical polymerization (ATRP) conditions by reacting C_{60} with bromo-terminated polystyrene (PSt-Br) and poly (methyl methacrylate) (PMMA-Br) with designed molecular weights and narrow molecular weight distributions. The fluorescence of PMMA-C_{60}-Br and PSt-C_{60}-Br is quenched by triethylamine or fumaronitrile, which indicates that C_{60} still retains its strong electron-accepting and electron-donating properties after modification by macromolecules. Zhang et al. also studied the self-assembly properties of this type of polymeric C_{60} derivative in solution [97]. They observed two narrow distributions by DLS with hydrodynamic radii 29.5 and 1.3 nm, which they

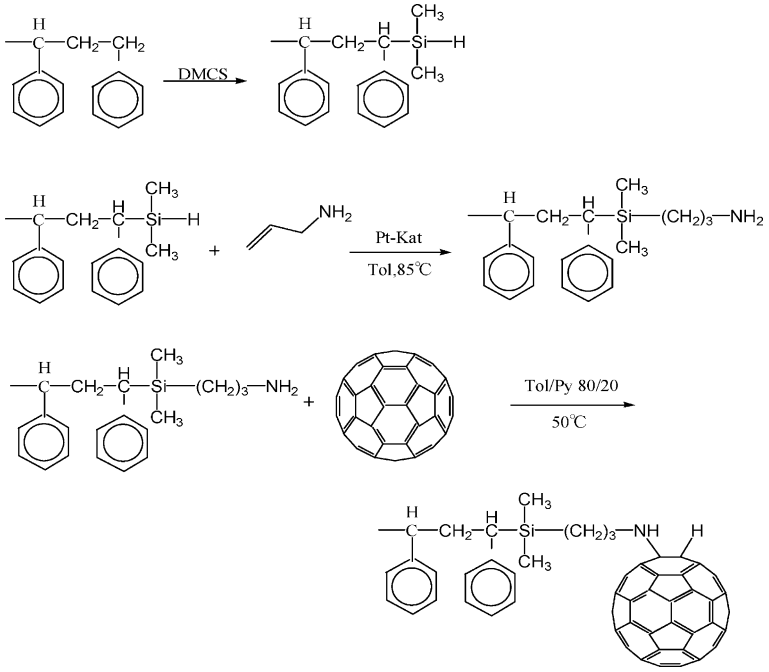

Scheme 32. A polystyrene-based copolymer with C_{60} termini (DMCS is dimethyl-carbosilane) [93].

attributed to aggregates and single polymer molecules, respectively. In GPC elution diagram, two distributions were also observed, and attributed to the aggregates and the single hammer-like polymer.

Using conducting polymer to prepare mono-C_{60}-end-capped polymer is also a very interesting project, Gu et al. prepared mono-C_{60}-end-capped oligophenylenevinylene (OPV) [98]. The synthesis procedure is depicted in Scheme 33. This molecular approach appears to be particularly interesting for solar energy conversion, since the bicontinuous network obtained by chemically linking the hole-conducting OPV moiety to the electron-conducting fullerene subunit prevents any problems arising from bad contacts at the junction, as observed in polymer/C_{60} blends. Furthermore, this new synthetic approach also offers great versatility for tuning the photovoltaic system. Interestingly, increasing the donor ability of the conjugated oligomer substituents due to the presence of the aniline group, increases the efficiency and sensitivity of photovoltaic devices by an order of magnitude.

Mono- and bi-C_{60}-end-capped PEOs were prepared using the reaction of the azide group with C_{60} [99,100]. First, the hydroxyl groups of PEO were converted to chlorine groups through reaction with thionyl chloride. The chloro-terminated PEO was then reacted with sodium azide to form azido-terminated PEO, which subsequently underwent a cycloaddition reaction with C_{60} to afford C_{60}-end-capped PEO. Martineau et al. [101] prepared various (mono-, bi- and tri-) C_{60}-end-capped oligothienylenevinylenes (nTVs) (Scheme 34). They studied electrochemical and optical properties, and found the band gap of the highest occupied molecular orbital and lowest unoccupied molecular orbital (LUMO) to be small enough for light harvesting in organic photovoltaic devices. Cloutet et al. [102] reported a hexa-C_{60}-end-capped star polymer. Functionalization of six branch termini of a star polymer with azido and amino groups led to a functional polymeric product that was further reacted with C_{60} to furnish hexafullerene star polymer (Scheme 35).

2.7. Immobilization of fullerene on solid surfaces

Fullerene-based thin films on solid surfaces are of high interest because of the possibility of transferring the distinctive fullerene properties to bulk materials by surface coating.

One method is to immobilize amine groups on indium tin oxide (ITO) surfaces and then react the

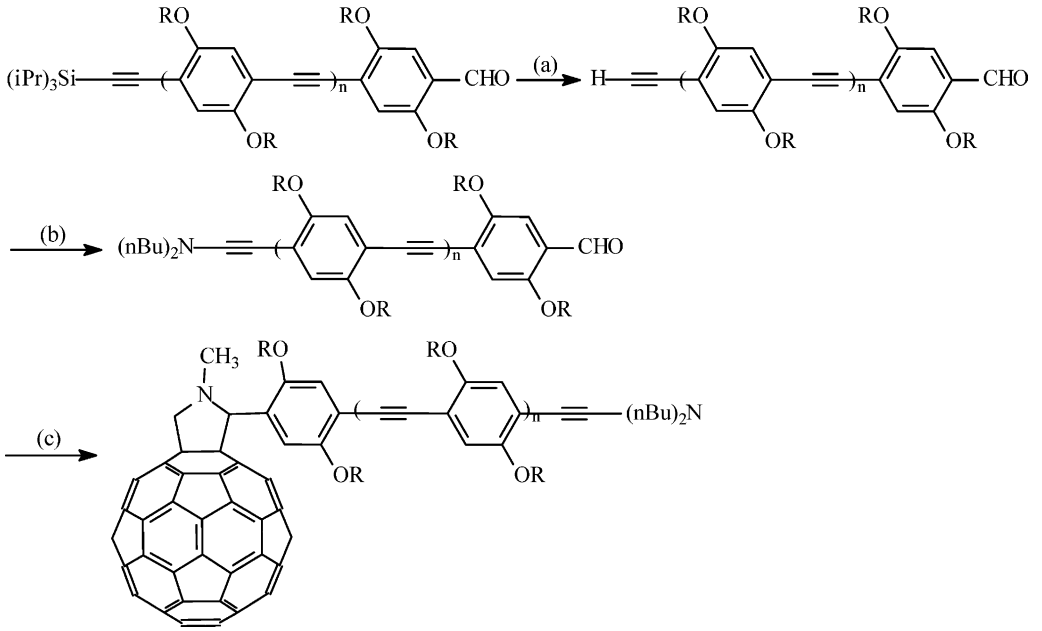

Scheme 33. Synthesis of mono-C_{60}-end-capped oligophenylenevinylene. Reagents and reaction conditions: (a) TBAF, THF, 0 °C; (b) 4-iodo-*N*,*N*-dibutylaniline, $PdCl_2(PPh_3)_2$, CuI, Et_3N, 25 °C; (c) C_{60}, *N*-methylglycine, tolune, △ [98].

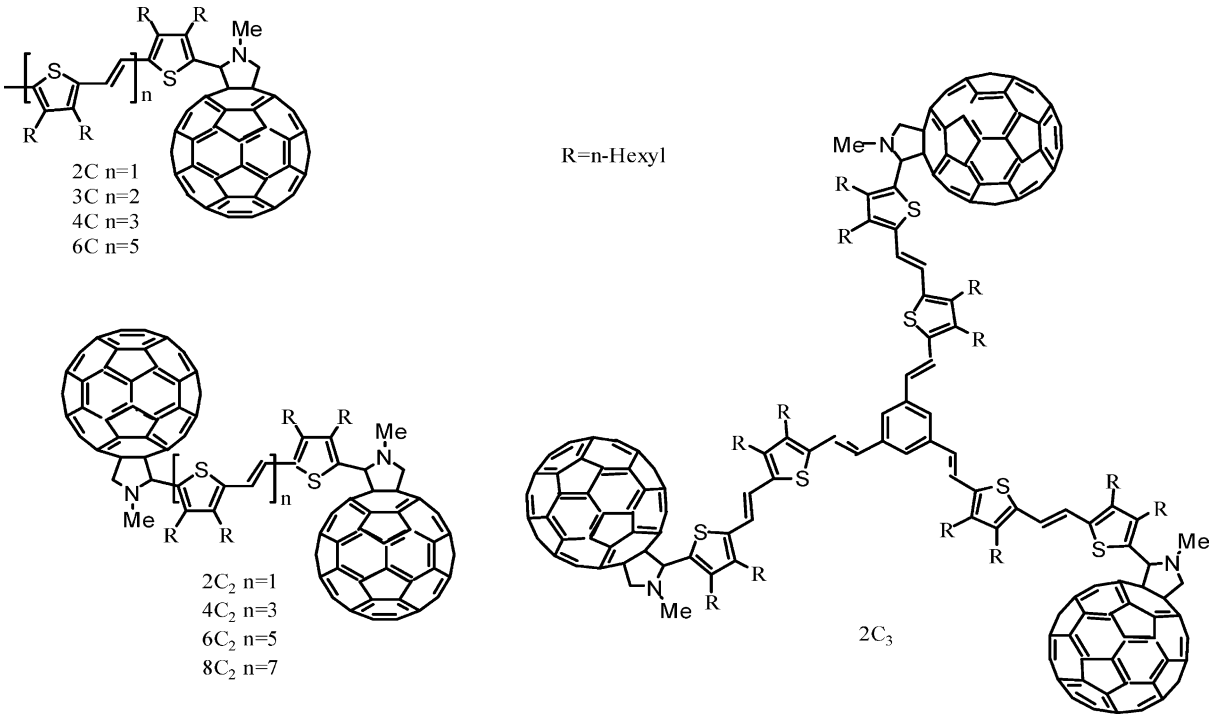

Scheme 34. Structures of mono-, bi- and tri-C_{60}-end-capped oligothienylenevinylenes [101].

amine groups with C_{60} [103]. Another method is to attach covalently a pyridyl-terminated, self-assembled monolayer of C_{60} to a silicon oxide surface [104]. After immobilization of (11-bromo-undecanyl) trichlorosilane on the surface of quartz or Ge/Si multilayer substrates and reaction with OsO_4 in toluene, C_{60} is allowed to react and thus to produce a coordination complex. Covalent attachment of C_{60} onto a functionalized polyethylene film also has been described [105] as follows. Diphenylmethyl-terminated oligomers are prepared by reaction with 1,1-diphenylethylene followed by protonation. A film containing about 3 wt% of the oligomers is formed by spin casting. Treatment the film with *n*-BuLi-TMEDA (*N*,*N*,*N*′,*N*′-tetramethylethylenediamine) leads to a lithiated film, which is then reacted with C_{60}.

Silicon alkoxide functionalized fullerenes can be profitably used in the preparation of HPLC stationary phases [106]. The silicon alkoxide group, in fact, guarantees chemical grafting to silica (Scheme 36). Standard chromatographic tests with simple aromatic compounds reveals that the modified stationary phase affords high efficiency both in organic and water-rich media. Specific interactions with complex solutes are capable of establishing multipoint contacts with the spheroidal fullerene. Accordingly, exceptionally high size-selectivities are obtained for cyclic oligomeric compounds like calixarenes and cyclodextrins in organic and water-rich media. A number of helical peptides, containing hydrophobic cavities complementary in size to C_{60}, bind selectively to the grafted fullerene.

2.8. Crosslinked fullerene polymers

Photochemical addition of C_{60} to furan derivatives has been used to prepare crosslinked furan-containing polymers. A polymer having furan units on the side chains was synthesized by the reaction of poly(2-hydroxyethylmethacrylate) with 2-furoic chloride [107], and then a 1,1,2,2-tetrachloroethane solution of the polymer was exposed to visible light in the presence of C_{60}. The solution turned to a gel after 10 h and then solidified completely. This photo-crosslinking process was applied to a photoresist with sensitivity in the visible region. The first example of

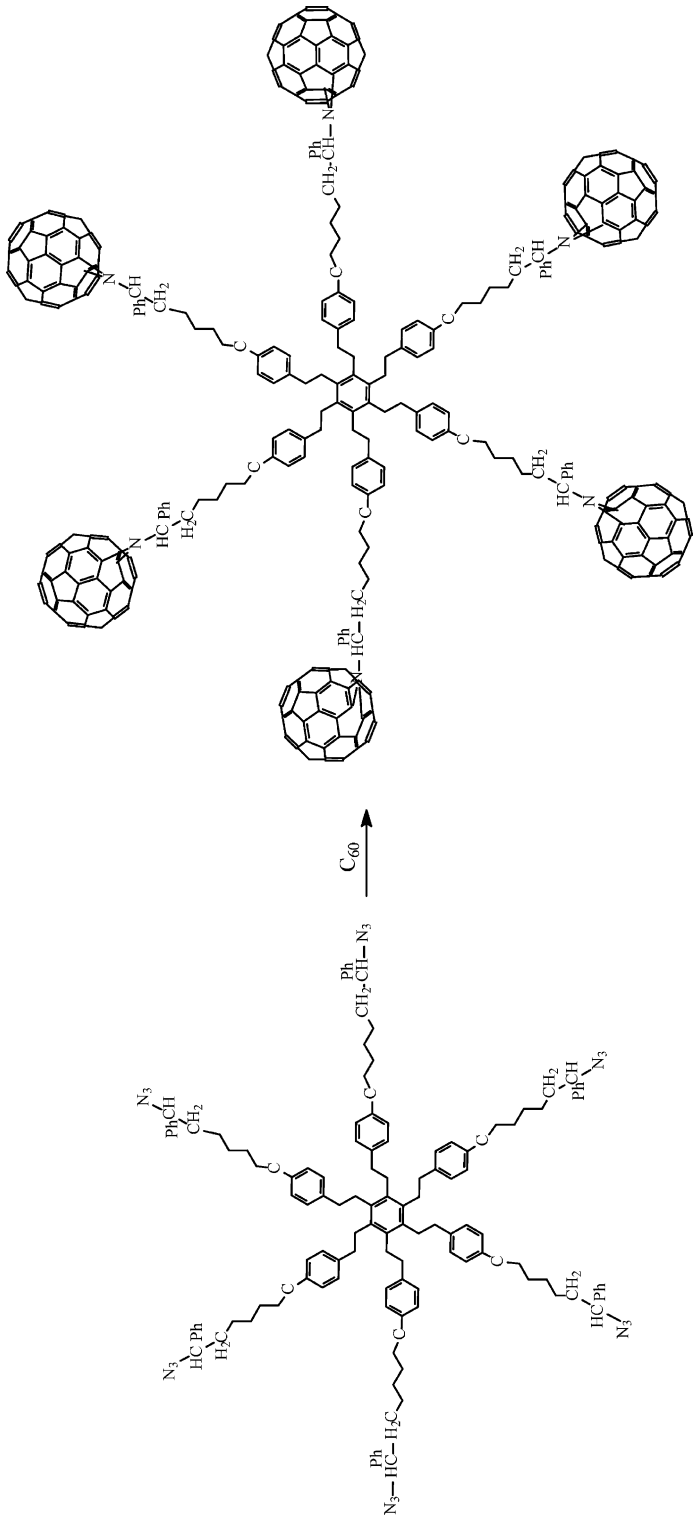

Scheme 35. Hexafunctional star adduct and hexafullerene star polymer [102].

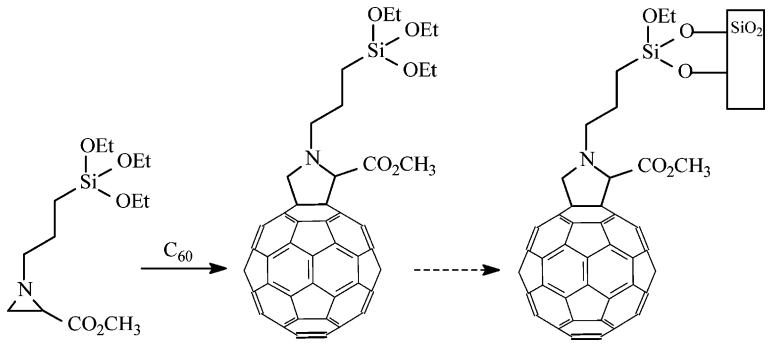

Scheme 36. Grafting of C_{60} onto a silica surface [106].

micron-size photolithographic patterning was achieved using the furan-containing polymer/fullerene system. Another interesting photosensitive system, ethylidene norbornene with C_{60}, was prepared by Jiang et al. [108]. A cast film of EPDM (ethylene–propylene ethylidene norbornene terpolymer) containing C_{60} kept in the dark remains soluble but exposure to light results in a crosslinked rubber (Scheme 37). A highly uniform photoconductive film can be obtained from the solution.

Under high pressure, crosslinked C_{60}-containing polymer has also been synthesized by free radical polymerization of styrene and C_{60} [109]. Fig. 1 shows the pressure dependence of the fraction of insoluble product in chloroform. This fraction has a maximum value at about 0.5 GPa. The insoluble product synthesized under 0.3–0.5 GPa was swollen in chloroform. The degree of swelling in chloroform (weight ratio of the swollen sample to the dry sample) was 28–34. Polystyrene synthesized under high pressure contained no insoluble material.

Controlled three-dimensional structures including C_{60} molecules as nodes were described by Nuffer et al. [110] (Scheme 38). For this synthesis, THF soluble $C_{60}^{2-}(K^+)^2$ was reacted with living polystyrene chains bearing a carbanion at each end. The use of the fullerene dianion is necessary to avoid complications originating from electron transfer from the carbanions to C_{60}. In the same paper, Nuffer et al. also developed a method to increase the functionality of the nodes by reacting C_{60} with high-functionality polystyrene stars with each branch bearing a carbanion at its end.

2.9. 'All-fullerene' polymers

'All-fullerene' polymers refer specifically to structures in which fullerene cages are directly connected covalently. In 1993, Rao et al. [111] first reported that solid C_{60} film undergoes a photo transformation reaction when exposed to visible or ultraviolet light to yield toluene-insoluble species, which were characterized as all-fullerene polymers formed by [2+2] cycloaddition between neighboring C_{60} molecules. In later studies, many methods have been used to polymerize fullerenes [112], including

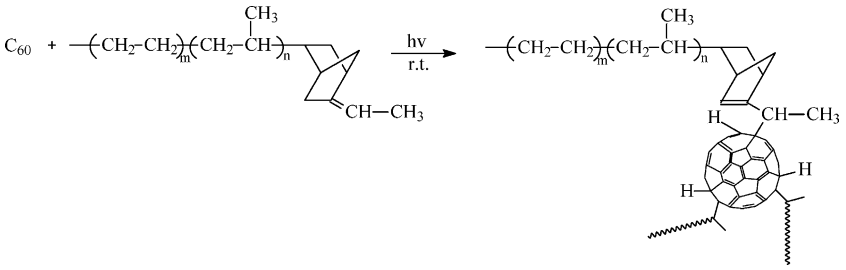

Scheme 37. EPDM-C_{60} network [108].

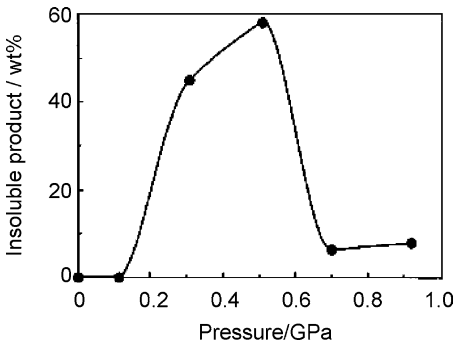

Fig. 1. Influence of pressure on fraction of insoluble product. Reprinted with permission from Ref. [109] (J Appl Polym Sci 1997;65:2781–3, Copyright (1997) Wiley).

photopolymerization [113–116], electron beam-induced polymerization [117,118], pressure-induced photopolymerization [117–120], and plasma-induced polymerization [121,122]. These fullerene structures include one-dimensional (linear chain), two-dimensional, and three-dimensional polymers.

Usually, synthesis of all-fullerene polymers is difficult; the synthesis methods usually entail specific physical conditions [123–125]. Following their discovery that C_{60} can form stable clusters in a solvent mixture, Ma and co-workers [123–125] synthesized high molecular weight polyfullerenes by photochemical reactions of C_{60} clusters in carefully deoxygenated toluene–acetonitrile solutions at room temperature. These authors believe that the photochemical reaction of fullerene clusters most likely follows the same mechanism as the phototransformation of solid fullerene films (Scheme 39). Crosslinking of fullerene molecules is assumed to occur through a photochemical [2+2] cycloaddition reaction in excited triplet states of the fullerene. The involvement excited triplet states is supported by the fact that the photopolymerization does not occur in air-saturated fullerene cluster solutions. The excited singlet-state lifetime of C_{60} is ca. 1.2 ns. This short lifetime is due to rapid and efficient intersystem crossing to form excited triplet states. The triplet states of C_{60} are much longer-lived (40–50 s), so that quenching due to dissolved oxygen is substantial. The structure of the polymers is probably random. There seems to be no

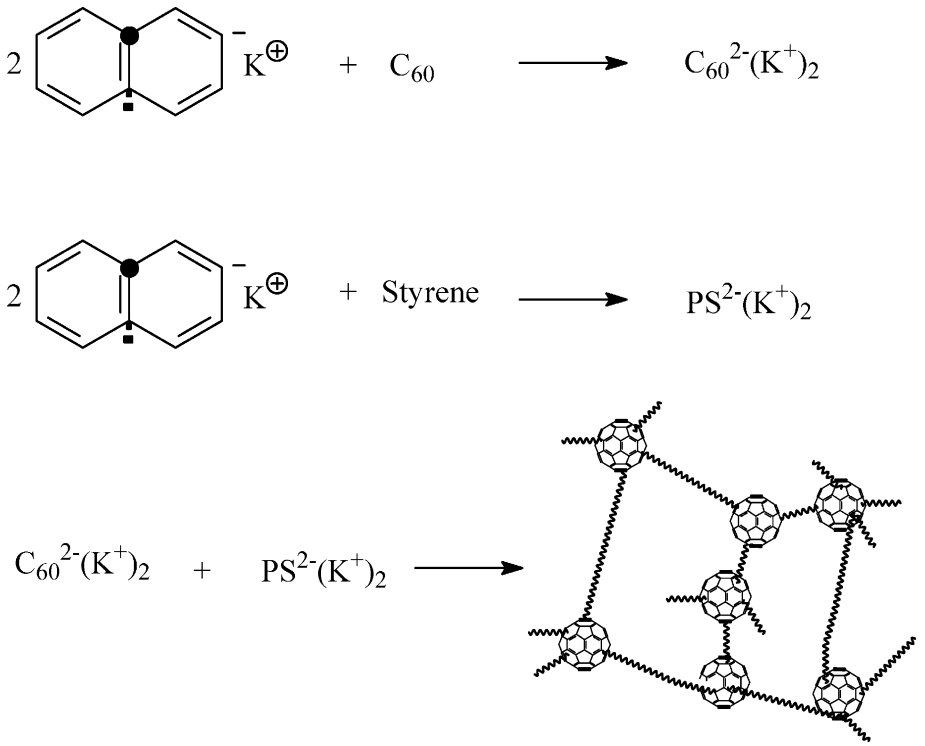

Scheme 38. Schematic representation of a network formed by reacting C_{60} with living polystyrene [110].

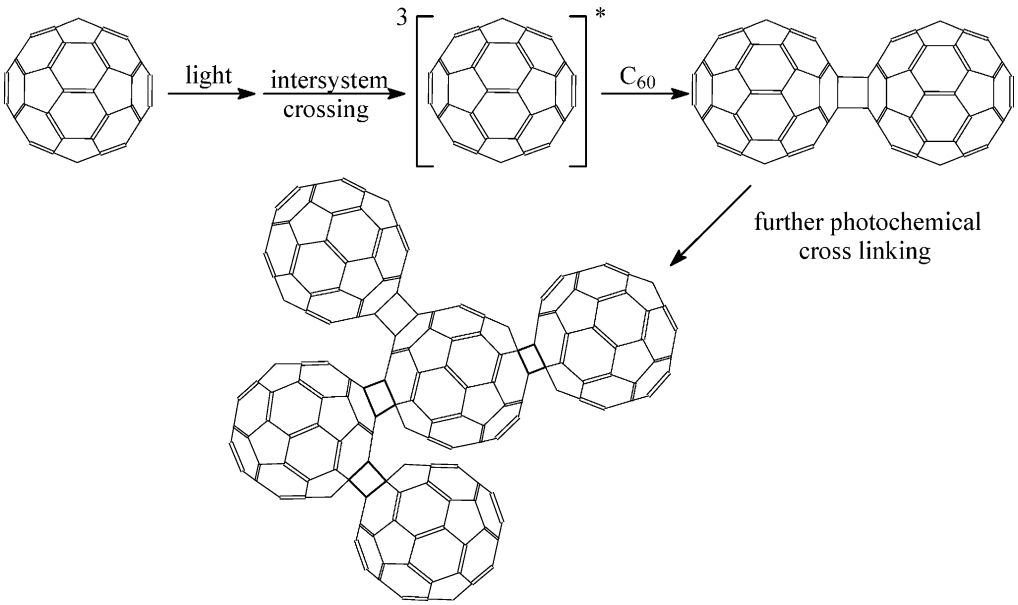

Scheme 39. Suggested mechanism of photopolymerization of C_{60} in solution [114].

fundamental differences among the polymers generated from C_{60} clusters. Also, the polyfullerenes and the clusters from which the polymers are of comparable sizes, which suggest that the photopolymerization is primarily due to intracluster reactions.

In 2000, Sun and Reed reported a novel method of obtaining a linear polymer of C_{60} cages by a crystal engineering method [126]. The co-crystallate of C_{60} and a calixarene [127] was packed in octahedrally shaped MgO containers and wrapped with Re foil for heating. The pressure was increased gradually to the desired value of 5 GPa over a 30 min period followed by 1 h of heating at 200 °C. The black obsidian-like product was proved by spectroscopic methods (energy dispersive X-ray spectroscopy, IR, and Raman) to be linear $(C_{60})_n$ with symmetrical [2+2] addition linkages (Scheme 40). The authors suggested that the linear C_{60} polymer they obtained could not be considered a nanowire but rather functioned as a nanofuse.

Cataldo [116] studied the photopolymerization of C_{60} in CCl_4, CH_2Cl_2, cyclohexane, and decalin. Irradiation of the C_{60} solutions under nitrogen flow produced C_{60} photopolymers, the structure of which was comparable to that of C_{60} photopolymers prepared by solid-state photopolymerization or by C_{60} piezopolymerization (polymerization under high pressure). Cataldo also investigated the role of oxygen as a photopolymerization inhibitor in cyclohexane and in the formation of oxygenated photopolymers in halogenated solvents. He reported that at $\lambda > 265$ nm, CCl_4 is photolysed and plays a role in promoting photopolymerization, while for $\lambda > 300$ nm no interference from CCl_4 occurs.

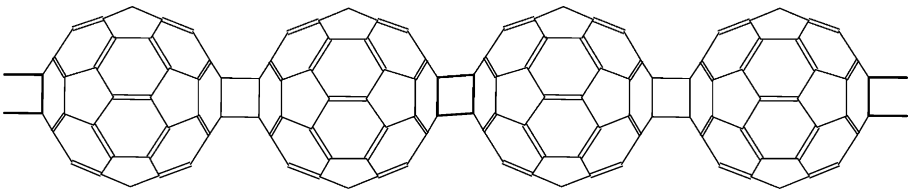

Scheme 40. C_{60} linear polymer [127].

3. Fullerene doped polymers

3.1. Fullerene doped conducting polymers

3.1.1. General aspects

Conducting polymers have attracted much interest owing to the drastic changes of electrical, optical and magnetic properties caused by doping. Many scientists are working on synthesizing new conducting polymers and searching for new effective and stable dopants [128–131]. Thus far, various compounds, such as halides, metal halides, and Lewis acids have been used as p-type dopants in conducting polymers [132]. Skugimoto and Takeda [131] found that a large-size dopant can improve the stability of a doped system. Thus the search for new large-size dopants seems to be quite important. That the C_{60} molecule can withdraw up to six electrons from an alkali metal reflects its very strong electron affinity and suggests it as a potential electron-acceptor candidate in organic solids and conducting polymers.

When C_{60} was doped into conducting polymer, two cases were found: (i) Marked changes in absorption spectra, obvious quenching of photoluminescence, slight enhancement of conductivity, and slight changes in ESR spectra—which suggested effective doping in the ground state [133]. In this case, the electronic wave functions of polymer and C_{60} were mixed to some extent in the ground state. (ii) Small changes in the absorption spectra, conductivity, and ESR signal, with obvious quenching of photoluminescence and enhancement of photoconductivity—which indicated ineffective doping in the ground state [134,135]. A photoinduced charge-transfer effect can be observed [134] in these systems. Till now, the latter case has been extensively studied in physics, chemistry, biology, and in the areas of overlap between the traditional disciplines, because theoretical studies in photophysics and photochemistry can provide an approach to deeper understanding of solar energy conversion in green plants [136].

3.1.2. Effective doping systems in the ground state

When C_{60} is doped into certain conducting polymers, such as poly(3-alkylthiophene) (PAT) and polyaniline, the electronic functions are mixed significantly in the ground state and absorption spectra are changed [133,137]. Fig. 2 shows absorption spectra of PAT film doped with various concentration of C_{60}. The high-energy peak originating from the interband transition is suppressed by doping and a new absorption peak evolves in the near infrared region around $E = 1.1$ eV with increasing C_{60} concentration. The new absorption peak is a typical indicator of the forming of a ground-state charge-transfer complex. The suppression of the interband absorption may be explained by transfer of electrons from the conjugated chain of PAT to C_{60} in the ground state. Morita et al. [133] considered that the strong electron–lattice interaction in the one-dimensional system would dramatically modify and distort the conjugated polymer system, and that polarons P^+ or bipolarons BP^{++} would be formed. Therefore, the density of states in the upper energy range of the valence band would be decreased, resulting in suppression of the interband absorption, especially in the lower energy range. They proposed the energy diagram in Fig. 3, which shows that transfer of free electrons between the rigid bands (those relatively insensitive to doping) of C_{60} and PAT is nearly impossible since charge-transfer (CT) requires positive energy $\delta_{CT} = 0.1$–0.2 eV. However, charge-transfer from polymer to C_{60} may occur if polaronic effects are taken into account, both in the polymer (P^+ level ~ 0.2 eV, while BP^{++} ~ 0.7 eV above the valence band top [138]) and in C_{60} molecules. In C_{60} a shape deformation effect [139,140] will lead to splitting of the threefold degenerate LUMO of C_{60} in the ionic

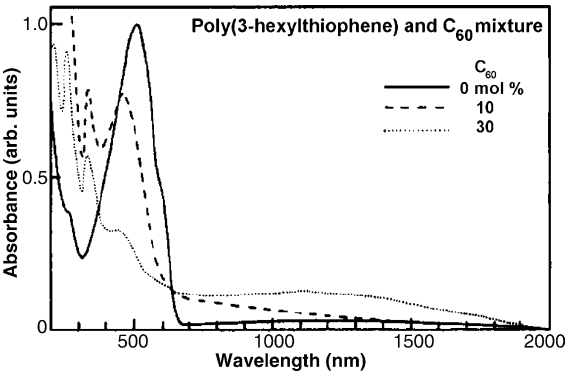

Fig. 2. Absorption spectra of poly(3-hexylthiophene) for various C_{60} concentrations. Reprinted with permission from Ref. [133] (Solid State Commun 1992;82(4):249–52, Copyright (1992) Elsevier).

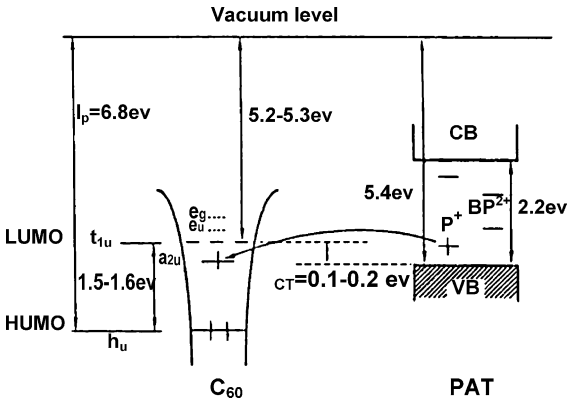

Fig. 3. Energy diagram of poly(3-hexylthiophene) and C_{60}. Reprinted with permission from Ref. [133] (Solid State Commun 1992;82(4):249–52, Copyright (1992) Elsevier).

state due to polaronic distortion; in other words, Jahn–Teller distortion will occur. In the latter case the t_{1u} level should split into three levels of different symmetries as sketched in Fig. 3, and the transferred electron should occupy the lowest split level. Moreover, it has been reported [141] that, in weak doping with slightly positive CT energy, the Coulomb attraction of the P^+ polaron and the dopant can additionally stabilize the charge transfer due to the creation of polarons P^+ in the ground state with C_{60}, even if Jahn–Teller or polaronic gain (which is still not found experimentally) is not as large as estimated in Ref. [139]. In this system, quenching of photoluminescence was also confirmed. It is believed that this is due to a rate of energy transfer from polymer to C_{60} much larger than the reciprocal lifetime, $10^7\ s^{-1}$ [142,143]. Polyaniline/C_{60} composites were prepared either by solid-state blending of both components or by the introduction of fullerene during polymerization of aniline [137]. FTIR spectroscopy indicates strong interaction between polyaniline (PANI) and fullerene in the ground state. The characteristic polaron $C–N^{+\cdot}$ band of PANI appears at 1240 cm^{-1}. Conductivity of pure PANI is low. After doping with C_{60}, the conductivity of PANI increases almost three orders of magnitude. The same conductivity level was reported for PANI/C_{60} composites prepared by a standard method using solution blending in NMP solvent [144].

More studies have been reported on similar systems, such as poly(3-octylthiophene) (P3OT) doped with C_{60} [145]. A large change in the P3OT/C_{60} absorption spectrum was reported, indicating significant mixing of the P3OT and C_{60} ground-state electron wave functions [128]. It is believed that the interaction between P3OT and C_{60} is not a full charge separation $D^+–A^-$ (D for donor, A for acceptor), but rather a partial charge transfer in the ground state, $D + A \rightarrow D^{\delta+}–A^{\delta-}$, since no C_{60} anion signal can be observed in ESR. Later, near steady-state photoinduced absorption (PIA) spectroscopy was used to study the P3OT/C_{60} composite, and a significant change of PIA was observed. Under the photoinduction conditions, full charge separation occurred and resulted in the formation of both $P3OT^{+\cdot}$ ($P^{+\cdot}$) and $C_{60}^{-\cdot}$. Steady-state light-induced electron-spin resonance (LESR) provides the evidence that $C_{60}^{-\cdot}$ is formed upon photoexcitation. Fig. 4 shows two spin signals, in which the $g \approx 2.000$ spin with $\Delta H_{FWHM} \approx 4$ G is assigned to the P3OT polaron radical (donor cation radical), and the $g \approx 1.9935$ spin with $\Delta H_{FWHM} \approx 3.7$ G is assigned to the $C_{60}^{-\cdot}$ anion radical. Accumulative effect of the charged separated upon successive illumination cycles is not observable, implying a short lifetime for the charge-separated configuration.

Recently, Marumoto et al. studied regioregular PAT (poly(3-alkylthiophene))/C_{60} composite [146].

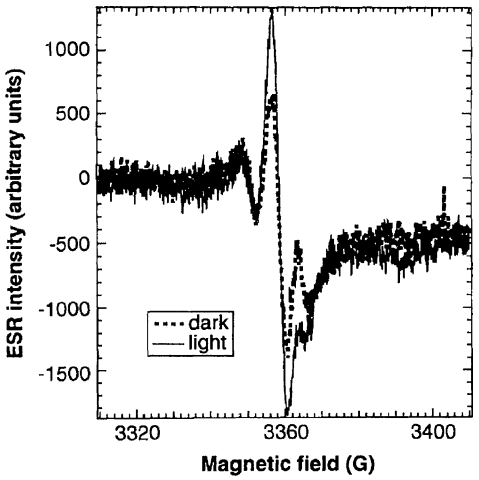

Fig. 4. LESR spectra of P3OT/C_{60} upon successive illumination with 2.41 eV argon ion laser at 100 mW. The ESR dark signal is the dashed line and the LESR signal is the solid line. Reprinted with permission from Ref. [149] (Science 1992;258(5087):1474–6, Copyright (1992) AAAS).

They observed two transient LESR signals below 200 K, due to photoinduced electron transfer between PAT and C_{60}. Marked enhancement of the LESR signals in the excitation spectrum near 1.8 eV was found as compared with pure regioregular PAT. This is consistent with the enhancement of the photoconductivity at about 1.8 eV, where an optically forbidden transition of C_{60} occurs. The spin–lattice relaxation time of the polaron spins of PAT is at least approximately 18 times longer than that of C_{60} as determined from the inhomogeneous broadening of the ESR line by hyperfine interactions. Prompt and persistent LESR signal components are observed in the transient response of the LESR signal (Fig. 5). The prompt contribution shows a monotonic increase with increasing excitation light intensity, while the persistent contribution is independent of excitation intensity owing to the deep traps of the photogenerated polarons.

Luzzati et al. [147,148] prepared random copolymers of 3-butylthiophene and 3,4-dibuthylthiophene in various ratios. The steric hindrance of 3,4-dibutylthiophene units induces a twist of the conjugated backbone. The degree of conformational disorder increases with increasing fraction of bisubstituted monomer in the copolymer together with a reduction in the conjugation length and consequent blue shift of the absorption–emission spectrum. Luzzari et al. found the energy gap of the copolymers to be tunable. The photoluminescence and steady-state photoinduced spectra (PIA) prove that there is electron transfer from the photoexcited copolymer to C_{60}. The efficiency of charge transfer depends on the miscibility of the two components, which is easily controlled by varying the copolymer composition.

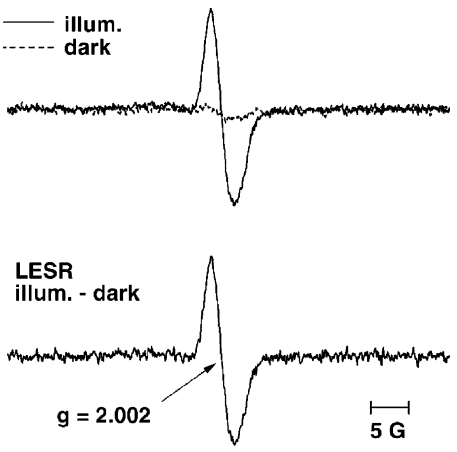

Fig. 5. Upper curves: ESR spectra of PAT-C_{60} composite in the dark (dotted line) and with 700 nm illumination (solid line) at 60 K. Lower curve: LESR spectrum of PAT-C_{60} composite obtained by subtracting the dark spectrum from that under 700 nm illumination at 60 K. Reprinted with permission from Ref. [146] (Synth Met 2002;129(3):239–47, Copyright (2002) Elsevier).

Based on the above, it can be concluded that the interaction mechanism in this type of conducting polymer (D) with C_{60} (A) is the following:

Step 1: charge transfer in the ground state: $D + A \rightarrow (D^{\delta+}\text{–}A^{\delta-})$.

Step 2: photoinduced ion radical pair formation: $(D^{\delta+}\text{–}A^{\delta-})^* \rightarrow (D^{+\cdot}\text{–}A^{-\cdot})$.

Step 3: charge separation: $(D^{+\cdot}\text{–}A^{-\cdot}) \rightarrow D^{+\cdot} + A^{-\cdot}$.

In these reactions, the donor and acceptor units are spatially close, but are not covalently bonded. At each step, the D–A system can relax back to the ground state, either by releasing energy to the 'lattice' in the form of heat or by emitting light, provided the radiational transition is allowed.

3.1.3. Other doping systems in the ground state

3.1.3.1. Photoinduced charge-transfer systems. A photoinduced charge-transfer system has little or no mixing of electron wave functions in the ground state. Unless it is 'short circuited' by a faster mixing process, the photoinduced charge-transfer can take place whenever the donor–acceptor couple satisfies the inequality, $I_{D^*} - A_A - U_C < 0$, where I_{D^*} is the ionization potential of the excited stated D* of the donor, A_A is the electron affinity of the acceptor, and U_C is the coulomb energy of the separated radicals (including polaronization effects). A typical example of such a system is the PPV/C_{60} composite. Sariciftci et al. [149] found that the spectrum of the poly[2-methoxy, 5-(ethyl-hexyloxy)-*p*-phenylene vinylene/C_{60}], [(MEH-PPV)/C_{60}], composite film is a simple superposition of the two components without any indication of new states below the π–π^* gap of the conducting polymer. Thus there is little or no interaction between the two materials in the ground state. They also found that the strong photoluminescence of MEH-PPV is

quenched by a factor of more than 10^3, and that the luminescence decay time is reduced from $\tau \approx 550$ ps to $\tau \ll 60$ ps (the instrumental resolution), indicating a rapid quenching process. They proposed that the luminescence is quenched by rapid electron transfer from MEH-PPV to C_{60}. They estimated the electron-transfer rate to be faster than $10^{12}\,s^{-1}$ [149]. In addition, the PIA experiment is consistent with rapid photoinduced charge transfer. The definitive evidence of charge transfer and charge separation is obtained by LESR upon illuminating the (MEH-PPV)/C_{60} composite film with light of $h\nu = E_{\pi-\pi^*}$, i.e. the energy gap of the MEH-PPV component. Two photoinduced ESR signals can be resolved, one is at $g = 2.000$ and the other is at $g = 1.995$ [11]. The higher g-value is assigned to the MEH-PPV cation radical (polaron) and the lower g-value line is attributed to the C_{60} anion radical. Similar results have been reported for MDMO-PPV/C_{60} composites by Zoriniants [150].

Doping C_{60} in polymers such as poly(*p*-phenylene vinylene) (PPV) can improve the photo-voltage response dramatically [151,152]. If dopant C_{60} traps the electrons that are photogenerated in the polymer for less than 1 ps [152,153], geminate electron–hole recombination will be eliminated. Then the hole recombination rate and photoconductivity along the polymer chains will be increased dramatically [152]. Hence, in pure and C_{60}-doped polymers, the holes are the majority photocarriers, while the minority-carrier electrons remain trapped in the fullerene molecules. Recently, Balberg et al. [154] reported that the unipolar or bipolar action can be 'tuned' by the C_{60} content C_f (i.e. C_{60} per polymer repeat unit) in polymer/C_{60} composites. In the system they studied, for $C_f \leq 0.05$ or $C_f \geq 0.43$, the transport was unipolar. However, for $C_f = 0.11$, very clear bipolar behavior with apparent coupling of the recombination in the two carriers systems was found. In this composite, the very sharp peak in the conductance and photoconductance at 250 K, which results from the well-known phase transition in C_{60} films, confirms the continuous nature of the C_{60} network [155–157]. On the other hand, the high polymer content ($1 - C_f = 0.89$) assures that the polymer system also forms a continuous network. These observations indicate clearly that only a polymer/C_{60} composite, in which both components form continuous networks (Fig. 6) can exhibit the observed bipolar behavior.

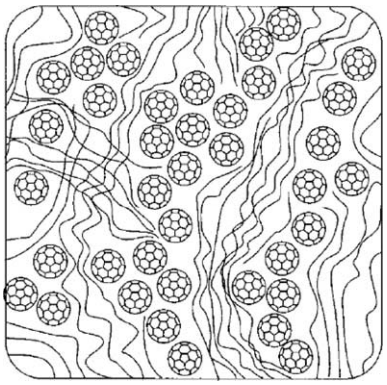

Fig. 6. Illustration of a C_{60}-polymer network in a composite as suggested by Balberg. Reprinted with permission from Ref. [154] (Appl Phys Lett 2001;79(2):197–9, Copyright (2001) American Institute of Physics).

Some other systems, such as phenylmethyl polysilane (PMPS)/C_{60} composites [142,158], have also been reported. The electroabsorption spectrum of the composite film was measured in ground state and no evidence of charge-transfer transition was found. When light with $h\nu > 2$ eV illuminates the composite film, a photoinduced charge-transfer takes place. Here, it is necessary to note that polysilanes are a unique class of photoconductive polymers, with the backbone consisting entirely of tetrahedrally coordinated silicon atoms. There is extensive delocalization of σ-conjugation along the silicon chain, causing improvements to many interesting electronic properties [159,160]. Thus carrier transport along the silicon backbone is very efficient. The hole mobility, about $10^{-4}\,cm^2/V \cdot s$ [161–163], is the highest observed in the polymers studied. In spite of this hole mobility, the photoinduced charge-generation efficiency in polysilane is low [161]. Several doping experiments using organic donors and acceptors did not enhance the charge-generation efficiency significantly, but doping with does enhanced the charge-generation efficiency greatly and makes fullerene-doped polysilane one of the leading polymeric photoconductor candidates. Recently, Mikhailova et al. [164] reported that the doping of fullerene into polyimide film could increase the carrier mobility in photoconduction 10-fold as compared with fullerene-free polymer films.

Electron transfer processes in solution are quite different from those in solid films. Photoinduced

electron transfer reactions between C_{60} and poly(*N*-vinylcarbazole) (PVK) in polar benzonitrile solution have been investigated by observing the transient absorption bands in the visible and near-IR regions [165]. In polar benzonitrile solution, the charge-transfer complex of C_{60} and PVK is responsible for the generation of photoinduced carriers; and several photoinduced electron transfer processes other than photoexcitation of a charge transfer complex were found in these systems. The contribution of these processes to the charge generation should depend largely on experimental conditions: e.g. the nature of the medium and the excitation wavelength.

Incompatibility of C_{60} and a conducting polymer will strongly influence film properties and photo-induced charge transfer processes. Many papers [166–169] have been published on functionalized C_{60} with solubilizing side chains. The most common conjugated polymer is MDMO-PPV and the fullerene derivative is PCBM (Scheme 41). Dyakonov et al. [166] reported detailed studies on MDMO-PPV/PCBM composites using light-induced electron-spin-resonance (LESR) technique. Two overlapping LESR lines are observed, from positive polarons on the polymer chains and negative charges on the fullerene moieties. Microwave power saturation shows different relaxation times for these two spins, ruling out spin-exchange correlations and giving clear evidence of independent spins. The unusually high relaxation rate of the fullerene monoanionic spins is of intrinsic origin. Further, Dyakonov et al. observed two distinct contributions to LESR signals: a prompt one and a persistent one. The excitation light intensity dependence of the prompt contributions to the $P^{+\cdot}$ and $C_{60}^{-\cdot}$ ESR signals is of the bimolecular type ($I^{0.5}$), and implies mutual annihilation of the created ($P^{+\cdot}\cdots C_{60}^{-\cdot}$) pair. The persistent contribution is independent of excitation intensity, and is proposed to originate from deep traps due to disorder. Further results have been reported on this composite by De Cuester et al. [167]. After illumination, two radicals in the sample are formed. One is the remaining positive polaron $P^{+\cdot}$ on the polymer backbone and the other is the $C_{61}^{-\cdot}$ radical anion (Fig. 7). Brabrec et al. [168] reported ultrafast spectroscopic studies using optical excitation of the above system by sub-10-fs pulses. Phonon modes which are strongly coupled to the electronic excitation of the conjugated polymer are directly observed as coherent oscillations during the pump-probe experiment, mirroring the resonant/non-resonant Raman spectrum of the conjugated polymer. For the first time, the kinetics of this charge transfer process were time resolved with a forward transfer time of around $\tau_{ct} \sim 45$ fs. In a study of efficiency of solar cells, Padingger et al. [169] found that addition of up to 10% of conventional polymer to the electroactive composite is possible without lowering the efficiency of the device.

Recently, the Meijer group [170,171] synthesized a functional supramolecular hydrogen-bonded *p*-conjugated polymer that exhibit true macroscopic polymeric properties. A photoinduced charge-separated state was generated within spin-coated blends of the supramolecular polymer with PCBM, and promising photovoltaic devices were obtained. These results create multiple possibilities for using supramolecular architectures in electronic devices in which the well-defined character of *p*-conjugated oligomers is combined with the material properties of polymers.

Through molecular design, the energy gap and electronegativity can be controlled. Conducting

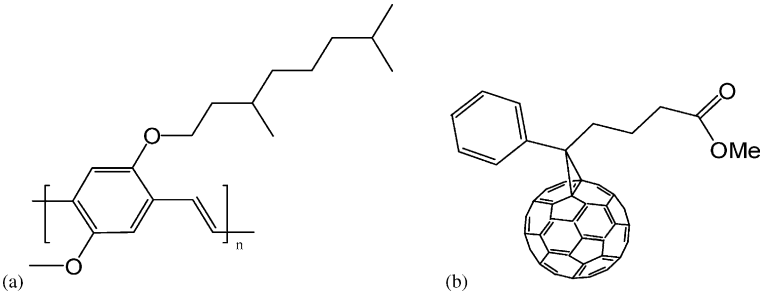

Scheme 41. Conjugated polymer MDMO-PPV (a) and fullerene derivative PCBM (b) [166].

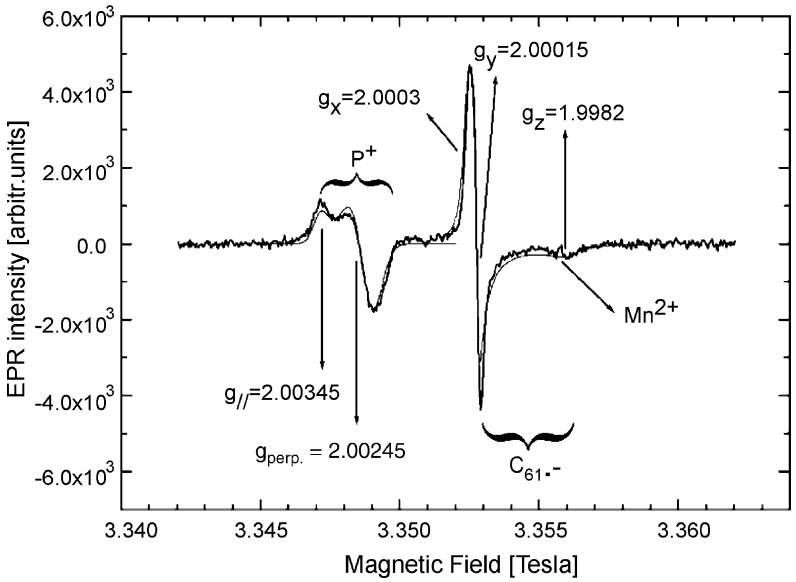

Fig. 7. LESR spectrum of a MDMO-PPV/PCBM composite. Reprinted with permission from Ref. [167] (Synth Met 2001;124:99–101, Copyright (2001) Elsevier).

polymers with a range of ionization potentials and electron affinities can be synthesized [172]. Considering the breadth of opportunity associated with this class of materials, it is important to establish the universal mechanism of photoinduced charge-transfer from conjugated polymer to C_{60}. The process can be described as follows (Scheme 42).

Step 1. Excitation of D:D + A → D* + A
Step 2. Excitation delocalization on the complex: D* + A → (D–A)*
Step 3. Charge transfer initiation: (D–A)* → $(D^{\delta+}–A^{\delta-})$*
Step 4. Ion radical pair formation: $(D^{\delta+}–A^{\delta-})$* → $(D^{+\cdot}–A^{-\cdot})$
Step 5. Charge separation: $(D^{+\cdot}–A^{-\cdot}) \rightarrow D^{+\cdot} + A^{-}$

3.1.3.2. Nonphotoinduced charge-transfer system. A nonphotoinduced charge-transfer composite poly[1,6-heptadiene]/C_{60}, was studied by Yoshino et al. [135]. Its absorption spectrum was a simple superposition of the spectra of the two components and the PIA spectrum showed no significant change upon mixing with C_{60}. Because PHDK has no detectable luminescence, luminescence quenching could not be used to check charge transfer. Thus, two cases involving no changes in PIA spectrum have to be considered: (i) photoinduced electron transfer does occur, but back transfer is so rapid ($\ll$microseconds) that the separated charge cannot be detected; or (ii) photoinduced charge transfer does not occur owing to a faster competing process.

Since the estimated photoinduced electron-transfer time in the (MEH-PPV)/C_{60} composite is about 10^{-12} s [172], longer than is required for the formation of a soliton in a polymer with degenerate ground state ($\leq 10^{-13}$ s) [132], photoexcitons will relax into soliton–antisoliton pairs in the donor polymer before electron transfer occurs. The lower energy of the soliton–antisoliton pair (relative to the initial photoexcited electron–hole pair) and the energy barrier for breaking the soliton–antisoliton pair into a pair of polarons prevent charge transfer. Thus, charge transfer does not occur in PHDK/C_{60} composites because the stabilized-charge solitons form more quickly.

The experimental results clarify an important criterion for the design of donor–acceptor couples suitable for electron transfer and long-lived charge separation. As in the case of conjugated polymers with a degenerate ground state, the excited-state dynamics of the donor unit can quench electron

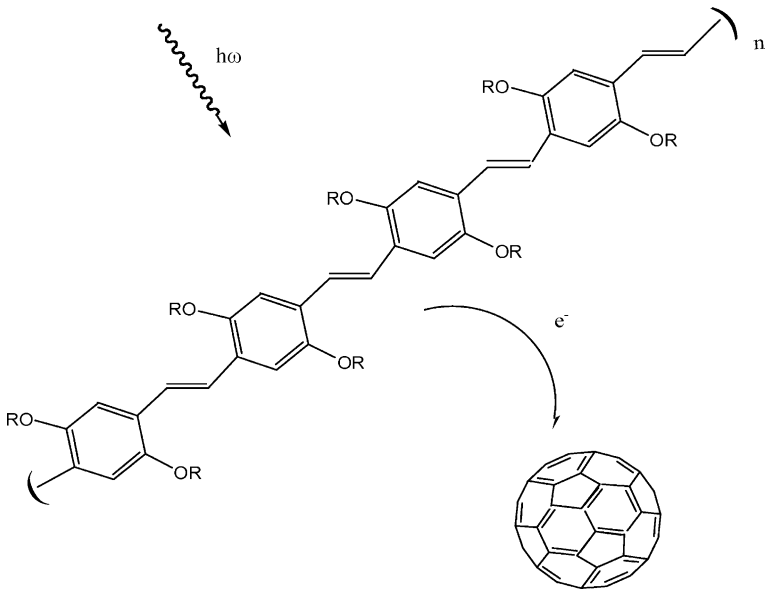

Scheme 42. Photoinduced electron transfer from semiconducting polymers to C_{60}.

transfer. Because this effect is hard to validate by experiment and has no potential value for applications, scarcely any further reports have been published.

3.2. Fullerene-doped nonconjugated polymers

In nonconjugated systems strong direct interactions of C_{60} with polymer as in the above conjugated system, cannot take place, but incorporation of C_{60} in a nonconjugated system can also improve its properties, just as in blending suitable pairs of polymer to produce new polymeric materials. Using a fullerene-containing polymer as a blend component offers a simple means to impart its properties to other polymers.

Polotskaya et al. [173] investigated the behavior of polystyrene/fullerene compositions containing up to 3 wt% C_{60}. They found that the addition of fullerene to polystyrene (PS) leads to an increase of molecular packing density and thus influences the transport of small molecules through polymer film. Gas diffusion through films of PS/fullerene compositions is slower than through PS films, but gas separation capabilities are greater. Dielectric studies showed that the fullerene is distributed as clusters in a rigid polymer matrix prepared from a toluene solution of PS and fullerene. Heating in the absence of air to temperatures above the PS glass transition leads to increased relaxation time for the α-transition in PS in compositions containing 1 wt% fullerene. This effect is caused by rather strong interaction of PS chains induced by fullerene molecules in the PS–fullerene complex. When the C_{60} content is 1 wt%, the probability of interaction between C_{60} molecules in the PS/C_{60} system may be sufficient to cause physical linking of PS chains in the film. Substituted C_{60} derivatives have been used to increase the miscibility of polystyrene and C_{60} [174]. Experimental results confirmed that C_{60} derivative molecules can be monomolecularly dispersed in a polystyrene matrix, up to a maximum content of 6.3 wt%. C_{60}-bearing polymers were dispersed in a blend film or a single-polymer film, either monomolecularly or in aggregates, depending on the chain length of the polymer moiety and the blend composition.

Adding the C_{60} to polyethylene (PE) film [175] causes a notable increase in the microhardness of the film, depending on the concentration of fullerene particles in the film. In addition, a substantial hardening of the composites is obtained by annealing at high temperature ($T_a = 130$ °C) and long annealing time ($t_a = 10^5$ s). The hardening of the composites by annealing has been identified with the thickening of

the PE crystalline lamellae. Comparison of X-ray scattering data and the microhardness values upon annealing leads to the conclusion that C_{60} molecules phase separate from the polyethylene crystals. The temperature dependence represents the independent contribution of the PE matrix of the C_{60} aggregates to the hardness value. Because of the poor compatibility of PE with C_{60} [176,177], C_{60} readily forms large particles (30–50 mm) in PE from solution that tend to be concentrated on the surface of the PE composite. Substituted C_{60} derivatives have been used to improve the compatibility of C_{60} with PE. Benzylaminofullerene ($C_{60}H_{4.7}(NHCH_2C_6H_5)_{4.7}$)/low-density polyethylene (BAF/LDPE) composites containing up to 10 wt% BAF have been prepared from solution. BAF is evenly distributed as small particles of 1–5 mm diameter in polyethylene. The BAF molecules do not aggregate even when PE is heated to melting. The dielectric permittivity and loss factor have been studied as functions of BAF loading and frequency. The composites have almost the same small dielectric loss as LDPE alone, partly owing to the volume increase after mixing. The introduction of BAF does not affect the crystal structure and the crystallinity of PE, indicating that BAF is in the amorphous region of PE. The composites show higher storage and loss moduli than LDPE; but higher BAF loading has an adverse effect on the modulus.

Zhang et al. [178] prepared PPO/PS–C_{60} blends. With increasing C_{60} content in PS–C_{60} and PS–C_{60} content in the blend, the color becomes deeper. Each blend has a composition-dependent T_g, showing that all the blends are miscible. None of the blends show any sign of phase separation, even when heated to 300 °C. The formation of a miscible blend requires the presence of favorable intermolecular interaction between the two component polymers. For PPO/PS blends, Wellinghoff et al. [179] suggested that miscibility arises from van der Waals interactions between the phenyl groups of PPO and PS. They show that PS containing 13.6 wt% C_{60} is still miscible with PPO. It is possible that the 'aromatic' C_{60} may also interact with the phenylene rings of PPO.

Troitskii et al. [180] used thermogravimetry to study the inhibition of thermo-oxidative degradation of PMMA and PS in the presence of C_{60}. They found that the weight loss decreased dramatically in the presence of fullerene (Fig. 8). They explored the correlation between the kinetics of the depropagation reaction of PMMA radicals $R^{\cdot}$ and their interaction with oxygen and showed that the retarding influence of oxygen on PMMA depropagation increases with increasing oxygen concentration and with decreasing degradation temperature. They suggested that in the thermo-oxidative degradation of PMMA at elevated temperatures, the inhibiting effect of C_{60} is due to its interaction with $R^{\cdot}$ and oxygen-containing radicals to form less active compounds. In the case of PS, the retarding influence of fullerene is mainly connected

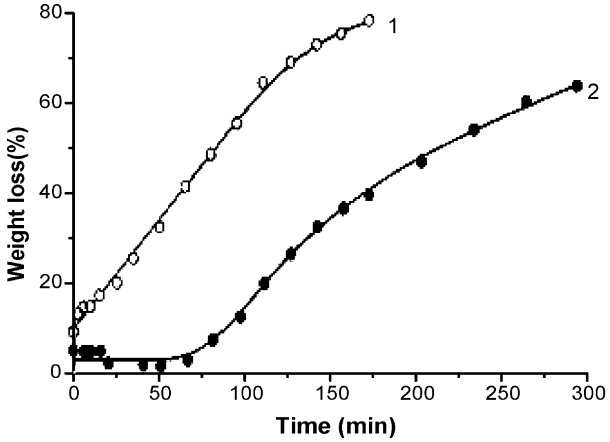

Fig. 8. Dependence of weight loss (%) on time in the thermo-oxidative degradation of PMMA under oxygen (initial pressure 200 mm, 282 °C): (1) without additive, and (2) with 0.2 mol% C_{60}. Reprinted with permission from Ref. [180] (Eur Polym J 2000;36:1073–84, Copyright (2000) Elsevier).

with its reaction with oxygen-containing radicals, but interaction of C_{60} with $R^{\cdot}$ cannot be ruled out.

4. Polymers with carbon nanotubes

4.1. General aspects

As a new kind of quasi one-dimensional material, CNTs have stimulated a much interest in the scientific world since they were discovered in 1991 [5]. Because of their intrinsic structural properties (e.g. large aspect ratio and chirality), CNTs exhibit remarkable properties that have made them one of the most celebrated novel materials in the world [181–187]. For example, large-scale aligned CNTs [188] could be used to make electron field emitters [189]. Various nano-electronic devices might be fabricated from CNTs [190]. CNTs are exceptionally stiff and strong materials along their length [191]. In general, CNTs are expected to show their unique effects in multidisciplinary fields and should assume important roles as novel nanomaterials in the 21st century.

With the advances in fabrication and purification of CNTs, these fantastic materials show potential in physics, materials science, and engineering. However, their poor solubility has hindered their chemical manipulation and their potential applications. It is apparent that chemical and physical modification of the surface of CNTs will be necessary to realize many of their potential applications.

Surface modification of CNTs may be realized either by covalent or noncovalent bonding (wrapping) of polymer molecules on the surface of CNTs [192–194].

4.2. Covalent modification of CNTs with polymers

Covalent modification of CNTs is an emerging area in research on CNTs-based materials. Currently, two main strategies are employed: direct sidewall modification of CNTs and modifications based on surface-bound carboxylic acids on CNTs. Modification of CNTs with small molecules has been reported extensively. Covalent macromolecular modification of CNTs has also made progress, but the modification is not easy and more work is needed.

In 2000, Riggs et al. [195] prepared polymer-modified CNTs soluble in both organic and aqueous solutions. The surface-bound carboxylic acid groups produced by acid treatment of CNTs were converted to acylchloride groups and then reacted with the linear copolymer poly-(propionyl-ethylenmine)-*co*-ethylenmine (PPEI-EI). In this way, the CNTs can be attached to the linear polymer, just like 'fishing'. According to the scanning tunneling microscopy (STM) results of Czerw et al. [196], the solubilized tubes appear homogeneous, containing the repeat units of the hexagonal structure along the tube axis presenting a self-assembled pattern. They also report the polymer-bound solubilized nanotubes to be luminescent. The luminescence is dependent on the excitation wavelength and can cover the entire visible range with quantum yields up to 0.1. Using similar strategies, Czerw et al. also realized covalent functionalization of CNTs by other polymers, such as PVA-VA, PVK-PS, and PS [197,198]. The functionalization breaks up nanotube bundles, a step which is essential for solubility.

For various polymer functionalized CNTs, there is direct microscopy evidence for wrapping of the polymer around individual nanotubes. Their solubilization provides opportunities for solution NMR studies of the CNTs. Although no meaningful nanotube carbon signals could be detected in ^{13}C solution NMR measurements of solubilized CNTs (including ^{13}C-enriched samples), both ^{1}H and ^{13}C NMR results provide valuable information on the functional groups in functionalized SWNT and MWNT samples in solution. Usually, the ^{1}H NMR signals of the attached moieties become very broad, which is believed to be associated with diamagnetic species of low mobility, the nanotube-attached moieties. The optical limiting of the PPEI-EI-CNTs was measured in a chloroform solution using nanosecond laser pulses at 532 nm [199]. The relatively weaker optical limiting effect suggests a different optical limiting mechanism from the nonlinear scattering mechanism for CNT suspensions [200].

The featureless absorption of PVK–SWNT is an indication of successful functionalization of SWNTs, in which the introduction of sp^3-hybridized carbon atoms disrupts the extended π-network of the bare sp^2-hybridized nanotubes (Fig. 9). The Raman spectrum of pristine SWNTs displays an intense

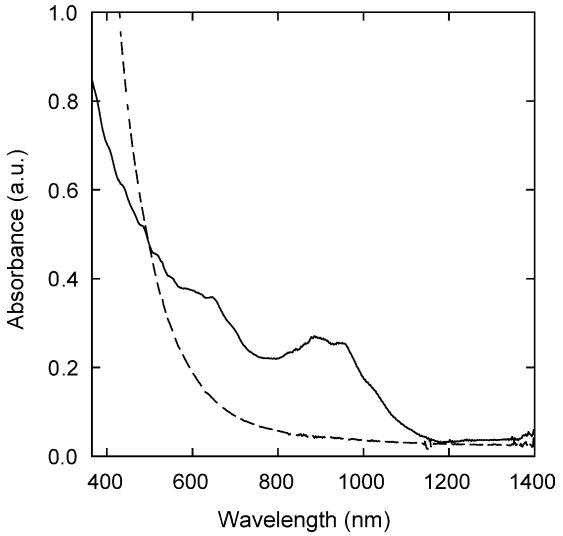

Fig. 9. UV–Vis–NIR absorption spectra of SWNT (solid line) in DMF and PVK–SWNT (dashed line) in chloroform.

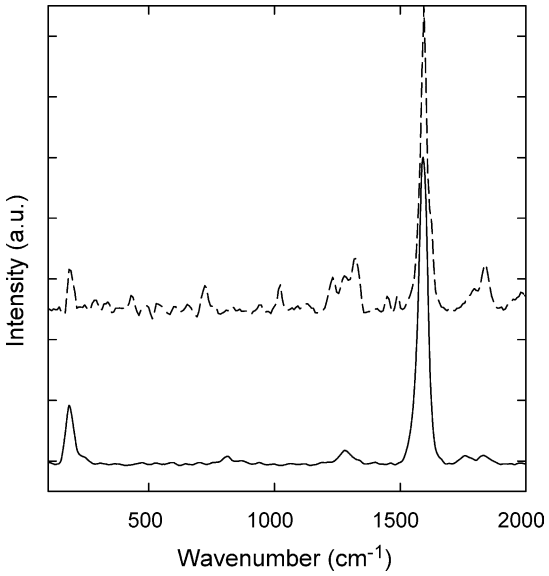

Fig. 10. Raman spectra of pristine SWNT (solid line) and PVK–SWNT (dash line).

peak at 1595 cm^{-1}, attributable to the E_{2g} tangential mode, with a small disorder-induced peak at 1280 cm^{-1} (D line). There is an also clear characteristic peak in the radial breathing mode (RBM) spectral region. The corresponding Raman spectrum of PVK–SWNT displays an intense peak at 1595 cm^{-1} together with other peaks derived from PVK. Compared with that of pristine SWNT, the intensity of the D line of PVK–SWNT at 1280 cm^{-1} is obviously increased (Fig. 10). This is an expected result of introduction of covalently bound moieties on the CNT framework, wherein some of the sp^2 carbons have been converted to sp^3 by hybridization [201]. Meanwhile, the existence of the RBM Raman line of the PVK–SWNT sample in the low-frequency range strongly suggests that the tubular structures of the sample are retained. Surprisingly, there is evidence of photo-induced electron transfer from PVK to SWNTs, which was detected by LESR. There are no ESR signals for both pure PVK and PB samples either with or without UV illumination. The ESR spectrum of pristine SWNTs shows only a very strong ferromagnetic resonance signal that is not affected by illumination. However, the ESR spectrum of PB-SWNT displays a strong, symmetric signal at $g \approx 2.003$ (where g is the electron g-factor) with peak-to-peak linewidth $\Delta H_{pp} \approx 2.7$ G. The g-value is similar to that of Haddon's solubilized SWNTs ($g = 2.003 \pm 0.001$) [194]. Under UV light illumination, no change in the signal was observed. The ESR spectrum of PVK–SWNT (Fig. 11), however, reveals a relatively wide unsymmetric line shape with $g \approx 2.004$ and $H_{pp} \approx 7.1$ G. When the sample was illuminated, two additional photoinduced spin signals were resolved at $g \approx 1.997$ with $\Delta H \approx 14$ G, and at $g \approx 2.009$ with $\Delta H \approx 20$ G, while the signal at $g = 2.004$ did not change. As the ESR spectra of PB-SWNT and pristine PVK do not change under the same illumination, the two new signals in the ESR spectrum of PVK–SWNT must be due to photoinduced interaction between PVK and SWNT. The g-value of 2.009 is assigned to $(PVK)^+$, and the other g-value of 1.997 can be assigned to the $SWNT^-$. Thus the new spin signals under illumination indicate that there is photoinduced electron transfer from PVK to SWNTs.

Recently, Yao et al. [202], Qin et al. [203] and Kong et al. [19] reported grafting of polymer chains from the ends and sidewalls of SWNT or MWNT via ATRP. Yao et al. [202] attached phenol groups to single-walled CNTs using the 1,3-dipolar cycloaddition reaction, then derivatized the phenols with 2-bromoisobutyryl bromide. These initiators were found to be active in the polymerization of methyl

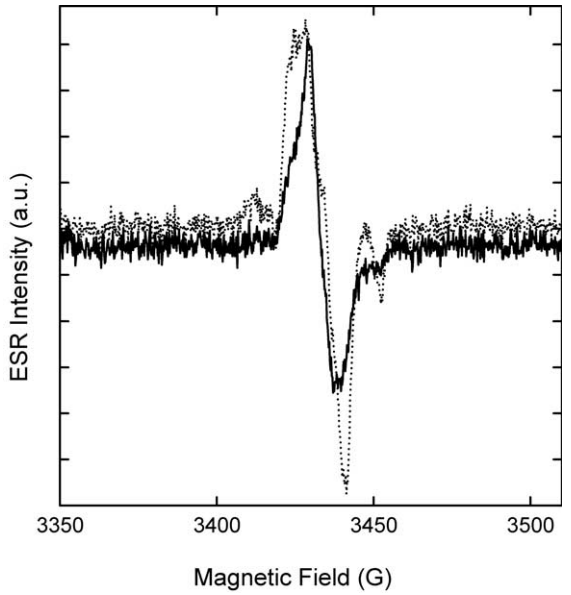

Fig. 11. ESR spectra of PVK–SWNT without (solid line) and with (dotted line) UV illumination.

methacrylate and *tert*-butyl acrylate from the surface of the nanotubes; but the polymerizations were not controlled, leading to production of high molecular weight polymers with relatively large polydispersities. Qin et al. [203] and Kong et al. [19] first introduced carboxylic acid groups on SWNT or MWNT by nitric acid oxidation and then covalently attached the ATRP initiator (2-hydroxyethyl-2′-bromopropionate) to the SWNT or MWNT. Qin et al. added methyl 2-bromopropionate (MBP) as free initiator during the grafting to control growth of the graft chains and to monitor the polymerization kinetics. Experimental results show that the molecular weight of free poly(*n*-butyl methacrylate) (PBMA) increased linearly with BMA monomer conversion. PBMA cleaved from the SWNT after high conversion had the same molecular weight as PBMA produced in solution. Kong et al. not only prepared the homopolymer grafting chain from MWNT, but also prepared block copolymer grafting chain from MWNT. Through this modification, MWNT-PMMA and MWNT-PMMA-*b*-PHEMA can be well dispersed in a suitable solvent, forming a stable, clear, transparent systems. The best 'solubility' of MWNT-PMMA-*b*-PHEMA is around 0.8 mg/ml. The modification of CNTs with biomacromolecules is of great current interest because of potential uses, such as building blocks in complex nanostructures, or in very sensitive, reversible biosensors. Baker et al. [204] and Khitrov [205] recently made a covalent adduct of DNA to SWNTs. The carboxylic acid groups on the surface of the nanotubes were converted to amide functionalities which were then treated with the cross-linker succinimidyl 4-(*N*-maleimidomethyl) cyclohexane-1-carboxylate (SMCC) to produce maleimide functionalized nanotubes. In the final step, the maleimide groups were covalently attached to DNA (Scheme 43). The assemblies were detected by labeling the DNA with a fluorescein dye group and measuring its photoluminescence, or by linking unlabeled DNA to the tubes and then hybridizing the DNA-SWNT adducts with dye labeled DNA. They demonstrate that despite being strongly bound to a SWNT, the DNA retains all the chemical properties of a free molecule. Thus, the covalent attachment would still allow the utilization of the DNA-SWNT adduct in very selective binding assays or the construction of complex nanostructures, and would result in systems with improved stability.

Williams et al. [206] unite SWNTs with the specific molecular-recognition features of DNA by coupling SWNTs to peptide nucleic acid (PNA, an uncharged DNA analog). The SWNTs with carboxylic acid groups on the surface were dispersed in DMF and incubated in 1-ethyl-3-(3-dimethylaminopropyl) carbodiimide hydrochloride and *N*-hydroxysuccinimide (NHS) to form SWNT-bearing NHS esters. PNA adducts were formed by reacting this material in DMF for 1 h with excess PNA (sequence: NH2-Glu-GTGCTCATGGTG-$CONH_2$, where Glu is a glutamate residue and the central block represents

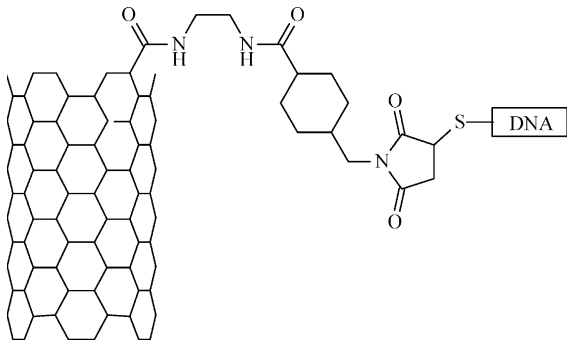

Scheme 43. DNA modified SWNTs [204].

nucleic-acid bases). AFM confirmed that fragments of double-stranded DNA were hybridized to the PNA-SWNT (Scheme 44). This method may provide a new, versatile means of incorporating SWNTs into larger electronic devices by recognition-based assembly, and of using SWNTs as probes in biological systems by sequence-specific attachment.

Huang et al. [207] functionalized CNTs with bovine serum albumin (BSA) via diimide-activated amidation under ambient conditions. The nanotube-BSA conjugates thus obtained are highly water-soluble, and nearly all the protein in the nanotube-BSA conjugates remains bioactive. Dwyer et al. [208] also proved that CNTs with surface-bound carboxylic acid groups can be functionalized with amino-terminated DNA strands.

4.3. Noncovalent modification of CNTs with polymers (polymer wrapping)

Like the fullerene-doped conducting polymer systems we discussed in Section 3, the CNT-doped conducting polymer systems also exhibit effective and noneffective doping in the ground state. Effective doping can improve the miscibility of CNTs with conducting polymers.

The sp^2 bonded graphene structures at the sidewalls of CNTs contain highly delocalized π electrons which can form functionalized CNTs with other π electron-rich compounds through π–π interaction. This organic functionalization method does not destroy the intrinsic structures of CNTs and gives structurally intact CNTs with functionalities. Recently, the potential interaction between the highly delocalized π-electrons of CNTs and the π-electrons correlated with the lattice of the polymer skeleton has generated much interest and provided the motivation for studying the optical and electronic properties of composites of CNTs and π-conjugated polymers.

An international group of investigators [209–215] doped CNTs into poly(*m*-phenylenevinylene-*co*-2,5-dioctoxy-*p*-phenylene vinylene) (PmPV) (Scheme 65), a conjugated luminescent polymer, and obtained a CNT-PmPV composite formed through π–π interaction. They found that the solution of the semiconjugated organic polymer was capable of suspending nanotubes indefinitely, while the accompanying amorphous graphite settled out. This method can be used to purify CNTs effectively and non-destructively [210–212]. A fairly strong interaction between SWNTs and PmPV was further demonstrated [209] by transmission electron microscopy and STM. The spectroscopic behavior of the composite was dramatically affected by CNT doping (effective doping in the ground state) [209]. Moreover, after doping by a small amount of MWNTs, the electrical conductivity of the polymer is increased by up to eight orders of magnitude. Composite light-emitting diodes

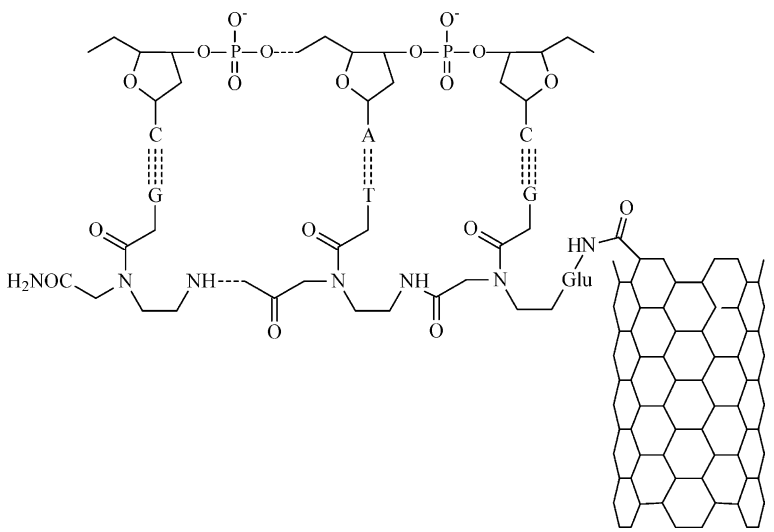

Scheme 44. PNA modified SWNTs [206].

(LEDs) fabricated from such solution show lifetimes up to five times longer than LEDs without MWNTs in air. The authors suggested that the MWNTs act as heat sinks in the polymer matrix dissipating the heat generated in the PmPV during operation [213]. Star et al. [216] also prepared a composite material based on PmPV wrapped SWNTs. They also confirmed the strong interaction of PmPV with SWNTs. They found that the surface coverage becomes highly uniform and the average diameter of the SWNT bundles decreases as the polymer concentration is increased.

Ago et al. [217,218] studied the electronic interaction between photoexcited poly(*p*-phenylene vinylene) (PPV) and MWNTs using absorption, photoluminescence (PL) and PIA spectroscopy. They found that the MWNTs interact strongly with the photoexcited PPV, while there is no significant interaction in the ground state (noneffective doping in the ground state). There was a slight blue-shift (40 meV) of the strongest PPV peak in the absorption spectrum of the composite. This blue-shift signifies that the effective π-conjugation length of PPV is shortened in the composite, because the local nanoscopic structure of PPV modified by MWNTs leads to more intrachain disorder. However, apart from the small change of the peak position, there was no significant change in the absorption spectrum of the composite, indicating the absence of electronic interaction in the ground state of PPV and MWNTs. In addition, the PL and PIA quenching in the PPV–MWNT composite is regarded as a consequence of electronic interaction between PPV and MWNTs, and the main electronic interaction is energy transfer from photoexcited PPV to the MWNTs. It is believed that the high efficiency arises from a complex interpenetrating network of PPV chains with MWNTs and the relatively high work function of the MWNT film. The present results suggest the possible application of CNTs as a new interesting electrode material in macroscale devices.

Star et al. [216] demonstrated that PmPV and nanotube components of a wrapped structure are in intimate electrical contact. They considered that this probably results from the helical conformation of PmPV, which aids in overcoming steric barriers to wrapping. This nanotubes/polymer composite behaves like a photoamplifier, producing a current of a thousand and more electrons for each photon the polymer absorbs. In the meantime, the electrical properties of SWNTs are largely unperturbed by the associated polymer. In addition, Steuerman et al. [219] investigated the composite of SWNTs and poly{(2,6-pyridinylene-vinylene)-*co*-[(2,5-dioctyloxy-*p*-phenylene)vinylene]} (PPyPV) (Scheme 45), which can also promote solubilization of SWNTs in chloroform. The fundamental difference between PPyPV and PmPV is that the former is a base and is readily protonated by addition of HCl. Steuerman et al. found that the SWNT/PPyPV interaction lowers the pK_a of PPyPV. For PmPV-wrapped tubes, the wavelength dependence of this effect correlates with the absorption spectrum of PmPV. For PPyPV, the wavelength dependence correlates with the

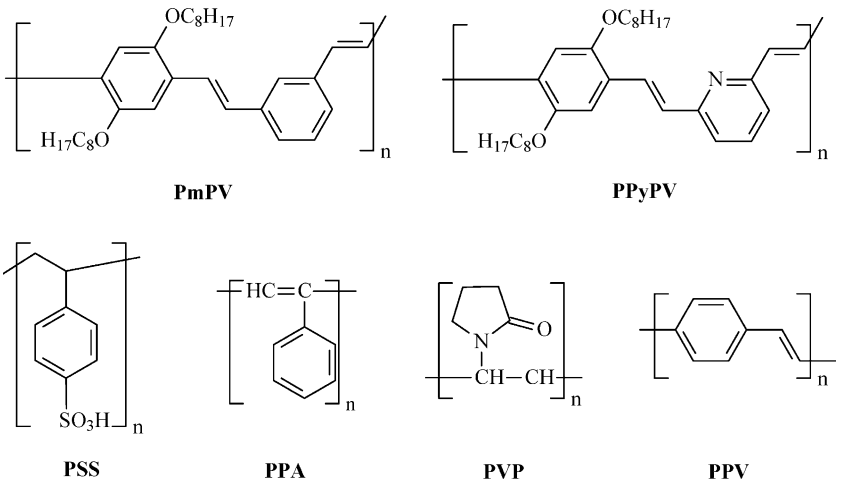

Scheme 45. Selected polymers that can noncovalently modify CNTs.

absorption spectrum of protonated PPyPV, indicating that SWNTs assist in charge stabilization.

In situ polymerization of a conducting polymer in the presence of nanotubes is also a good method to improve the miscibility of CNTs and conducting polymer. Tang et al. [220] prepared MWNTs-containing poly(phenylacetylene) (PPAs) by in situ catalytic polymerization of phenylacetylene in the presence of nanotubes. They found that the nanotubes in CNT/PPAs were helically wrapped with PPA chains. Short nanotubes thickly wrapped with PPA chains are soluble in common organic solvents including THF, toluene, chloroform, and 1,4-dioxane. Shearing of the CNT/PPA solutions readily aligns the nanotubes along the direction of the applied mechanical force. The nanotubes exhibit a strong photostabilization effect, protecting the PPA chains from photodegradation under intense laser irradiation with incident fluence as high as 10 J/cm^2. This CNT/PPA nanocomposite also shows good optical limiting properties. Fan et al. [221, 222] obtained a new type of polymer-wrapped CNTs by in situ polymerization of conducting polypyrrole (PPY) on MWNTs. Cochet et al. [223] reported the synthesis of MWNT composite with polyaniline (PANI). They found that in situ polymerization led to effective site-selective interactions between the equinoid ring of PANI and the MWNTs, facilitating charge transfer between the two components. This confirmed the formation of an overall material, which is more conducting than the starting components. Zengin et al. [224] also reported the preparation of PANI/MWNT composite by in situ methods. They found the composite to exhibit an order magnitude increase in electrical conductivity over neat PANI, and found that the MWNTs were well dispersed and isolated.

O'Connell et al. [225] found SWNTs could be solubilized in water by noncovalently associating them with linear polymers, most successfully with polyvinyl pyrrolidone (PVP) and polystyrene sulfonate (PSS) (Scheme 45). They proposed a general thermodynamic interpretation, wherein the polymer drove the wrapping by disrupting both the hydrophobic interface with water and the smooth tube–tube interactions in the aggregates. The nanotubes could be unwrapped by changing the solvent system. This solubilization process opens the door to solution chemistry on pristine nanotubes, as well as their introduction into biologically relevant systems.

In addition to the CNT doped conducting polymer composites, many papers have been concerned with CNT doped nonconducting polymer systems. Because of their good elasticity and extremely high Young's modulus [9,10], as well as their high aspect ratios, CNTs are expected to find uses as effective reinforcing additives in composite materials. Many studies carried out on CNT/polymer composites [12, 226–230] show that three main factors greatly influence the reinforcement of the CNT/polymer composites: (1) good dispersion of the CNTs in the polymer matrix [12,226–228], (2) strong interfacial bonding between CNTs and polymer [228–230], and (3) good alignment of the CNTs in the polymer matrix [213,231–233]. Because of the weak interaction between polymer matrix and CNTs and the strong van der Waals forces between CNTs, CNTs tend to agglomerate in composites and the composite strength may not be effectively enhanced by CNTs. It has been suggested that sufficient dispersion is one of the key factors needed to realize nano-reinforcement of the composite. Various approaches have been taken to improve the dispersion of MWNTs in a polymer matrix: Gong et al. [226] used nonionic surfactants to aid the dispersion of CNTs in epoxy, which resulted higher T_g and elastic modulus; Jin et al. [227] used PVDF to assist the melt-blending of MWNTs in PMMA, which led to a significant improvement in the storage modulus of the MWNT/PMMA composite at low temperatures.

Recently, chemical functionalization of CNTs has been realized, and high solubility of CNTs in some solvents can be achieved [187,193,234]. This is very important for application of CNTs as additives for reinforcement of polymer materials because the functionalization of CNTs not only simplifies the fabrication process of CNT/polymer composites, but also improves the interfacial bonding between the polymer matrix and the CNT. Preliminary results are encouraging but further studies are needed.

5. Applications

5.1. Photoconductivity

The photoconductivity of a conducting polymer can be markedly enhanced by doping with C_{60}. C_{60}

doped polymers that have been studied include PVK [151], PMPS [158], and OO-PPV [11]. The performance of these materials is comparable with some of the best photoconductors available, such as thiapyrylium dye aggregates [235]. Interestingly, PMPS shows no detectable surface discharge upon illumination under tungsten lamp light because of its low charge-generation efficiency. When 1.6 mol% C_{60} was doped into PMPS, the photoinduced discharge rate increased several orders of magnitude. Similar results were obtained when the samples were irradiated with monochromatic irradiation at 340 nm. Fig. 12 shows that C_{60}-doped PMPS film has low dark conductivity, and the photo-induced discharge is fast and complete. These properties are very important for electron-photographic applications. C_{60}-doped PMPS and polycarbonate film doped with thiapyrylium dye, one of the best commercial photoconductors, have comparable photo-induced discharge responses over a 40-fold change in tungsten light intensity.

In 1999, Gu et al. [236] synthesized fullerenated polymethylphenylsilane (C_{60}-PMPS) by two methods: (1) synthesis of PMPS via a Wurtz type reduced coupling reaction followed by a Friedel–Crafts reaction with C_{60}; (2) by direct copolymerization of dichloromethylphenylsilane with C_{60}. They found that the C_{60} moieties were bonded to the pendant benzene ring of PMPS by the Friedel–Crafts reaction and incorporated into the main chain by direct copolymerization. The C_{60}-PMPS copolymers

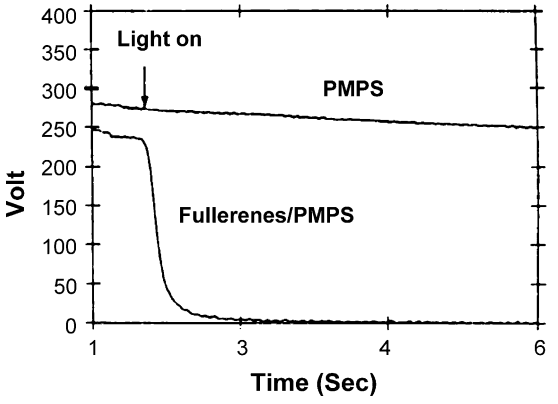

Fig. 12. Comparison of photo-induced discharge curves of PMPS and PMPS/C_{60}. Reprinted with permission from Ref. [158] (J Am Chem Soc 1993;115(9):3844–5, Copyright (2000) American Chemical Society).

prepared by direct copolymerization have very good photoconductivity in contrast with pure PMPS and Friedel–Crafts C_{60}-PMPS, which show hardly any photoconductivity.

In the PVK/C_{60} system [237–240], charge-generation might be due either to excitation of fullerene (followed by electron hopping from carbazole to fullerene) or to direct excitation of the fullerene/carbazole CT complex. Because the absorption spectrum of the C_{60}/carbazole CT complex differs from that of pure C_{60} by a broadened absorption in the 500 nm region, it is very difficult to distinguish the two possibilities from the spectra alone. We studied these spectra and proved the existence of fullerene/carbazole CT complexes by several methods. Incorporation of C_{60} into the PVK chain by covalent bonds improves the miscibility of C_{60} and PVK, and the photoconductivity is greatly enhanced [237]. *N*-vinylcarbazole copolymers with different C_{60} contents were synthesized in lithium naphthalene-initiated anionic polymerization reactions by Chen [238]. ^{13}C NMR provided strong evidence for the covalent attachment of PVK units to the C_{60} core. This system has very good photoconductivity. Using a very simple method, we [239] prepared C_{60} grafted PVK and found that the photoconductivity of PVK is enhanced greatly by grafted C_{60}. The decay half time $t_{1/2}$ of the light is only 0.35 s, and film forming properties are also improved. To increase the miscibility of C_{60} with polymer, some soluble chains, such as 2-(1′,1′,2′,2′-tetracyanomethanoxymethano) fullerene have to be bonded to C_{60} [240]. Doping this compound into PVK, Long et al. [240] found much higher photoconductivity than could be obtained by doping with pure C_{60}.

The photoconductivity of the OO-PPV/C_{60} system has also been studied in detail [11]. The photoconductivity is strongly enhanced by introduction of a small amount of C_{60}. However, the photoconductivity tends to saturate at C_{60} concentrations exceeding 5 mol%. Similar enhancement of photoconductivity by doping PMPS with C_{60} was also reported [158]. This enhancement can be interpreted in terms of photoinduced charge transfer, and is observed when the top of the valence band of the conducting polymer is at lower energy than the LUMO of C_{60}. Yoshino et al. [11] gave the energy diagram of OO-PPV/C_{60} (Fig. 13), and proposed that electron transfer from

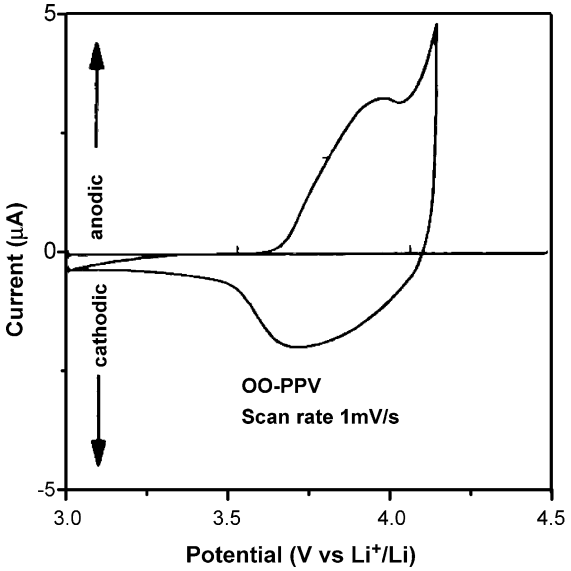

Fig. 13. Cyclic voltammogram of OO-PPV in 0.1 mol/l LiBF4/-propylene carbonate and lithium plates as counter and reference electrodes, respectively. Reprinted with permission from Ref. [11] (Jpn J Appl Phys 2 1993;32(3A):L357–360, Copyright (1993) The Institute of Pure and Applied Physics).

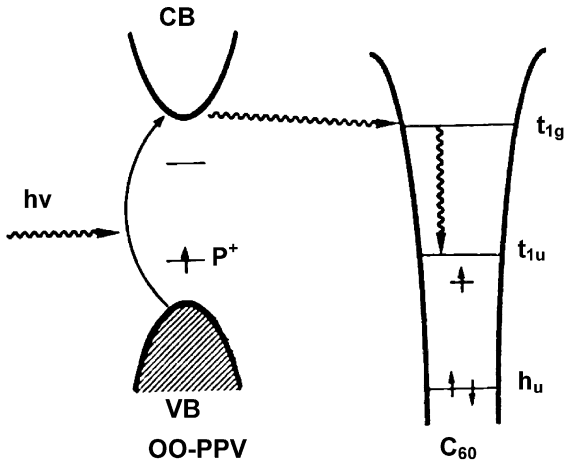

Fig. 14. Energy diagram of OO-PPV and C_{60}. Reprinted with permission from Ref. [11] (Jpn J Appl Phys 2 1993;32(3A):L357–60, Copyright (1993) The Institute of Pure and Applied Physics).

OO-PPV to C_{60} is difficult in the ground state. Upon irradiation of light with photon energy exceeding the band gap energy (2.2 eV) of OO-PPV, the interband optical transition will create excitons or exciton-polarons (Ex-P) in OO-PPV. The migration from the Ex-P to the vicinity of neutral C_{60} is an autoionization process (Fig. 14), since electron tunneling from the Ex-P level to t_{1g} or t_{1u} states of C_{60} is favored. The probability of this tunneling (or photon-assisted hopping) is determined by the overlapping of π orbitals of OO-PPV and C_{60} and the extent of Ex-P. Electrons transferred to C_{60} by this photoinduced charge-transfer process relax to immobile negative polarons $C_{60}^{\cdot -}$, but holes in OO-PPV relax to mobile positive polarons $P^{\cdot +}$, resulting in the enhancement of photoconductivity. This enhancement is observed over a C_{60} concentration range from 1 or 2 mol% to saturation. This can be explained as follows: for enhancement of photocarrier generation, the photo-excited Ex-P must encounter a C_{60} molecule during its lifetime. There is one C_{60} molecule per 50–100 monomer units of OO-PPV at a concentration of 1–2 mol% of C_{60}. Hence, the enhancement of photo-conductivity mainly occurs in the concentration range below 1–2 mol%, suggesting that Ex-P migrates along about 50–100 monomer units during its lifetime. At higher concentrations of C_{60} to saturation, the Ex-P will encounter C_{60} more frequently and the lifetime of mobile positive polarons P^+ may become shorter. Thus no further enhancement of photoconductivity will occur.

Interestingly, we found that C_{60} can enhance the photoconductivity of nonconducting as well as conducting polymers. A series of C_{60}-MMA copolymers synthesized by free radical polymerization [241] showed obvious photoconductivity. In order to obtain unambiguously structured nonconducting polymeric C_{60} derivatives, we prepared two kinds of side-chain polymeric C_{60} derivatives [242]. In one type, C_{60}-containing polystyrene resins with C_{60} in the side-chains at mass fractions about 2.9, 6.7 and 11%, photoconductivity increases markedly with increasing C_{60} content. Another system is C_{60}-containing styrene-acrylamide (St-Am) copolymer [243], in which the maximal C_{60} content in the copolymer is 1.45 wt.%. Experimental results indicate that these polymers with 1.45% C_{60} have good photoconductivity; $t_{1/2}$ of the best one is about 1.88 s. The photoconductivity can be enhanced by increasing the C_{60} content. We also studied the photoconductivity of a PVK/MWNTs blend [244]. A PVK/MDDA (didecylamine modified MWNT) blend showed good photoconductivity. However, the PVK/MWNT blend

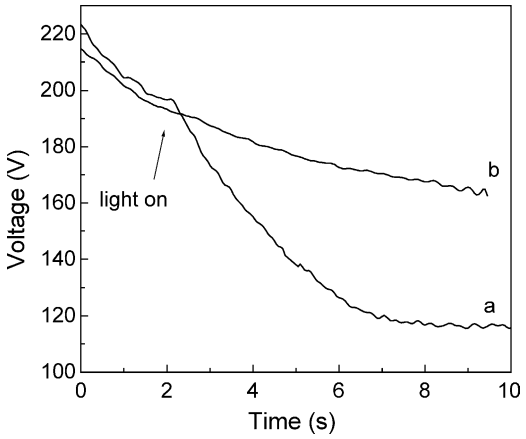

Fig. 15. Qualitative comparison of photo-induced discharge curves for (a) PVK/MDDA blend and (b) PVK/pMWNT blend. Reprinted with permission from Ref. [244] (Chem Phys Lett 2002;364(1–2):196–9, Copyright (2002) Elsevier).

exhibited little photoconductivity (Fig. 15). Fluorescence studies indicated that MDDA can act as an electron acceptor in either the ground or excited state, while PVK serves as an electron donor. As solubilized CNTs can improve the mobility and the dispersibility of CNTs, the solubilized CNTs may be used to improve the interaction with certain polymers in CNT/polymer composites.

It can be predicted that, with further study, polymer composites with C_{60} or CNT will be developed into practical photoconductive materials. In the near future, these materials should find uses in photoelectric, electrophotographic, and other devices.

5.2. Photorefractivity

The potential application of photorefractive (PR) materials is in data storage devices. The photorefractive effect has been observed in a variety of inorganic crystals, such as $LiNbO_3$, $KNbO_3$ and $LiTaO_3$. Organic and polymeric materials are potential candidates for nonlinear optical (NLO) applications because of their NLO properties, high optical damage threshold, and easy processability [245]. The requirements for the photorefractive effect can be fulfilled simultaneously in an organic composite containing both photoconductive and electro-optic components. Polymers doped with C_{60} have been studied extensively in last decade. Zhang et al. [246] reported the observation of photorefractivity in a charge transport polymer system, i.e. PVK doped with fullerene and a second-order NLO molecule, diethyl-amino-nitrostyrene (DEANST) (with a first hyper-polarizability of $\beta = 2.2 \times 10^{-20}$ esu). Study of the electric-field dependence of the photocharge, generation quantum efficiency, and four-wave mixing diffraction efficiency showed that this system fulfills the three necessary characteristics for a photorefractive material (absorption, photoconduction, and electron-optic activity). Degenerate four-wave mixing demonstrated the existence of the photorefractive effect, and a maximum diffraction efficiency of 2×10^{-5} was obtained. PVK doped with a liquid crystal, 4-butyloxy-4′-cyanobiphenyl, and C_{60} was studied by a two-beam coupling experiment [247]. The results showed that the photorefractivity is enhanced by phase separation. A hybrid photorefractive liquid-crystal cell was prepared with PVK as a photoconduction layer [248]. The hybrid structure increased the diffraction efficiency and transmittance by eliminating light loss by undesirable scattering of the incident beam through the liquid-crystal cell. The use of a photoalignment layer in the hybrid liquid-crystal structure resulted in a gain coefficient over 900 cm^{-1}, diffraction efficiency over 13%, and transmittance over 85%. These results indicate that the hybrid cell design can provide high efficiency for many applications in real-time holography and data storage devices.

Acrylate-type copolymers (TPA-DCV) consisting of a triphenylamine (TPA) unit as a hole transport agent and dicyanovinyl aniline (DCV) as a second-order NLO chromophore on a side chain were synthesized by Park et al. [249]. The polymers showed good solubility and sufficient morphological stability after film formation. The diffraction efficiency and gain coefficient increased as the glass transition temperature decreased TPA-DCV composite doped with fullerene (C_{60}) and dibutyl phthalate had a high photoconductivity of 5.1×10^{-12} S/cm at an applied electric field of 50 V/μm. Diffraction efficiency and response rate were measured as functions of the parameters determining the photoconductivity (e.g. applied electric field, the density of the photocharges generated, and writing beam intensity). The maximum diffraction efficiency, gain coefficient, and maximum response time were

12.9%, 64 cm^{-1}, and 700 ms, respectively, at an applied electric field of 80 V/μm. Photoconductivity, response rate, and diffraction efficiency increased with increasing applied field. The field dependence of the response rate is attributed to the charge generation efficiency and/or the drift mobility. A similar power dependence of photoconductivity and response rate on the writing beam intensity was observed. The response rate and diffraction efficiency showed a good linear relationships with the logarithm of the photoconductivity.

Ono and Kawatsuki [250,251] observed high-performance photorefractivity in the thick-grating regime for high-molar-mass liquid crystal (H-LC) and low-molar-mass liquid crystal (L-LC) mixtures (HL-LCMs) doped with C_{60}. The photorefractive performance strongly depended on the concentration ratio of H-LC and L-LC. A high net gain coefficient over 600 cm^{-1} was achieved with low applied DC fields (0.7 V/μm) and a fringe spacing of 2.8 mm. The gain coefficients and the resolution increased with increasing concentration of H-LC. The photorefractive grating formation time was varied between 0.12 and 3.5 s, depending on the concentration of H-LCs. In view of the above findings, we anticipate that C_{60} doped conducting polymer or LC systems have high potential for applications to real-time holography and data storage devices. Development of better preparative methods can be expected to lead to major improvements in photorefractivity.

5.3. Photovoltaic cells and photodiodes

Photoinduced electron transfer between semiconducting conjugated polymers and fullerenes has recently attracted considerable scientific and technological attention. 'Bulk heterojunction' polymer photovoltaic devices and photodiodes have been constructed with composite films of semiconducting polymer as electron donors and fullerene derivatives as electron acceptors [252,253]. The primary step in these polymer photovoltaic devices is an ultrafast photoinduced electron transfer reaction at the donor–acceptor interface, which results in a metastable charge-separated state. The quantum efficiency of this step is assumed to be close to unity [254,255]. However, the overall conversion efficiency of these devices is limited by the carrier collection efficiency, which is greatly influenced by the morphology of the active film [253,256]. In order to achieve better performance of fullerene-based photovoltaic devices, novel types of 'double-cable' polymer photovoltaic devices and photodiodes have been constructed very recently in which the p-type conjugated backbones (donor-cable) bear directly grafted or tethered fullerene moieties (acceptor-cable). In this way, the effective donor/acceptor interfacial area is maximized, while phase separation and clustering phenomena should be prevented. In addition, the interaction between the donor conjugated backbone and the acceptor moieties may be tuned by varying the chemical structure (nature and length) of their connecting fragment [257].

In 2001, Rarcos et al. [42,258] reported the preparation of a solar cell based on a novel double-cable polymer (Scheme 12). Compared with the corresponding pristine polymer, the photoluminescence of C_{60} linked polymers in toluene solution was quenched by two orders of magnitude. Photoluminescence quenching was also observed in thin solid films. The quenching mechanism is believed to be photoinduced electron transfer. Accordingly, the photoinduced Vis–NIR absorption spectrum of the C_{60} linked polymers in the solid state exhibits the band typical of methanofullerene radical-anions at about 1.2 eV accompanied by two broad bands, at 0.62 and 1.53 eV, characteristic of positive polarons on a conjugated chain. The lifetime of the photogenerated charges in the C_{60} linked polymers extends to the millisecond time domain.

Photovoltaic devices based on the C_{60} linked polymers were fabricated by spin-coating [42]. Current vs. voltage (*I*/*V*) curves recorded in the dark and under white-light illumination (100 mW cm^{-2}) revealed a J_{SC} value of 0.42 mA cm^{-2}, V_{OC} = 830 mV, and FF = 0.29. The IPCE showed an onset at 550 nm and a maximum of 6% at 480 nm. It is worthy of note that the performance of this first example of double-cable based solar cells, which were not optimized, is already competitive with that of devices prepared following the *p*/*n*-heterojunction as well as the 'bulk-heterojunction' approaches [252,253,259]. Moreover, this performance is given by a double-cable with a fullerene loading of 31.5 wt%, a value considerably smaller than that commonly used in 'bulk-heterojunction' solar cells (about 75 wt%).

Zhang et al. [41] reported another interesting family of soluble double-cable copolythiophenes carrying fulleropyrrolidine moieties (Scheme 11). Copolymers contained 7 mol% fullerene monomer (corresponding to 14.5 wt% n:m = 93:7) and 14 mol% (corresponding to 24.2 wt%, n:m = 43:7) of fullerene monomer, respectively. Both copolymers exhibited a color change from orange to blue upon exposure to chloroform vapor at room temperature. In this blue-phase, both copolymers displayed a broad electronic absorption band covering a wide range of the solar spectrum, which is in itself an interesting property for PV materials. The solubility of *a* and *b* allowed the fabrication of photodiodes. The devices based on *b*, the more highly fullerene-loaded double-cable, showed an IPCE more than twofold higher than that of devices prepared with *a*. A significant improvement of the IPCE was obtained in both cases after treating the photoactive films with chloroform just before evaporation of the Al electrode. This effect reflects the change in the absorption spectra while going from the orange to the bluephase of the copolymers. Devices prepared using *b* where characterized under monochromatic light (λ = 505 nm) illumination with an intensity of 0.1 mW cm^{-2}. The FF was 0.25 and the power conversion efficiency was 0.6%. The diodes not treated with chloroform gave the highest photovoltages, V_{OC} = 750 mV. This value is higher than that reported for PEOPT/C_{60} 'bulk-heterojunction' solar cells [246]. After treatment with chloroform vapor, the V_{OC} of the device dropped to 450 mV. This behavior is a consequence of the altered energy levels between the orange and the blue phases [260].

Nava et al. [261] prepared fullerene-containing polyesters by polycondensation of bifunctional fullerene adducts with tetraethyleneglycol or polyethyleneglycol (Scheme 46a and b). These polymers show both good solubility in common organic solvents and good film-forming properties. One of the compounds was fabricated into solar cells together with MDMO-PPV (Scheme 46). Although the cell performance was poor, probably due to the presence of the large solubilizing groups attached to the fullerene monomer, Nava et al. believe that device performances could be improved by optimizing the processing of the fullerene-functionalized polymer/MDMD-PPV active layer.

Oligo(*p*-phenylenevinylene)-fullerene dyads were prepared by several research groups in order to avoid the incompatibility and macrophase separation problem of regular fullerene-based photovoltaic devices [98,262–266]. For example, Eckert et al. [262,263] synthesized fullerene-OPV hybrids (a) and (b) in Scheme 47 through 1,3-dipolar cycloaddition of azomethine ylides to C_{60}. Photovoltaic devices incorporating these hybrids produced a photocurrent, showing that photoinduced electron transfer takes place. However, the efficiency of the devices is limited by the fact that photoinduced electron transfer from the OPV moiety to the C_{60} sphere must compete with an efficient energy transfer.

Janssen et al. [255] synthesized a homologous series of oligo(*p*-phenylene vinylene)-

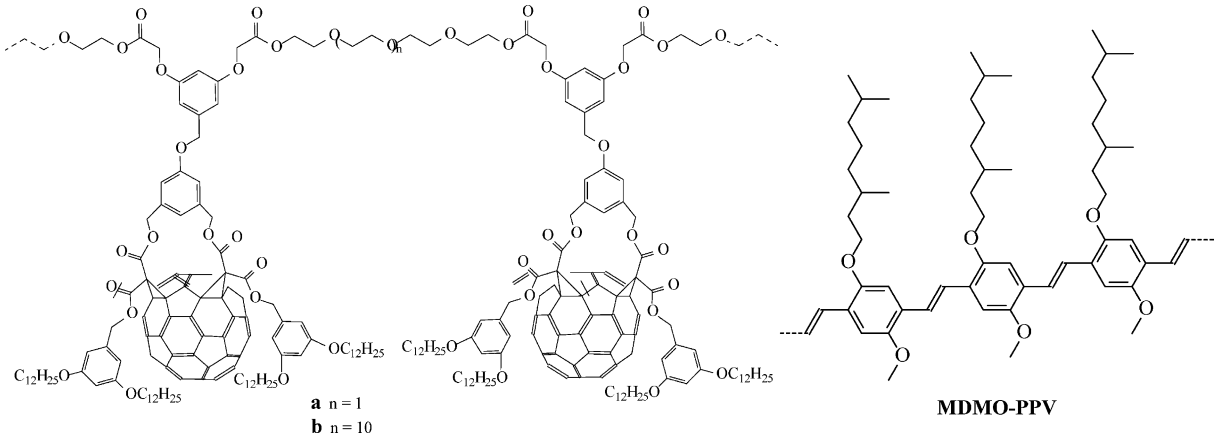

Scheme 46. C_{60}-containing polyesters and MDMO-PPV [261].

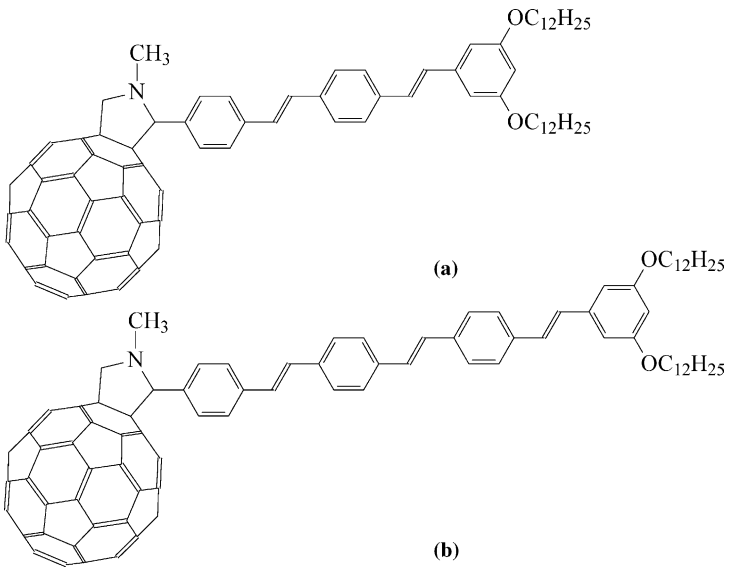

Scheme 47. Oligo(*p*-phenylene vinylene)-fullerene dyads [262].

fulleropyrrolidines (Scheme 48). The photophysical properties of these donor–acceptor dyads and the corresponding model compounds and *N*-methylfulleropyrrolidine were studied as a function of the conjugation length in solvents of different polarity and as thin films. Fast singlet energy transfer occurred in an apolar solvent after photoexcitation of the oligo(*p*-phenylene vinylene) (OPV) adjacent to the fullerene. Photoexcitation of the dyads in a polar solvent resulted in electron transfer in *c* and *d* and to some extent in *b*, but not for *a*. In thin solid films of *c* and *d*, a long-lived charge-separated state is was formed after photoexcitation. The long lifetime in the film was attributed to the migration of charges to different molecules. A flexible photovoltaic device was prepared from *d*, indicating that the donor–acceptor dyads form a bicontinuous donor–accepter network. This may be an important clue for design of more efficient molecular bulk heterojunction materials.

Beside the applications in photovoltaic devices and photodiodes, polymer-modified fullerenes can also be used to fabricate organic light-emitting devices. Wang et al. [267] fabricated a multilayer organic light-emitting device by mixing together a C_{60}-based poly(phenylene vinylene) dyad and an emissive conjugated polymer POMPV (Scheme 49). Their primary study showed that the PPV-C_{60} dyad can improve the light-emitting performance.. For example, the maximum luminance of the device is higher than that of the pure-POMPV device. The mechanism of the enhancement is under investigation. Using this composite [209,210], Wang et al. also fabricated photovoltaic devices and obtained quantum efficiency of 1.8% at 2.9–3.2 eV, about twice that of the standard ITO device.

5.4. Optical limiting

Owing to their unique molecular symmetry with π electrons highly delocalized over nearly spherical surfaces, fullerenes, especially C_{60}, possess exhibit

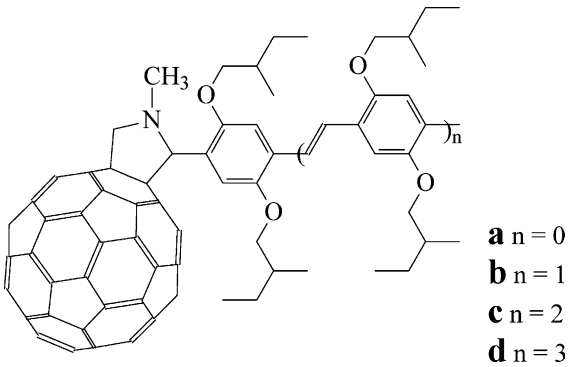

Scheme 48. Oligo(*p*-phenylene vinylene)-fulleropyrrolidines [255].

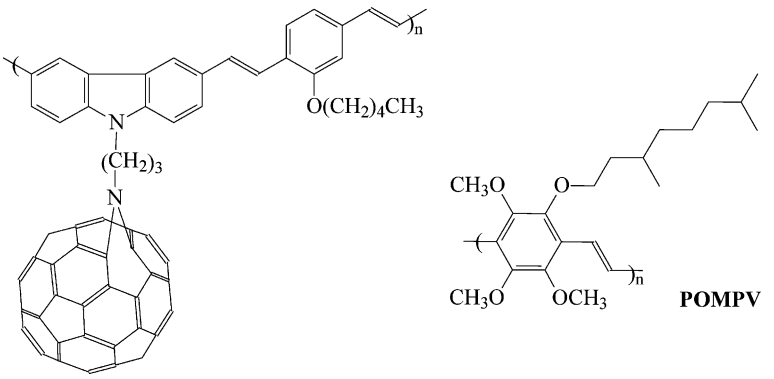

Scheme 49. C_{60}-based poly(phenylene vinylene) dyad and POMPV [267].

highly NLO properties [13]. One of the most attractive NLO properties of fullerenes is optical limiting [268–272]. Optical limiting occurs when the optical transmission of a material decreases with increasing laser fluence [268], a property that is desirable for protection of sensors and human eyes from intense laser radiation. For laser radiation at 532 nm, C_{60} and its derivatives are among the best materials showing optical limiting properties. The mechanism of optical limiting of C_{60} and its derivatives is believed to be reverse saturable absorption (RSA), which occurs when excited states formed through optical pumping of the ground state have a higher absorption cross-section than the ground state [268–271].

For practical application, it is necessary to make solid-state optical limiting devices. In this context, C_{60}-doped polymer matrices has been investigated [153,272,273]. However, as C_{60} itself is hardly processible into a solid optical material, owing to its very low solubility in most organic solvents, preparation of fullerene derivatives with better solubility, but maintaining the NLO properties of C_{60}, are obviously crucial to obtaining better optical limiting devices. One strategy is functionalization of C_{60} with solubilized polymers.

The first optical limiting study of polymer-bound C_{60} was reported by Kojima et al. in 1995 [274]. The polystyrene-bound C_{60} was prepared by high-pressure polymerization of styrene in the presence of C_{60}. The optical limiting of a circular disk made from the resulting C_{60}-bound polymer was measured by using a frequency-doubled Nd:YAG laser with an 8 ns pulse width. The limiting was about five times greater than that of a C_{60} styrene solution.

Sun et al. [275] prepared linear polystyrene-bound C_{60} (Scheme 50) in which the fullerene cages are covalently attached to polystyrene chains, in primarily pendant linkages, by a Friedel–Crafts type reaction using $AlCl_3$ catalyst. These soluble pendant C_{60}–PS polymers have better defined structures than the copolymers reported by Kojima et al. The optical limiting behavior of the polymer is attributed to the nonlinear absorptions of the pendant C_{60}, which follow the RSA mechanism. Although the optical limiting of the polystyrene-bound C_{60} at 532 nm (Nd:YAG laser) is not as good as that of pristine C_{60} in solution, this polymer can be fabricated into supported or free-standing films of high optical quality. Since C_{60} cages are polymer-bound, their dispersion in the films should be homogeneous. Such polymer films may well play a significant role in the development of optical limiting devices.

Lu et al. [276] synthesized copolymers of benzylaminofullerene ($C_{60}H_2(NHCH_2C_6H_5)_2$) with methyl methacrylate or ethyl methacrylate by free-radical

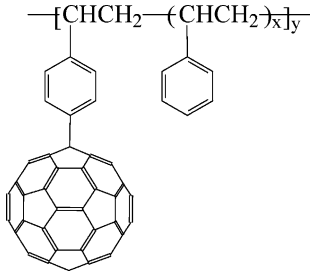

Scheme 50. Polystyrene-bound C_{60} [275].

copolymerization. These copolymers have relatively good solubility in THF. Although benzylaminofullerene homopolymer shows good optical limiting performance comparable to that of C_{60}, the optical limiting of all of the copolymers is much weaker.

Tang et al. synthesized a series of copolymers of C_{60} with phenylacetylene (PA), with 1-phenyl-1-propyne (PP), and with 1-phenyl-1-butyne (PB), initiated by catalysts such as $MoCl_5Ph_4Sn$, and WCl_6-Ph_4Sn, etc. [92,277]. The resulting copolymers are soluble, stable, and film-forming. They contain up to 9.1 wt% C_{60} cages. The authors claim that the C_{60} cages are incorporated into the polymer structures through cyclopropanation reactions resulting in methanofullerene structures. For the PP modified C_{60}, only one, or at most two, poly-PP chains are bound to one C_{60} cage on average. However, for the PB modified C_{60}, usually more than two poly-PB chains are bound to one C_{60}, resulting in multiple addition patterns of the C_{60} cage. The authors' optical limiting investigation shows that at 532 nm (Nd:YAG laser) the poly-PP bound C_{60} exhibits much better optical limiting performance than C_{60} in solution at a linear transmission of 43%. Under the same experimental conditions, the multiple poly-PB chains bound C_{60} is also a better optical limiter than C_{60}. This is not consistent with other results from other research groups showing that that C_{60} derivatives with multiple addition patterns show much weaker optical limiting responses compared with the corresponding mono-addition C_{60} derivative as well as pristine C_{60}. This behavior is probably due to the high degree of functionalization of the fullerene cage as well as the involvement of optical limiting mechanisms other than RSA [278,279].

The optical limiting behavior of star polymer of polystyrene-modified C_{60} (C_{60}-(PSx)y) was studied by Venturini et al. [280]. In their experiments, two, four and six polystyrene arms of controllable length were grafted directly on the C_{60} cage in order to prevent aggregation of C_{60} cages and consequently to permit achievement of high C_{60} concentrations (equivalent to a solution of up to 37 mM). The optical limiting behavior of thin films made from pure PS–C_{60} or mixtures of PS–C_{60} and PS at various concentrations was measured below the damage threshold using nanosecond 532 nm laser radiation. It is clear that the two-arm $C_{60}(PS)_2$ entity, which exhibits recognizable residual bands of the C_{60} absorption spectrum, has a better optical limiting performance than structures having 4 or 6 PS arms. Venturini et al. suggested that polystyrene is not the best matrix since the damage threshold is rapidly reached. Further work has to be carried out to improve the optical limiting properties of such promising macromolecules up to the optical quality level required for practical NLO device applications.

Recently, fullerodendrimers were also studied for their optical limiting properties. Rio et al. [71] attached poly(aryl ether) dendritic branches terminated with peripheral triethyleneglycol chains to C_{60} cages to obtain a series of poly(aryl ether) modified fullerodendrimers. These fullerodendrimers (Scheme 21) were easily incorporated in mesoporous silica glasses and its optical limiting properties were measured by the frequency-doubled Nd:YAG laser emission at 532 nm. The pulse duration is about 30 ps, which is considerably shorter than the intersystem crossing time and the observed increase in absorption is dominated by the population of the excited singlet state. For all the compounds, transmission remains nearly constant for fluences lower than 3–10 mJ cm^{-2}. When the intensity increases above this threshold, the effect of induced absorption appears, and the transmission diminishes rapidly, thus showing the potential of these materials for optical limiting applications.

6. Conclusion and prospects for the future

With the development of fullerene organic chemistry, many low-molecular organic reactions can be used in polymeric modification of fullerene. By controlling the functional groups in polymers and reaction conditions, many well-defined fullerene polymers, such as side-chain fullerene polymers, main-chain fullerene polymers, dendritic fullerene polymers, star-shaped fullerene polymers, fullerene end-capped polymers, and so on, have been prepared. At the same time, many living polymerization methods have been introduced into the preparation of the polymer fullerenes. By anionic polymerization, well-defined six-arm star-shaped fullerene polymers can be obtained (the iniferter technique allows well-defined arms for the star fullerene polymer to be synthesized). With ATRP, mono- or bi-substituted

fullerene polymers with well-controlled polymer chain length can be prepared. Thus it is now possible to control the architecture of fullerene polymers precisely by methods that constitute a good platform for the practical applications of fullerene derivatives.

Covalent bonding of polymer chains to CNTs is a new field. The section on polymeric CNTs in this review shows that polymeric modification of CNTs is in its beginnings, but is destined to play an important role in research and development on CNT-based materials. The combination of the unique properties of CNTs with various functional polymers offers many opportunities for research in chemistry, physics, and materials science, that will produce novel materials with unusual electrical, magnetic, and optical properties.

Doping fullerene into polymer systems has found more and more uses in preparation of electronic and optical materials. Many conducting polymers doped with C_{60} and its derivatives have been studied. Among them, three interaction modes can be distinguished. (i) There are interactions between the ground-state wave functions of the polymer and C_{60}, as in P3OT/C_{60}. Upon photoexcitation, complete charge separation can occur from conducting polymer to C_{60}. (ii) There is no interaction between the ground-state wave functions of the polymer and C_{60}, but upon photoexcitation, photoinduced charge transfer can occur from conducting polymer to C_{60}, as in PPV/C_{60} and PMPS/C_{60} composites, etc. (iii) No charge transfer occurs in the ground state or upon photoexcitation, as in PHDK/C_{60} composite. The differences among (i), (ii) and (iii) type composites arise because the polymers in cases (i) and (ii) have nondegenerate ground states, whereas the polymers in case (iii) have a degenerate ground state. Thus, in case (iii), photoinduced charge transfer is 'short-circuited' by a competing process, and the short-circuited process is related to the formation of soliton–antisoliton pairs.

Conventional polymers such as polyethylene and polystyrene have been used as matrices for the functional composites. The structure and properties of these composites are strongly dependent on the properties and concentrations of the active component. In order to improve miscibility, many C_{60} derivatives have been used in composites.

Owing to the special electrochemical behavior and versatile chemical reactivity of C_{60} and CNTs, polymers with C_{60} or CNTs possess a broad range of potential applications, such as photosensitive drums for static copying machines, digital data storage media, photovoltaic cells and photodiodes, and optical limiting devices. Now, many opportunities can be expected to arise for combining fullerenes and CNTs with the familiar classical materials.

Acknowledgements

This work was supported by the National Science Foundation of China (Grant Nos 50173005, 20374012, and 50203015), the Major State Basic Research Development Program of China (Grant No. G2000077500), and The Chinese Academy of Sciences.

References

[1] Kroto HW, Heath JR, O'Brien SC, Curl RF, Smalley RF. C_{60} -buckminsterfullerene. Nature 1985;318(6042):162–3.
[2] Dornenburg E, Hintenberger H. Das auftreten vielatomiger kohlenstoffmolekule im hochfrequenzfunken zwischen graphitelektroden. Z Naturforsch Teil A 1959;14(8):765.
[3] Kratschmer W, Lamb LD, Fostiropoulos K, Huffman DR. Solid C_{60}—a new form of carbon. Nature 1990;347(6291): 354–8.
[4] Nakamura E, Isobe H. Functionalized fullerenes in water. The first 10 years of their chemistry, biology, and nanoscience. Acc Chem Res 2003;36(11):807–15.
[5] Nakamura E, Tahara K, Matsuo Y, Sawamura M. Synthesis, structure and aromaticity of a hoop-shaped cyclic benzenoid [10]-cyclophenacene. J Am Chem Soc 2003;125:2834–5.
[6] URL of Frontier Carbon; 2002. http://www.f-carbon.com/
[7] Iijima S. Helical microtubules of graphitic carbon. Nature 1991;354(6348):56–8.
[8] Treacy MMJ, Ebbesen TW, Gibson JM. Exceptionally high Young's modulus observed for individual carbon nanotubes. Nature (Lond) 1996;381(6584):678–80.
[9] Wong EW, Sheehan PE, Lieber CM. Nanobeam mechanics: elasticity, strength, and toughness of nanorods and nanotubes. Science 1997;277(5334):1971–5.
[10] http://www.rtpcompany.com/info/flyers/ntc.pdf
[11] Yoshino K, Yin XH, Muro K, Kiyomatsu S, Morita S, Zakhidov AA, et al. Marked enhancement of photoconductivity and quenching of luminescence in poly(2,5-dialkoxy-*p*-phenylene vinylene) upon C_{60} doping. Jpn J Appl Phys 1993;32(3A):L357–L360.

[12] Dalton AB, Collins S, Munoz E, Razal JM, Ebron VH, Ferraris JP, et al. Super-tough carbon-nanotube fibres—these extraordinary composite fibres can be woven into electronic textiles. Nature 2003;423(6941):703–3.
[13] Shinar J, Vardeny ZV, Kafafi ZH, editors. Optical and electronic properties of fullerenes and fullerene-based materials. New York: Marcel Dekker; 2000.
[14] Ruoff RS, Tse DS, Malhotra R, Lorents DC. Solubility of C_{60} in a variety of solvents. J Phys Chem 1993;97(13):3379–83.
[15] Taylor R, Walton DRM. The chemistry of fullerenes. Nature 1993;363(6431):685–93.
[16] Hirsch A. The chemistry of the fullerenes—an overview. Angew Chem Int Ed 1993;32(8):1138–41.
[17] Diederich F, Thilgen C. Covalent fullerene chemistry. Science 1996;271(5247):317–23.
[18] Prato M. [60]Fullerene chemistry for materials science applications. J Mater Chem 1997;7(7):1097–109.
[19] Kong H, Gao C, Yan D. Controlled functionalization of multiwalled carbon nanotubes by in situ atom transfer radical polymerization. J Am Chem Soc 2004;126(2):412–3.
[20] Kadish KM, Ruoff RS, editors. Fullerenes: chemistry, physics, and technology. New York: Wiley; 2000.
[21] Hirsch A, editor. Fullerenes and related structures. Berlin: Springer; 1999.
[22] Sariciftci NS. Role of buckministerfullerene, C_{60}, in organic photoelectric device. Prog Quant Electr 1995;19:131–59.
[23] Geckeler KE, Samal S. Syntheses and properties of macromolecular fullerenes, a review. Polym Int 1999;48: 743–57.
[24] Prato M. Fullerene materials. Top Curr Chem 1999;199: 173–84.
[25] Nierengarten JF. Fullerodendrimers: fullerene-containing macromolecules with intriguing properties. Top Curr Chem 2003;228:87–110.
[26] Shi S, Khemanikc KC, Li QC, Wudl F. A polyester and polyurethane of diphenyl-C61—retention of fulleroid properties in a polymer. J Am Chem Soc 1992;114(26):10656–7.
[27] Geckeler KE, Hirsch A. Polymer-bound C_{60}. J Am Chem Soc 1993;115(9):3850–1.
[28] Kuwashima SY, Kubota M, Kushida K, Ishida T, Ohashi M, Nogami T. Synthesis and structure of nitrene-C_{60} adduct, C_{60} nphth(phth = phthalimido). Tetrahedron Lett 1994;35(25): 4371–4.
[29] Sun YP, Liu B, Morton DK. Preparation and characterization of a highly water-soluble pendant fullerene polymer. Chem Commun 1996;(24):2699–700.
[30] Hawker CJ. A simple and versatile method for the synthesis of C_{60} copolymers. Macromolecules 1994;27(17):4836–7.
[31] Wang CC, Shu C, Fu SK. Synthesis of polystyrene with C-60 in the side group. Chem J Chin Univ 1996;17(9):1477–81.
[32] Lu ZH, Goh SH, Lee SY. Synthesis of fullerene-containing poly(alkyl methacrylate)s with narrow polydispersities. Polym Bull 1997;39(6):661–7.
[33] Goh HW, Goh SH, Xu GQ. Synthesis and miscibility studies of [60] fullerenated poly(2-hydroxyethyl methacrylate). J Polym Sci Polym Chem 2002;40(8):1157–66.
[34] Sato H, Matsuda D, Ogino K. Synthesis and polymerization of methacrylate having fullerene. Polym J 1998;30(11): 904–9.
[35] Ferraris JP, Yassar A, Loveday DC, Hmyene M. Grafting of buckminsterfullerene onto polythiophene: novel intramolecular donor–acceptor polymers. Opt Mater 1998;9(1–4): 34–42.
[36] Wang ZY, Kuang L, Meng XS, Gao JP. New route to incorporation of [60] fullerene into polymers via the benzocyclobutenone group. Macromolecules 1998;31(16): 5556–8.
[37] Kraus A, Mullen K. [60] Fullerene-containing poly(dimethylsiloxane)s: easy access to soluble polymers with high fullerene content. Macromolecules 1999;32(13): 4214–9.
[38] Li FY, Li YL, Guo ZX, Zhu DB, Song YL, Fang GY. Synthesis and optical limiting properties of polycarbonates containing fullerene derivative. J Phys Chem Solids 2000; 61(7):1101–3.
[39] Tang BZ, Leung SM, Peng H, Yu NT, Su KC. Direct fullerenation of polycarbonate via simple polymer reactions. Macromolecules 1997;30(10):2848–52.
[40] Liu B, Bunker CE, Sun YP. Preparation and characterization of soluble pendant [60]fullerene-polystyrene polymers. Chem Commun 1996;10:1241–2.
[41] Zhang F, Svensson M, Andersson MR, Maggini M, Bucella S, Menna E, et al. Soluble polythiophenes with pendant fullerene groups as double cable materials for photodiodes. Adv Mater 2001;13(24):1871–4.
[42] Ramos AM, Rispens MT, van Duren JKJ, Hummelen JC, Janssen RAJ. Photoinduced electron transfer and photovoltaic devices of a conjugated polymer with pendant fullerenes. J Am Chem Soc 2001;123(27):6714–5.
[43] Fang H, Wang S, Xiao S, Li Y, Shi Z, Du C, et al. Synthesis and characterization of new dyads containing different percentages of C_{60} and PPV covalently linked macromol. Chem Phys 2002;203:1931–5.
[44] Wang S, Xiao SX, Li YL, Shi ZQ, Du CM, Fang HJ, et al. Synthesis and characterization of new C_{60}-PPV dyads containing carbazole moiety. Polymer 2002;43(7):2049–54.
[45] Yang J, Lin H, Wang S, Li Y, Bai F, Zhu D. Photophysical characteristics of soluble oligo(*p*-phenylenevinylene)-fullerene dyad. J Polym Sci Polym Chem 2001;39:3981–8.
[46] Chen Y, Cai RF, Huang ZE, Kong SQ. A novel and versatile method for the synthesis of soluble fullerenated polymers. Polym Bull 1995;35(6):705–10.
[47] Chen Y, Huang ZE, Cai RF, Kong SQ, Chen SM, Shao QF, et al. Synthesis and characterization of soluble C_{60} chemically modified poly(*p*-bromostyrene). J Polym Sci Polym Chem 1996;34(16):3297–302.
[48] Cai RF, Bai X, Chen Y, Huang ZE. Preparation and structural characterization of C_{70} chemically modified poly(*N*-vinylcarbazole). Eur Polym J 1998;34(1):7–12.
[49] Dai LM, Mau AWH, Griesser HJ, Spurling TH, White JW. Grafting of buckminsterfullerene onto polydiene—a new route to fullerene-containing polymers. J Phys Chem 1995; 99(48):17302–4.

[50] Dai LM, Mau AWH, Zhang XQ. Synthesis of fullerene- and fullerol-containing polymers. J Mater Chem 1998;8(2): 325–30.
[51] Dai LM, White JW. Soluble conducting polymers from polyisoprene. Polymer 1991;32(12):2120–7.
[52] Dai LM. Charge-transfer complexes between polyacetylene-type polymers and iodine in solution. J Phys Chem 1992; 96(15):6469–71.
[53] Dai LM, Mau AWH, Griesser HJ, Winkler DA. Conducting polymers from polybutadiene—molecular-configuration effects on the iodine-induced conjugation reactions. Macromolecules 1994;27(23):6728–35.
[54] Sanchez L, Rispens MT, Hummelen JC. A supramolecular array of fullerenes by quadruple hydrogen bonding. Angew Chem Int Ed 2002;41(5):838–40.
[55] Benincori T, Brenna E, Sannicolo F, Trimarco L, Zotti G, Sozzani P. The first charm bracelet conjugated polymer: an electroconducting polythiophene with covalently bound fullerene moieties. Angew Chem Int Ed 1996;35(6):648–51.
[56] Gugel A, Belik P, Walter M, Kraus A, Harth E, Wagner M, et al. The repetitive Diels–Alder reaction: a new approach to [60]fullerene main-chain polymers. Tetrahedron 1996; 52(14):5007–14.
[57] Okamura H, Terauchi T, Minoda M, Fukuda T, Komatsu K. Synthesis of 1,4-dipolystyryldihydro[60]fullerenes by using 2,2,6,6-tetramethyl-1-polystyroxypiperidine as a radical source. Macromolecules 1997;30(18):5279–84.
[58] Nie B, Rotello VM. Thermally controlled formation of fullerene-diene oligomers and copolymers. Macromolecules 1997;30(13):3949–51.
[59] Taki M, Takigami S, Watanabe Y, Nakamura Y, Nishimura J. Synthesis of polyesters containing the [60]fullerene moiety in the main chain. Polym J 1997;29(12): 1020–2.
[60] Xiao L, Shimotani H, Ozawa M, Li J, Dragoe N, Saigo K, et al. Synthesis of a novel fullerene pearl-necklace polymer, poly(4,4*-carbonylbisphenylene *trans*-2-fullerenobisacetamide). J Polym Sci Polym Chem 1999;37:3632–7.
[61] Yu G, Gao J, Hummelen JC, Wudl F, Heeger AJ. Polymer photovoltaic sells—enhanced efficiencies via a network of internal donor–acceptor heterojunctions. Science 1995; 270(5243):1789–91.
[62] Kohler A, Dos Santos DA, Beljonne D, Shuai Z, Bredas JL, Holmes AB, et al. Charge separation in localized and delocalized electronic states in polymeric semiconductors. Nature 1998;392(6679):903–6.
[63] Yu G, Gao J, Yang C, Heeger AJ. Future generation photovoltaic technologies. AIP Conf Proc 1997;404:317–24.
[64] Hecht S, Frechet JMJ. Dendritic encapsulation of function: applying nature's site isolation principle from biomimetics to materials science. Angew Chem Int Ed 2001;40(1):74–9.
[65] Gorman CB, Smith JC. Structure–property relationships in dendritic encapsulation. Acc Chem Res 2001;34(1):60–71.
[66] Rio Y, Accorsi G, Nierengarten H, Rehspringer J-L, Honerlage B, Kopitkovas G, et al. Fullerodendrimers with peripheral triethyleneglycol chains: synthesis, mass spectrometric characterization, and photophysical properties. New J Chem 2002;26(9):1146–54.
[67] Nierengarten J-F, Armaroli N, Accorsi G, Rio Y, Eckert JF. [60]Fullerene: a versatile photoactive core for dendrimer chemistry. Chem Eur J. 2003;9(1):37–41.
[68] Stiriba SE, Frey H, Haag R. Dendritic polymers in biomedical applications: from potential to clinical use in diagnostics and therapy. Angew Chem Int Ed 2002;41(8): 1329–34.
[69] Wooley KL, Hawker CJ, Frechet JMJ, Wudl F, Srdanov G, Shi S, et al. Fullerene-bound dendrimers-soluble, isolated carbon clusters. J Am Chem Soc 1993;115(21):9836–7.
[70] Hawker CJ, Wooley KL, Frechet JMJ. Dendritic fullerene—a new approach to polymer modification of C_{60}. J Chem Soc Chem Commun 1994;8:925–6.
[71] Rio Y, Accorsi G, Nierengarten H, Rehspringer JL, Honerlage B, Kopitkovas G, et al. Fullerodendrimers with peripheral triethyleneglycol chains: synthesis, mass spectrometric characterization, and photophysical properties. New J Chem 2002;26(9):1146–54.
[72] Murata Y, Ito M, Komatsu K. Synthesis and properties of novel fullerene derivatives having dendrimer units and the fullerenyl anions generated therefrom. J Mater Chem 2002; 12:2009–20.
[73] Brettreich M, Hirsch A. A highly water-soluble dendro[60]-fullerene. Tetrahedron Lett 1998;39(18):2731–4.
[74] Berberan-Santos MN, Fedorov A, Brettreich M, Schonberger H, Hirsch A, Leach S, et al. Photophysics and photochemistry of a water-soluble C_{60} dendrimer: fluorescence quenching by halides and photoinduced oxidation of I-Texier I. J Phys Chem A 2001;105(45):10278–85.
[75] Dardel B, Deschenaux R, Even M, Serrano E. Synthesis, characterization, and mesomorphic properties of a mixed [60]fullerene-ferrocene liquid-crystalline dendrimer. Macromolecules 1999;32(16):5193–8.
[76] Dardel B, Guillon D, Heinrichb B, Deschenaux R. Fullerene-containing liquid-crystalline dendrimers. J Mater Chem 2001;11:2814–31.
[77] Bunker CE, Lawson GE, Sun YP. Fullerene-styrene random copolymers, novel optical properties. Macromolecules 1995; 28:3744–6.
[78] Cao T, Webbers SE. Free radical copolymerization of styrene and C_{60}. Macromolecules 1996;29(11):3826–30.
[79] Chen Y, Lin KC. Radical polymerization of styrene in the presence of C_{60}. J Polym Sci Polym Chem 1999;37:2969–75.
[80] Ford WT, Nishioka T, McCleskey SC, Mourey TH, Kahol P. Structure and radical mechanism of formation of copolymers of C_{60} with styrene and with methyl methacrylate. Macromolecules 2000;33(7):2413–23.
[81] Chiang LY, Wang LY, Tseng SM, Wu JS, Hsieh KH. Fullerenol derived urethane-connected polyether dendritic polymers. J Chem Soc Chem Commun 1994;(23):2675–6.
[82] Wang L, Chiang LY, Kuo CS, Lin JG, Huang CY. Mater Res Soc Symp Proc 1996;413:571.

[83] Ederle Y, Mathis C. Grafting of anionic polymers onto C_{60} in polar and nonpolar solvents. Macromolecules 1997;30(9): 2546–55.
[84] Ederle Y, Mathis C. Carbanions on grafted C_{60} as initiators for anionic polymerization. Macromolecules 1997;30(15): 4262–7.
[85] Mathis C, Ederle Y, Nuffer R. Palm-tree and dumbbell like polystyrene structures based on C_{60}. Synth Met 1999;103: 2370–1.
[86] Ederle Y, Mathis C. Palm-tree and dumbbell like polymer architecture based on C_{60}. Macromolecules 1999;32(3): 554–8.
[87] Mathis C, Nunige S, Audouin F, Nuffer R. Thermal stability of a C_{60}–polystyrene bond. Synth Met 2001;121(1–3):1153–4.
[88] Pantazis D, Pispas S, Hadjichristidis N. Synthesis and stability of linear and star polymers containing [C_{60}] fullerene. J Polym Sci Polym Chem 2001;39:2494–507.
[89] Mignard E, Hiorns RC, Francois B. Synthesis and characterization of star copolymers consisting of fullerene and conjugated polyphenylene: 6-star-C_{60}[styrene-poly(1,4-phenylene)-*block*-polystyrene] and 6-star-C_{60}[polystyrene-*block*-poly(1,4-phenylene). Macromolecules 2002;35(16):6132–41.
[90] Anantharaj V, Wang LY, Canteenwala T, Chiang LY. Synthesis of starburst hexa(oligoanilinated) C_{60} using hexanitro[60]fullerene as a precursor. J Chem Soc Perkin Trans 1999;22:3357–66.
[91] He JD, Wang J, Li SD, Cheung MK. New synthetic method for soluble starlike C_{60}-bonding polymers. J Appl Polym Sci 2001;81:1286–90.
[92] Tang BZ, Xu HY, Lam JWY, Lee PPS, Xu KT, Sun QH, et al. C_{60}-containing poly(1-phenyl-1-alkynes): synthesis, light emission, and optical limiting. Chem Mater 2000;12: 1446–55.
[93] Weis C, Friedrich C, Muelhaupt R, Frey H. Fullerene-end-capped polystyrenes, monosubstituted polymeric C_{60} derivatives. Macromolecules 1995;28(1):403–5.
[94] Wang CC, He JP, Fu SK, Jiang KJ, Cheng HZ, Wang M. Synthesis and characterization of the narrow polydispersity fullerene-end-capped polystyrene. Polym Bull 1996;37(3): 305–11.
[95] Zhou P, Chen GQ, Hong H, Du FS, Li ZC, Li FM. Synthesis of C_{60}-end-bonded polymers with designed molecular weights and narrow molecular weight distributions via atom transfer radical polymerization. Macromolecules 2000;33(6):1948–54.
[96] Zhou P, Chen GQ, Li CZ, Du FS, Li ZC, Li FM. Synthesis of hammer-like macromolecules of C_{60} with well-defined polystyrene chains via atom transfer radical polymerization (ATRP) using a C_{60}-monoadduct initiator. Chem Commun 2000;(9):797–8.
[97] Zhang WC, Zhou P, Du FS, Li ZC, Li FM. The morphology investigation of hammer-like C_{60} conjugated polystyrene in solution. Acta Polym Sin 2001;(4):557–60.
[98] Gu T, Tsamouras D, Melzer C, Krasnikov V, Gisselbrecht P, Gross M, et al. Photovoltaic devices from fullerene oligophenyleneethynylene conjugates. Chem Phys Chem 2002;3(1):124–7.
[99] Huang XD, Goh SH, Lee SY. Miscibility of C_{60}-end-capped poly(ethylene oxide) with poly(*p*-vinylphenol). Macromol Chem Phys 2000;201(18):2660–5.
[100] Huang XD, Goh SH. Interpolymer complexes through hydrophobic interactions: C_{60}-end-capped poly(ethylene oxide)/poly(methacrylic acid) complexes. Macromolecules 2000;33(23):8894–7.
[101] Martineau C, Blanchard P, Rondeau D, Delaunay J, Roncali J. Synthesis and electronic properties of adducts of oligothienylenevinylenes and fullerene C_{60}. Adv Mater 2002;149(4):283–7.
[102] Cloutet E, Gnanou Y, Fillaut J, Astruc D. C_{60} end-capped polystyrene stars. Chem Commun 1996;13:1565–6.
[103] Chen KM, Caldwell WB, Mirkin CA. Fullerene self-assembly onto $(MeO)_3Si(CH2)_3NH_2$-modified oxide surfaces. J Am Chem Soc 1993;115(3):1193–4.
[104] Chupa JA, Xu ST, Fischetti RF, Strongin RM, Mccauley JP, Smith AB, et al. A monolayer of C_{60} tethered to the surface of an inorganic substrate—assembly and structure. J Am Chem Soc 1993;115(10):4383–4.
[105] Bergbreiter DE, Gray HN. Grafting of C_{60} onto polyethylene surfaces. J Chem Soc Chem Commun 1993;7:645–6.
[106] Bianco A, Gasparrini F, Maggini M, Misiti D, Polese A, Prato M, et al. Molecular recognition by a silica-bound fullerene derivative. J Am Chem Soc 1997;119(32):7550–4.
[107] Tajima Y, Tazuka Y, Yajima H, Ishii T. Photo-crosslinking polymers by fullerene. Polymer 1997;38(20):5255–7.
[108] Jiang A, Hamed GR. Photo-induced crosslinking of ethylene propylene diene monomer (EPDM) by buckminsterfullerene. Polym Bull 1998;40:499–502.
[109] Kojima Y, Matsuoka T, Takahashi H, Kuruchi T. High-pressure synthesis of polystyrene-bound C_{60} gel. J Appl Polym Sci 1997;65:2781–3.
[110] Nuffer R, Ederle Y, Mathis C. Preparation of networks with C60 knots using anionic polymers. Synth Met 1999;103: 2376–7.
[111] Rao AM, Zhou P, Wang KA, Hager GT, Holden JM, Wang Y, Cornett DS, Duncan MA, Amster IJ, et al. Photoinduced polymerization of C_{60} films. Science 1993; 259:955–7.
[112] Eklund PC, Rao AM, editors. Fullerene polymers and fullerene polymer composites. Berlin: Springer; 2000.
[113] Pusztai T, Oszlanyi G, Faigel G, Kamaras K, Granasy L, Pekker S. Bulk structure of phototransformed C_{60}. Solid State Commun 1999;111(11):595–9.
[114] Sun YP, Ma B, Bunker CE, Liu B. All-carbon polymers (polyfullerenes) from photochemical reactions of fullerene clusters in room-temperature solvent mixtures. J Am Chem Soc 1995;117(51):12705–11.
[115] Nisha JA, Premila M, Sridharan V, Sundar CS, Radhakrishnan TS. UV-irradiation studies on C_{70} clusters in mixed solvents. Carbon 1998;36(5/6):637–9.
[116] Cataldo F. On C_{60} fullerene photopolymerization. Polym Int 1999;48(2):143–9.
[117] Iwasa Y, Arima T, Fleming RM, Siegrist T, Zhou O, Haddon RC, et al. New phases of C_{60} synthesized at high-pressure. Science 1994;264(5165):1570–2.

[118] Rao AM, Eklund PC, Hodeau JL, Marques L, NunezRegueiro M. Infrared and Raman studies of pressure-polymerized C_{60}. Phys Rev B 1997;55(7):4766–73.
[119] Yamawaki H, Yoshida M, Kakudate Y, Usuba S, Yokoi H, Fujiwara S, et al. Infrared study of vibrational property and polymerization of C_{60} and C_{70} under pressure. J Phys Chem 1993;97(43):11161–3.
[120] Blank VD, Buga SG, Dubitsky GA, Serebryanaya NR, Popov MY, Sundqvist B. High-pressure polymerized phases of C_{60}. Carbon 1998;36(4):319–43.
[121] Takahashi N, Dock H, Matsuzawa N, Ata M. Plasma-polymerized C_{60}/C_{70} mixture films—electric-conductivity and structure. J Appl Phys 1993;74(9):5790–8.
[122] Zou YJ, Zhang XW, Li YL, Wang B, Yan H, Cui JZ, et al. Bonding character of the boron-doped C_{60} films prepared by radio frequency plasma assisted vapor deposition. J Mater Sci 2002;37(5):1043–7.
[123] Ma B, Riggs JE, Sun YP. Photophysical and nonlinear absorptive optical limiting properties of [60]fullerene dimer and poly[60]fullerene polymer. J Phys Chem B 1998; 102(31):5999–6009.
[124] Ma B, Milton AM, Sun YP. Infrared spectroscopy of all-carbon poly[60]fullerene polymer and [60]fullerene dimer model. Chem Phys Lett 1998;288(5/6):854–60.
[125] Sun YP, Bunker CE. C-70 in solvent mixtures. Nature 1993; 365(6445):398–8.
[126] Sun DY, Reed CA. Crystal engineering a linear polymer of C_{60} fullerene via supramolecular pre-organization. Chem Commun 2000;(23):2391–2.
[127] Barbour LJ, Orr GW, Atwood JL. Supramolecular assembly of well-separated, linear columns of closely-spaced C_{60} molecules facilitated by dipole induction. Chem Commun 1998;(17):1901–2.
[128] Yoshino K, Nakajima S, Park DH, Sugimoto R. Thermochromism, photochromism and anomalous temperature-dependence of luminescence in poly(3-alkylthiophene) film. Jpn J Appl Phys 1988;27(4):L716–L718.
[129] Yoshino K, Peter L. Jpn J Appl Phys 1988;27:L2388.
[130] Yoshino K, Nakao K, Sugimoto R. Poly(3-alkylthiophene) gel and its properties. Jpn J Appl Phys 1989;28(3): L490–L492.
[131] Skugimoto R, Takeda S. Chemistry Express 1988;1:639.
[132] Heeger AJ, Kivelson S, Schrieffer JR, Su WP. Solitons in conducting polymers. Rev Mod Phys 1988;60(3):781–850.
[133] Morita S, Zakhidov AA, Yoshino K. Doping effect of buckminsterfullerene in conducting polymer—change of absorption-spectrum and quenching of luminescence. Solid State Commun 1992;82(4):249–52.
[134] Morita S, Zakhidov AA, Kawai T, Araki H, Yoshino K. Electrical-conductivity and esp-spectrum of buckminsterfullerene-doped poly(3-alkylthiophene). Jpn J Appl Phys 1992; 31(7A):L890–L893.
[135] Yoshino K, Morita S, Kawai T, Araki H, Yin XH, Zakhidov AA. ICSM'92 Proc.
[136] Fox MA, Chanon M, editors. Photoinduced electron transfer, Parts A and D. Amsterdam: Elsevier; 1988.
[137] Sapurina I, Mokeev M, Lavrentev V, Zgonnik V, Trchov M, Drahomira H, et al. Polyaniline complex with fullerene C_{60}. Eur Polym J 2000;36:2321–6.
[138] Onoda M, Manda Y, Morita S, Yoshino K. Temperature-dependence of the doping effect of poly(3-alkylthiophene) and polaronic state. J Phys Soc Jpn 1989;58(6):1895–8.
[139] Harigaya K. Lattice and electronic-structures of undoped and doped C_{60} molecules by the extended su-schrieffer-heeger model. J Phys Soc Jpn 1991;60(12):4001–4.
[140] Kato T, Kodama T, Oyama M, Okazaki S, Shida T, Nakagawa T, et al. ESR and optical studies of the radical-anion of C_{60}. Chem Phys Lett 1991;186(1):35–9.
[141] Zakhidov AA. Proceedings of the International Conference on 'Electronics of Organic Materials'. Moscow: Elorma'87; 1987 p. 216.
[142] Kepler RG, Cahill PA. Photoinduced charge-transfer and charge-carrier generation in polysilane films containing C_{60} molecules. Appl Phys Lett 1993;63(11):1552–4.
[143] Thorne JRG, Williams SA, Hochstrasser RM, Fagan PJ. Radiative lifetimes of confined excitations in sigma-conjugated silane oligomers. Chem Phys 1991;157(3):401–8.
[144] Li M, Wan M. Doped polyaniline with C_{60}. Solid State Commun 1995;93(8):681–4.
[145] Smilowitz L, Sariciftci NS, Wu R, Gettinger C, Heeger AI, Wudl F. Photoexcitation spectroscopy of conducting-polymer-C_{60} composites—photoinduced electron-transfer. Phys Rev B 1993;47(20):13835–42.
[146] Marumoto K, Takeuchi N, Ozaki T, Kuroda S. ESR studies of photogenerated polarons in regioregular poly(3-alkylthiophene)-fullerene composite. Synth Met 2002; 129(3):239–47.
[147] Luzzati S, Panigoni M, Catellani M. Spectroscopical evidences of photoinduced charge transfer in blends of C60 and thiophene-based copolymers with a tunable energy gap. Synth Met 2001;116:171–4.
[148] Catellani M, Luzzati S, Mendichi R, Schieroni AG, Stein PC. Poly(3-butyl-*co*-3, 4-dibutylthiophene) copolymers: a new series of conjugated materials with a different energy-gap. Polymer 1996;37(7):1059–64.
[149] Sariciftci NS, Smilowitz L, Heeger AI, Wudl F. Photo-induced electron-transfer from a conducting polymer to buckminsterfullerene. Science 1992;258(5087):1474–6.
[150] Zoriniants G, Dyakonov V, Scharber M, Brabec CJ, Tanssen RAJ, Hummelen JC. Light-induce ESR studies in conjugated polymer-fullerene com posites. Synth Met 1999; 102:1241–2.
[151] Wang Y. Photoconductivity of fullerene-doped polymers. Nature 1992;356(6370):585–7.
[152] Yoshino K, Yin XH, Muro K, Kiyomatsu S, Morita S, Zakhidov AA, et al. Fullerene-doped conducting polymers. In: Roth S, editor. Solid-State Physics. New York: Springer; 1993. p. 286.
[153] Cha M, Sariciftci NS, Heeger AJ, Hummelen JC, Wudl F. Enhanced nonlinear absorption and optical limiting in semiconducting polymer methanofullerene charge transfer films. Appl Phys Lett 1995;67(26):3850–2.

[154] Balberg I, Naidis R, Lee MK, Shinar J, Fonseca LF. Bipolar phototransport in π-conjugated polymer/C_{60} composites. Appl Phys Lett 2001;79(2):197–9.
[155] Mort J, Machonkin M, Ziolo R, Huffman DR, Ferguson MI. Temperature-dependence of photoconductivity in buckminsterfullerene films. Appl Phys Lett 1992;60(14):1735–7.
[156] Balberg I, Naides R, San G. Temperature dependence of the phototransport properties in C_{60} films. Fullerene Sci Technol 1998;6(1):39–57.
[157] Chiu KC, Wang JS, Lin CY. Temperature dependence of the band gap in C_{60} crystals. J Appl Phys 1996;79(3):1784–7.
[158] Wang Y, West R, Yuan CH. Fullerene-doped polysilane photoconductor. J Am Chem Soc 1993;115(9):3844–5.
[159] West R. In: Patai S, Rappoport Z, editors. The chemistry of organic silicon compounds. New York: Wiley; 1989. p. 1207–40.
[160] Miller RD, Michl J. Polysilane high polymers. Chem Rev 1989;89(6):1359–410.
[161] Kepler RG, Zeigler JM, Harrah LA, Kurtz SR. Photocarrier generation and transport in sigma-bonded polysilanes. Phys Rev B 1987;35(6):2818–22.
[162] Abkowitz M, Knier FE, Yuh HI, Weagley RJ, Stolka M. Electronic transport in amorphous-silicon backbone polymers. Solid State Commun 1987;62(8):547–50.
[163] Stolka M, Yuh HJ, Mcgrane K, Pai DM. Hole transport in organic polymers with silicon backbone (polysilylenes). J Polym Sci Polym Chem 1987;25(3):823–7.
[164] Mikhailova MM, Kosyreva MM, Kamanina NV. On the increase in the charge carrier mobility in fullerene-containing conjugated organic systems. Tech Phys Lett 2002;28(6):450–3.
[165] Fujitsuka1 M, Yahata Y, Watanabe A, Ito O. Transient absorption study on photoinduced electron transfer between C60 and poly(*N*-vinylcarbazole) in polar solvent. Polymer 2000;41:2807–12.
[166] Dyakonov V, Zoriniants G, Scharber M, Brabec CJ. Photoinduced charge carriers in conjugated polymer-fullerene composites studied with light-induced electron-spin resonance. Phys Rev B 1999;59(15):8019–9025.
[167] De Ceuster J, Goovaerts E, Bouwen A, Dyakonov V, Hummelen JC. A high-frequency light-induced electron spin resonance study of conjugated polymer/fullerene composites. Synth Met 2001;124:99–101.
[168] Brabec CJ, Zerza G, Cerullo G, De Silvestri S, Luzzati S, Hummelen JC, et al. Tracing photoinduced electron transfer process in conjugated polymer/fullerene bulk heterojunctions in real time. Chem Phys Lett 2001;340:232–6.
[169] Padinger F, Brabec CJ, Hummelen JC, Janssen RAJ, Sariciftci NS. CW-photocurrent measurements of conjugated polymers and fullerenes blended into a conventional polymer matrix. Synth Met 1999;102(1–3):1285–6.
[170] El-Ghayoury A, Schenning APHJ, van Hal PA, van Duren JKJ, Janssen RAJ, Meijer EW. Supramolecular hydrogen-bonded oligo(*p*-phenylene vinylene) polymers. Angew Chem Int Ed 2001;40(19):3660–3.
[171] Schenning APHJ, Fransen M, Van Duren JKJ, Van Hal PA, Janssen RAJ, Meijer EW. Side-chain-functionalized polyacetylenes. 2. Photovoltaic properties. Macromol Rapid Commun 2002;23(4):271–5.
[172] Salaneek WR, Clark DT, Samuelsoe EJ, editors. Science and application of conducting polymers. Bristol: Hilgen; 1991.
[173] Polotskaya GA, Gladchenko SV, Zgonnik VN. Gas diffusion and dielectric studies of polystyrene–fullerene compositions. J Appl Polym Sci 2002;85(14):2946–51.
[174] Okamura H, Minoda M, Fukuda T, Miyamoto T, Komatsu K. Solubility characteristics of C60 fullerenes with two well-defined polystyrene arms in a polystyrene matrix. Macromol Rapid Commun 1999;20:37–40.
[175] Calleja FJB, Giri L, Asano T, Mieno T, Sakurai S, Ohnuma M, et al. Structure and mechanical properties of polyethylene-fullerene composites. J Mater Sci 1996;31(19):5153–7.
[176] Lua Z, Hea C, Chunga TS. Composites of multifunctional benzylaminofullerene with low-density polyethylene. Polymer 2001;42:5233–7.
[177] Brabec CJ, Dyakonov V, Sariciftci NS, Grauoner W, Leising G, Hummelen JC. Investigation of photoexcitations of conjugated polymer/fullerene composites embedded in conventional polymers. J Chem Phys 1998;109(3):1185–95.
[178] Zhang JW, Goh SH, Lee SY. Miscibility of fullerene-containing polystyrene with poly(2,6-dimethyl-1,4-phenylene oxide) and with poly(vinyl methyl ether). Macromolecules 1997;30:8069–71.
[179] Wellinghoff ST, Koenig JL, Baer E. Spectroscopic examination of chain conformation and bonding in poly(phenylene oxide)–polystyrene blends. J Polym Sci Polym Phys 1977; 15(11):1913–25.
[180] Troitskii BB, Troitskaya LS, Dmitriev AA, Yakhnov AS. Inhibition of thermo-oxidative degradation of poly(methyl methacrylate) and polystyrene by C_{60}. Eur Polym J 2000;36: 1073–84.
[181] Dresselhaus MS, Dresselhaus G, Eklund PC. Science of fullerenes and carbon nanotubes. San Diego: Academic Press; 1996.
[182] Harris PJF. Carbon nanotubes and related structures: new materials for the twenty-first century. Cambridge: Cambridge University Press; 1999.
[183] Dekker C. Carbon nanotubes as molecular quantum wires. Phys Today 1999;52(5):22–8.
[184] Ajayan PM, Charlier JC, Rinzler AG. Carbon nanotubes: from macromolecules to nanotechnology. Proc Natl Acad Sci USA 1999;96(25):14199–200.
[185] Yakobson BI, Smalley RE. Fullerene nanotubes: $C_{1,000,000}$ and beyond. Am Sci 1997;85(4):324–37.
[186] Special issue: Carbon nanotubes. Acc Chem Res 2002;34(12).
[187] Baughman RH, Zakhidov AA, De Heer WA. Carbon nanotubes—the route toward applications. Science 2002; 297(5582):787–92.
[188] Li WZ, Xie SS, Qian LX, Chang BH, Zou BS, Zhou WY, et al. Large-scale synthesis of aligned carbon nanotubes. Science 1996;274(5293):1701–3.
[189] De Heer WA, Bonard JM, Fauth K, Chatelain A, Forro L, Ugarte D. Electron field emitters based on carbon nanotube films. Adv Mater 1997;9(1):87–9.

[190] Saito S. Carbon nanotubes for next-generation electronics devices. Science 1997;278:77–8.
[191] Zhu HW, Xu CL, Wu DH, Wei BQ, Vajtai R, Ajayan PM. Direct synthesis of long single-walled carbon nanotube strands. Science 2002;296(5569):884–6.
[192] Hirsch A. Functionalization of single-walled carbon nanotubes. Angew Chem Int Ed 2002;41(11):1853–9.
[193] Bahr JL, Tour JM. Covalent chemistry of single-wall carbon nanotubes. J Mater Chem 2002;12(7):1952–8.
[194] Niyogi S, Hamon MA, Hu H, Zhao B, Bhowmik P, Sen R, et al. Chemistry of single-walled carbon nanotubes. Acc Chem Res 2002;35(12):1105–13.
[195] Riggs JE, Guo Z, Carroll DL, Sun YP. Strong luminescence of solubilized carbon nanotubes. J Am Chem Soc 2000; 122(24):5879–80.
[196] Czerw R, Guo Z, Ajayan PM, Sun YP. Organization of polymers onto carbon nanotubes: a route to nanoscale assembly. Nano Lett 2001;1(8):423–7.
[197] Hill DE, Lin Y, Rao AM, Allard LF, Sun Y-P. Functionalization of carbon nanotubes with polystyrene. Macromolecules 2002;35(25):9466–71.
[198] Sun Y-P, Fu K, Lin Y, Huang W. Functionalized carbon nanotubes: properties and applications. Acc Chem Res 2002; 35(12):1096–104.
[199] Riggs JE, Walker DB, Carroll DL, Sun YP. Optical limiting properties of suspended and solubilized carbon nanotubes. J Phys Chem B 2000;104(30):7071–6.
[200] Vivien L, Lancon P, Riehl D, Hache F, Anglaret E. Carbon nanotubes for optical limiting. Carbon 2002;40(10):1789–97.
[201] Bahr JL, Yang JP, Kosynkin DV, Bronikowski MJ, Smalley RE, Tour JM. Functionalization of carbon nanotubes by electrochemical reduction of aryl diazonium salts: a bucky paper electrode. J Am Chem Soc 2001;123:6536–42.
[202] Yao Z, Braidy N, Botton GA, Adronov A. Polymerization from the surface of single-walled carbon nanotubes—preparation and characterization of nanocomposites. J Am Chem Soc 2003;125(51):16015–24.
[203] Qin S, Qin D, Ford WT, Resasco DE, Herrera JE. Polymer brushes on single-walled carbon nanotubes by atom transfer radical polymerization of *n*-butyl methacrylate. J Am Chem Soc 2004;126(1):170–6.
[204] Baker SE, Cai W, Lasseter TL, Weidkamp KP, Hamers RJ. Covalently bonded adducts of deoxyribonucleic acid (DNA) oligonucleotides with single-wall carbon nanotubes: synthesis and hybridization. Nano Lett 2002;2(12):1413–7.
[205] Khitrov G. Covalent nanoassemblies of carbon nanotubes and DNA oligo-nucleotides synthesized. Mrs Bull 2002; 27(12):940–0.
[206] Williams KA, Veenhuizen PTM, de la Torre BG, Eritja R, Dekker C. Nanotechnology—carbon nanotubes with DNA recognition. Nature 2002;420(6917):761–1.
[207] Huang WJ, Taylor S, Fu KF, Lin Y, Zhang DH, Hanks TW, et al. Attaching proteins to carbon nanotubes via diimide-activated amidation. Nano Lett 2002;2(4):311–4.
[208] Dwyer C, Guthold M, Falvo M, Washburn S, Superfine R, Erie D. DNA-functionalized single-walled carbon nanotubes. Nanotechnology 2002;13(5):601–4.
[209] Mc Carthy B, Coleman JN, Czerw R, Dalton AB, Carroll DL, Blau WJ. Microscopy studies of nanotube-conjugated polymer interactions. Synth Met 2001;121(1–3):1225–6.
[210] Curran S, Davey AP, Coleman JN, Dalton AB, Mc Carthy B, Maier S, et al. Evolution and evaluation of the polymer nanotube composite. Synth Met 1999;103(1–3):2559–62.
[211] Coleman JN, Dalton AB, Curran S, Rubio S, Davey AP, Drury A, et al. Phase separation of carbon nanotubes and turbostratic graphite using a functional organic polymer. Adv Mater 2000;12(3):213–6.
[212] Murphy R, Coleman JN, Cadek M, Mc Carthy B, Bent M, Drury A. High-yield, nondestructive purification and quantification method for multiwalled carbon nanotubes. J Phys Chem B 2002;106(12):3087–91.
[213] Curran SA, Ajayan PM, Blau WJ, Carroll DL, Coleman JN, Dalton AB, et al. A composite from poly(*m*-phenylenevinylene-*co*-2,5-dioctoxy-*p*-phenylenevinylene) and carbon nanotubes: a novel material for molecular optoelectronics. Adv Mater 1998;10(14):1091–3.
[214] Mc Carthy B, Dalton AB, Coleman JN, Byrne HJ, Bernier P, Blau WJ. Spectroscopic investigation of conjugated polymer/single-walled carbon nanotube interactions. Chem Phys Lett 2001;350(1/2):27–32.
[215] Dalton AB, Stephan C, Coleman JN, Mc Carthy B, Ajayan PM, Lefrant S, et al. Selective interaction of a semiconjugated organic polymer with single-wall nanotubes. J Phys Chem B 2000;104(43):10012–6.
[216] Star A, Stoddart JF, Steuerman D, Diehl M, Boukai A, Wong EW, et al. Preparation and properties of polymer-wrapped single-walled carbon nanotubes. Angew Chem Int Ed 2001;40(9):1721–5.
[217] Ago H, Petritsch K, Shaffer MSP, Windle AH, Friend RH. Composites of carbon nanotubes and conjugated polymers for photovoltaic devices. Adv Mater 1999;11(15):1281–5.
[218] Ago H, Shaffer MSP, Ginger DS, Windle AH, Friend RH. Electronic interaction between photoexcited poly(*p*-phenylene vinylene) and carbon nanotubes. Phys Rev B 2000; 61(3):2286–90.
[219] Steuerman DW, Star A, Narizzano R, Choi H, Ries RS, Nicolini C, et al. Interactions between conjugated polymers and single-walled carbon nanotubes. J Phys Chem B 2002; 106(12):3124–30.
[220] Tang BZ, Xu H. Preparation, alignment, and optical properties of soluble poly(phenylacetylene)-wrapped carbon nanotubes. Macromolecules 1999;32(8):2569–76.
[221] Fan JH, Wan MX, Zhu DB, Chang BH, Pan ZW, Xie SS. Synthesis, characterizations, and physical properties of carbon nanotubes coated by conducting polypyrrole. J Appl Polym Sci 1999;74(11):2605–10.
[222] Fan JH, Wan MX, Zhu DB, Chang BH, Pan ZW, Xie SS. Synthesis and properties of carbon nanotube-polypyrrole composites. Synth Met 1999;102(1-3):1266–7.
[223] Cochet M, Maser WK, Benito AM, Callejas MA, Martínez MT, Benoit JM, et al. Synthesis of a new polyaniline/nanotube composite: in-situ polymerisation and charge transfer through site-selective interaction. Chem Commun 2001;16:1450–1.

[224] Zengin H, Zhou W, Jin J, Czerw R, Smith Jr DW, Echegoyen L, et al. Carbon nanotube doped polyaniline. Adv Mater 2002;14(20):1480–3.
[225] O'Connell MJ, Boul P, Ericson LM, Huffman C, Wang Y, Haroz E, et al. Reversible water-solubilization of single-walled carbon nanotubes by polymer wrapping. Chem Phys Lett 2001;342(3/4):265–71.
[226] Gong XY, Liu J, Baskaran S, Voise RD, Young JS. Surfactant-assisted processing of carbon nanotube/polymer composites. Chem Mater 2000;12(4):1049–52.
[227] Jin ZX, Pramoda KP, Goh SH, Xu GQ. Poly(vinylidene fluoride)-assisted melt-blending of multi-walled carbon nanotube/poly(methyl methacrylate) composites. Mater Res Bull 2002;37(2):271–8.
[228] Qian D, Dickey EC, Andrews R, Rantell T. Load transfer and deformation mechanisms in carbon nanotube-polystyrene composites. Appl Phys Lett 2000;76(20):2868–70.
[229] Xu XJ, Thwe MM, Shearwood C, Liao K. Mechanical properties and interfacial characteristics of carbon-nanotube-reinforced epoxy thin films. Appl Phys Lett 2002;81(15): 2833–5.
[230] Cadek M, Coleman JN, Barron V, Hedicke K, Blau WJ. Morphological and mechanical properties of carbon-nanotube-reinforced semicrystalline and amorphous polymer composites. Appl Phys Lett 2002;81(27):5123–5.
[231] Andrews R, Jacques D, Rao AM, Rantell T, Derbyshire F, Chen Y, et al. Nanotube composite carbon fibers. Appl Phys Lett 1999;75(9):1329–31.
[232] Haggenmueller R, Gommans HH, Rinzler AG, Fischer JE, Winey KI. Aligned single-wall carbon nanotubes in composites by melt processing methods. Chem Phys Lett 2000; 330(3/4):219–25.
[233] Jin L, Bower C, Zhou O. Alignment of carbon nanotubes in a polymer matrix by mechanical stretching. Appl Phys Lett 1998;73(9):1197–9.
[234] Chen J, Hamon MA, Hu H, Chen YS, Rao AM, Eklund PC, et al. Solution properties of single-walled carbon nanotubes. Science 1998;282(5386):95–8.
[235] Borsenberger PM, Chowdry A, Hoesterey DC, Mey W. Aggregate organic photoconductor. 2. Photoconduction properties. J Appl Phys 1978;49(11):5555–64.
[236] Gu T, Xu JM, Chen WX, Xu ZD. Synthesis and photoconductivity of fullerenated polymethylphenylsilane. Chem J Chin Univ 1999;20(1):150–2.
[237] Wang CC, Deng BJ, Fu SK. Spectrm study of PVK/C_{60} charge transfer complex. Chem J Chin Univ—Chin 1994; 15(10):1559–62.
[238] Chen Y, Cai RF, Xiao LX, Huang ZE, Pan DC. Synthesis and characterization of photoconductive C-60-*N*-vinylcarbazole copolymers. J Mater Sci 1998;33(18):4633–41.
[239] Li L, Tao ZH, Wang CC, Yang WL, Fu SK. Preparation, characterization and photoconductivity of C-60 grafted poly(*N*-vinyl carbazole). Chem J Chin Univ—Chin 2000;21(5):816–8.
[240] Long CF, Bai FL, Zhu DB, Li FY, Li YL, Guo ZX. Photoconductivity of 1,2-(1′,1′,2′,2′-tetracyanomethanoxy-methano)[60]fullerene-doped PVK. J Appl Polym Sci 1999; 72(2):209–13.
[241] Wang CC, Tao ZH, Hu JH, Fu SK. Preparation and photoconductivity study of the C_{60}/MMA copolymers. Chem J Chin Univ—Chin 2000;21(5):805–8.
[242] Wang CC, Shu C, Fu SK, Jiang KJ, Chen HJ, Wang M. Photoconductivity of polystyrene with C-60 in the side group. Chem J Chin Univ—Chin 2000;21(8):1331–3.
[243] Wang CC, Tao KH, Yang WL, Fu SK. Synthesis and photoconductivity study of C-60-containing styrene/acrylamide copolymers. Macromol Rapid Commun 2001;22(2): 98–103.
[244] Wu W, Li JX, Liu L, Yang L, Guo Z-X, Dai L, et al. The photoconductivity of PVK-carbon nanotube blends. Chem Phys Lett 2002;364(1-2):196–9.
[245] Prasad PN, Williams DJ, editors. Introduction to nonlinear optical effects in molecules and polymers. New York: Wiley; 1991.
[246] Zhang Y, Cui Y, Prasad PN. Observation of photorefeactivity in a fullerene-doped polymer composite. Phys Rev B 1992; 46(15):9900–2.
[247] Bai Y, Chen X, Wan X, Zhou QF, Liu H, Zhang B, et al. Photorefractive properties in homogeneous and heterogeneous polymer/liquid crystal composites. Appl Phys B–Lasers Opt 2001;73(1):35–7.
[248] Kim HW, Yoon CS, Kim JY, Kim TM, Kim JD. Photorefractivity and optical transmittance of hybrid liquid crystal cell with homeotropically photoaligned layer and fullerene initiation. J Appl Phys 2001;40(11A): L1157–L1159.
[249] Park SH, Ogino K, Sato H. Synthesis and characterization of photorefractive polymers with triphenylamine unit and NLO chromophore unit on a side chain. Polym Adv Technol 2000; 11(7):349–58.
[250] Ono H, Kawatsuki N. High-performance photorefractivity in high- and low-molar-mass liquid crystal mixtures. J Appl Phys 1999;85(5):2482–7.
[251] Ono H, Kawatsuki N. Response characteristics of high-performance photorefractive liquid crystals. Jpn J Appl Phys 1999;38(2A):737–40.
[252] Brabec CJ, Sariciftci NS, Hummelen JC. Plastic solar cells. Adv Funct Mater 2001;11(1):15–26.
[253] Brabec CJ, Sariciftci SN. Recent developments in conjugated polymer based plastic solar cells. Monatsh Chem 2001; 132(4):421–31.
[254] Ouali L, Krasnikov VV, Stalmach U, Hadziioannnou G. Oligo(phenylenevinylene)/fullerene photovoltaic cells: influence of morphology. Adv Mater 1999;11(18):1515–8.
[255] Peeters E, van Hal PA, Knol J, Brabec CJ, Sariciftci NS, Hummelen JC, et al. Synthesis, photophysical properties, and photovoltaic devices of oligo(*p*-phenylene vinylene)-fullerene dyads. J Phys Chem B 2000;104(44):10174–90.
[256] Li JX, Sun N, Guo ZX, Li CJ, Li YF, Dai LM, et al. Photovoltaic devices with methanofullerenes as electron acceptors. J Phys Chem B 2002;106(44):11509–14.
[257] Cravino A, Sariciftci NS. Double-cable polymers for fullerene based organic optoelectronic applications. J Mater Chem 2002;12(7):1931–43.

[258] Ramos AM, Rispens MT, Hummelen JC, Janssen RAJ. A poly(*p*-phenylene ethynylene vinylene) with pendant fullerenes. Synth Met 2001;119(1–3):171–2.

[259] Roman LS, Andersson MR, Yohannes T, Inganas O. Photodiode performance and nanostructure of polythiophene/C_{60} blends. Adv Mater 1997;9(15):1164–8.

[260] Brabec CJ, Cravino A, Meissner D, Sariciftci NS, Fromherz T, Rispens MT, et al. Origin of the open circuit voltage of plastic solar cells. Adv Funct Mater 2001;11(5): 374–80.

[261] Nava MG, Setayesh S, Rameau A, Masson P, Nierengarten JF. Fullerene-functionalized polyesters: synthesis, characterization and incorporation in photovoltaic cells. N J Chem 2002;26(11):1584–9.

[262] Eckert JF, Nicoud JF, Nierengarten JF, Liu SG, Echegoyen L, Barigelletti F, et al. Fullerene-oligophenylenevinylene hybrids: synthesis, electronic properties, and incorporation in photovoltaic devices. J Am Chem Soc 2000; 122(31):7467–79.

[263] Nierengarten JF, Eckert JF, Nicoud JF, Ouali L, Krasnikov V, Hadziioannou G. Synthesis of a C_{60}-oligophenylenevinylene hybrid and its incorporation in a photovoltaic device. Chem Commun 1999;7:617–8.

[264] Nierengarten JF, Eckert JF, Felder D, Nicoud JF, Armaroli N, Marconi G, et al. Synthesis and electronic properties of donor-linked fullerenes towards photochemical molecular devices. Carbon 2000;38(11/12):1587–98.

[265] Gu T, Nierengarten JF. Synthesis of fullerene-oligophenyleneethynylene hybrids. Tetrahedron Lett 2001;42(18): 3175–8.

[266] Armaroli N, Accorsi G, Gisselbrecht JP, Gross M, Krasnikov V, Tsamouras D, et al. Photoinduced processes in fullerenopyrrolidine and fullerenopyrazoline derivatives substituted with an oligophenylenevinylene moiety. J Mater Chem 2002;12(7):2077–87.

[267] Wang S, Yang JL, Li YL, Lin HZ, Guo ZX, Xiao SX, et al. Composites of C_{60} based poly(phenylene vinylene) dyad and conjugated polymer for polymer light-emitting devices. Appl Phys Lett 2002;80(20):3847–9.

[268] Tutt LW, Boggess TF. A review of optical limiting mechanisms and devices using organics, fullerenes, semiconductors and other materials. Prog Quant Electron 1993; 17(4):299–338.

[269] Kohlman R, Klimov V, Smilowitz L, McBranch D. Optical limiting and excited-state absorption in fullerene solutions and doped glasses. In: Shinar J, Vardeny ZV, Kafafi ZH, editors. Optical and electronic properties of fullerenes and fullerene-based materials. New York: Marcel Dekker; 2000. p. 143–68.

[270] Sun YP, Riggs JE. Organic and inorganic optical limiting materials. From fullerenes to nanoparticles. Int Rev Phys Chem 1999;18(1):43–90.

[271] Tutt LW, Kost A. Optical limiting performance of C_{60} and C_{70} solutions. Nature 1992;356(6366):225–6.

[272] Brusatin G, Signorini R. Linear and nonlinear optical properties of fullerenes in solid state materials. J Mater Chem 2002;12(7):1964–77.

[273] Kost A, Tutt LW, Klein MB, Dougherty TK, Elias WE. Optical limiting with C_{60} in polymethyl methacrylate. Opt Lett 1993;18(5):334–6.

[274] Kojima Y, Matsuoka T, Takahashi H, Kurauchi T. Optical limiting property of polystyrene-bound C_{60}. Macromolecules 1995;28(26):8868–9.

[275] Sun YP, Riggs JE. Non-linear absorptions in pendant [60]fullerene-polystyrene polymers. J Chem Soc Faraday Trans 1997;93(10):1965–9.

[276] Lu ZH, Goh SH, Lee SY, Sun X, Ji W. Synthesis, characterization and nonlinear optical properties of copolymers of benzylaminofullerene with methyl methacrylate or ethyl methacrylate. Polymer 1999;40(10):2863–7.

[277] Xu HY, Tang BZ. Syntheses and optical properties of poly (C_{60}-*co*-phenylacetylene)s. J Macromol Sci Pure 1999;36(9): 1197–207.

[278] Riggs JE, Sun YP. Optical limiting properties of mono- and multiple-functionalized fullerene derivatives. J Chem Phys 2000;112(9):4221–30.

[279] Sun N, Guo ZX, Dai LM, Zhu DB, Wang YX, Song YL. Hexakisadduct C_{60}-Ag nanocomposite: fabrication and optical limiting effect. Chem Phys Lett 2002;356(1/2): 175–80.

[280] Venturini J, Koudoumas E, Couris S, Janot JM, Seta P, Mathis C, et al. Optical limiting and nonlinear optical absorption properties of C_{60}–polystyrene star polymer films: C_{60} concentration dependence. J Mater Chem 2002;12(7): 2071–6.